Noname manuscript No.
(will be inserted by the editor)

Evolving finite element methods with an artificial tangential velocity for mean curvature flow and Willmore flow

Jiashun Hu · Buyang Li

Received: date / Accepted: date

Abstract An artificial tangential velocity is introduced into the evolving finite element methods for mean curvature flow and Willmore flow proposed by Kovács, Li & Lubich in [40,41] in order to improve the mesh quality in the computation. The artificial tangential velocity is constructed by considering a limiting situation in the method proposed by Barrett, Garcke & Nürnberg in [7–9]. The stability of the artificial tangential velocity is proved. The optimal-order convergence of the evolving finite element methods with artificial tangential velocity are proved for both mean curvature flow and Willmore flow. Extensive numerical experiments are presented to illustrate the convergence of the method and the performance of the artificial tangential velocity in improving the mesh quality.

Keywords Evolving surface, mean curvature flow, Willmore flow, finite element method, artificial tangential velocity, stability, error analysis

1 Introduction

The evolution of surface under geometric curvature flows has been intensively investigated in the past decades. The most well-known examples are mean curvature flow and higher-order geometric flows driven by curvature, including Willmore flow and surface diffusion. The numerical computation of such

J. Hu
Department of Applied Mathematics, The Hong Kong Polytechnic University, Hung Hom, Hong Kong. Email address: jiashhu@polyu.edu.hk

B. Li (Corresponding author)
Department of Applied Mathematics, The Hong Kong Polytechnic University, Hung Hom, Hong Kong. Email address: buyang.li@polyu.edu.hk, libuyang@gmail.com

geometric curvature flows originates from the pioneering work of Dziuk [26], who proposed the first parametric finite element method (FEM) for mean curvature flow. It is known that the velocity of an evolving surface Γ under mean curvature flow is determined by

$$v = -Hn = \Delta_\Gamma \mathrm{id}, \tag{1.1}$$

where id denotes the identity function on $\Gamma \subset \mathbb{R}^3$, H and n denote the mean curvature and the outward normal vector of the surface Γ, and Δ_Γ denotes the Laplace–Beltrami operator on the surface. Assuming that $\Gamma(t_{m-1})$ is already approximated by a piecewise triangular surface Γ_h^{m-1}, Dziuk's method is to find a parametrization of the surface Γ_h^m, denoted by $u_h^m : \Gamma_h^{m-1} \to \mathbb{R}^3$, in a finite element space $S_h(\Gamma_h^{m-1})^3$ satisfying the following weak formulation:

$$\int_{\Gamma_h^{m-1}} \frac{u_h^m - \mathrm{id}}{\tau} \cdot \chi_h + \int_{\Gamma_h^{m-1}} \nabla_{\Gamma_h^{m-1}} u_h^m \cdot \nabla_{\Gamma_h^{m-1}} \chi_h = 0 \quad \forall \chi_h \in S_h(\Gamma_h^{m-1})^3. \tag{1.2}$$

The methods of parametrizing the unknown surface Γ_h^m by finite element functions on the known surface Γ_h^{m-1} are later referred to as parametric FEMs. The idea was widely adopted for approximating other geometric curvature flows, including surface diffusion, Willmore flow, Helfrich flow, and so on; see [3, 14, 28, 46, 48].

The parametric FEMs can successfully compute the evolution of surfaces under curvature flows within a short time, but the nodes may cluster and mesh may become distorted as the surface evolves. In this case, certain mesh redistribution technique may improve the computational results; see [3]. In order to improve the mesh quality without using mesh redistribution technique, Barrett, Garcke & Nürnberg proposed a different weak formulation for mean curvature flow, surface diffusion and Willmore flow in [7–9], with an intrinsic tangential velocity that is promising to make mesh points distribute more uniformly. The method of Barrett, Garcke & Nürnberg (BGN method) has been successful in improving the mesh quality in practical computation and adopted by many others in developing numerical methods for curvature flows, e.g., in the simulation of solid-state dewetting problems with anisotropic surface energies and contact line migration [4, 54]. The idea of BGN method was also used in computing the interface of two-phase flow by an unfitted or fitted bulk mesh; see [10, 11], and by the arbitrary Lagrangian–Eulerian (ALE) method; see [34, 35]. The tangential velocity in the BGN method appears only in the fully discretized scheme and the lack of counterpart in the continuous formulation increases the difficulty to prove the convergence of the BGN method. For mean curvature flow, an alternative approach to introducing tangential velocity was proposed by Elliott and Fritz [33] using the DeTruck trick. The additional tangential velocity of the continuous flow can be interpreted as a special re-parametrization under the harmonic map heat flow scaled by an adjustable parameter, and can generate good mesh properties as in the BGN method.

In the semidiscrete case, the parametric FEMs can be formulated into evolving surface FEMs [30] and then written into matrix-vector forms by using the notation of [42]. For example, in the semidiscrete case (as $\tau \to 0$), Dziuk's parametric FEM for mean curvature flow can be written as (see [44]): Find a vector $\mathbf{x}(t) \in \mathbb{R}^{3N}$ which collects all nodes in the triangulation of the surface (N is the number of nodes) satisfying the equation

$$\mathbf{M}(\mathbf{x})\frac{\mathrm{d}\mathbf{x}}{\mathrm{d}t} + \mathbf{A}(\mathbf{x})\mathbf{x} = \mathbf{0}, \tag{1.3}$$

where $\mathbf{M}(\mathbf{x})$ and $\mathbf{A}(\mathbf{x})$ are the mass and stiffness matrices on the surface $\Gamma_h[\mathbf{x}]$ determined by the nodal vector $\mathbf{x}$. Dziuk's fully discrete method (1.2) is equivalent to a semi-implicit scheme for (1.3), i.e.,

$$\mathbf{M}(\mathbf{x}^{m-1})\frac{\mathbf{x}^m - \mathbf{x}^{m-1}}{\tau} + \mathbf{A}(\mathbf{x}^{m-1})\mathbf{x}^m = \mathbf{0}. \tag{1.4}$$

The matrix-vector formulation has been a powerful tool in [40–42] for error analysis of evolving surface FEMs when the evolving surface is unknown.

The convergence results of different parametric and evolving surface FEMs for mean curvature flow and Willmore flow of *curves* were proved in [13, 17, 18, 27, 33, 47] and [43, 49, 53] for semidiscrete and fully discrete methods, respectively. For mean curvature flow and Willmore flow of *graph surfaces*, the convergence results of FEMs were proved in [15, 16, 21, 29]. Convergence of finite element semi-discretizations for the surface diffusion flow of *graphs* and axially symmetric surfaces has been proved; see [2, 19, 20]. For mean curvature flow of *closed surfaces*, the convergence of an evolving surface FEM using finite elements of degree $\geqslant 2$ was proved in [40] by using the evolution equations of mean curvature and normal vector field discovered in [37], i.e., by considering the following equivalent formulation of (1.1):

$$\partial_t X = v \circ X, \tag{1.5a}$$
$$v - \Delta_{\Gamma[X]} v = -Hn + \Delta_{\Gamma[X]}(Hn), \tag{1.5b}$$
$$\partial_t^\bullet n - \Delta_{\Gamma[X]} n = |\nabla_{\Gamma[X]} n|^2 n, \tag{1.5c}$$
$$\partial_t^\bullet H - \Delta_{\Gamma[X]} H = |\nabla_{\Gamma[X]} n|^2 H, \tag{1.5d}$$

where $X(\cdot, t) : \Gamma^0 \to \mathbb{R}^3$ is the flow map which maps the given initial surface Γ^0 to the current surface

$$\Gamma[X(\cdot, t)] = \{X(p, t) : p \in \Gamma^0\},$$

$\partial_t^\bullet n$ and $\partial_t^\bullet H$ denote the material derivatives of n and H, respectively, along the particle trajectory of the evolving surface. This treatment brings additional (about twice) computational cost, but provides full-order approximations to mean curvature and normal vector, and allows people to obtain rigorous error estimates for the numerical approximation. The techniques turn out to be also successful for constructing an evolving surface FEM for Willmore flow with rigorous convergence proof; see [41]. More recently, Dziuk's semidiscrete method for mean curvature flow of closed surfaces was proved to be convergent for high-order finite elements of degree $\geqslant 6$ in [44]. All these methods, which were proved convergent for mean curvature flow or Willmore flow of *closed surfaces*, do not contain tangential velocity to improve the mesh quality. For convergence analysis of algorithms with tangential velocity, there are some recent results which apply the DeTurck trick to introduce a tangential velocity and obtain optimal convergence order for mean curvature flow of two-dimensional axisymmetric surface [6, 22] and torus type surface [45].

In this article, we propose a new evolving surface FEM for mean curvature flow of *closed surfaces*, with a tangential velocity to improve the mesh quality, and then prove the convergence of the proposed method. The velocity of the surface consists of normal and tangential components, where the tangential velocity is determined by requiring $\Delta_{\Gamma[X]}v$ to be parallel to n, i.e.,

$$v \cdot n = -H, \tag{1.6}$$

$$\Delta_{\Gamma[X]}v = \kappa n \quad \text{for some auxiliary function } \kappa. \tag{1.7}$$

Our idea of determining the tangential velocity by (1.7) is inspired by considering the temporally semidiscrete version of the BGN method in [8]: Let u^{m+1} and H^{m+1} denote the position and the mean curvature of the surface Γ^{m+1} parametrized through Γ^m. Then the temporally semidiscrete version of the BGN method can be written as

$$\Delta_{\Gamma^m} u^{m+1} = -H^{m+1} n^m, \tag{1.8}$$

where n^m denotes the normal vector of Γ^m. Subtracting the identity $\Delta_{\Gamma^m}\mathrm{id} = -H^m n^m$ from (1.8) and dividing the result by the temporal step size τ, we obtain

$$\Delta_{\Gamma^m} \frac{u^{m+1} - \mathrm{id}}{\tau} = -\frac{H^{m+1} - H^m}{\tau} n^m,$$

which tends to the form of (1.7) as $\tau \to 0$. At the discrete level, since the BGN method can improve the mesh quality, it follows that the derived equations in (1.6)–(1.7) may similarly improve the mesh quality.

At the continuous level, it is easy to verify that solving equations (1.6)–(1.7) is equivalent to minimizing the energy functional

$$E[v] = \int_{\Gamma[X]} |\nabla_\Gamma v|^2$$

under the constraint $v \cdot n = -H$, with κ denoting a Lagrangian multiplier in this constraint optimization problem. For an evolving surface $\Gamma(t)$, $t \geqslant t_0$, the deformation tensor $\nabla_{\Gamma(t_0)}X(x,t)$ between the two surfaces $\Gamma(t)$ and $\Gamma(t_0)$ satisfies the following equation:

$$\partial_t \nabla_{\Gamma(t_0)} X(x,t) = \nabla_{\Gamma(t_0)} v(X(x,t),t).$$

By setting $t = t_0$ in the equation above we see that $\nabla_{\Gamma(t_0)}v(x,t_0)$ represents the instantaneous rate of deformation at time t_0. Therefore, minimizing the energy functional $E[v] = \int_{\Gamma[X]} |\nabla_\Gamma v|^2$ is equivalent to minimizing the instantaneous rate of deformation. Equivalently speaking, solving equations (1.6)–(1.7) is equivalent to minimizing the rate of deformation under the constraint $v \cdot n = -H$ (so that the mesh can be less deformed).

For mean curvature flow, the evolution equations governing H and n are used to couple with the velocity equations in (1.6)–(1.7):

$$\partial_t X = v \circ X, \tag{1.9a}$$

$$v \cdot n = -H, \tag{1.9b}$$

$$\kappa n = \Delta_{\Gamma[X]} v, \tag{1.9c}$$

$$\partial_t^\bullet n - v \cdot \nabla_{\Gamma[X]} n - \Delta_{\Gamma[X]} n = |\nabla_{\Gamma[X]} n|^2 n, \tag{1.9d}$$

$$\partial_t^\bullet H - v \cdot \nabla_{\Gamma[X]} H - \Delta_{\Gamma[X]} H = |\nabla_{\Gamma[X]} n|^2 H. \tag{1.9e}$$

In other words, we have replaced the velocity equation in (1.5) by (1.9b)–(1.9c). This can yield a tangential velocity which has similar effect as the BGN method. Due to the presence of tangential velocity, the flow map X in (1.9) is different from that in (1.5). It is noted that (1.9e) can be found as a special case of [12, Lemma 39]. We temporarily distinguish the two flow maps in (1.5) and (1.9) by $\tilde{X}$ and X, respectively, and add them to the subscripts of the associated material derivatives. Then, for f defined on $\mathcal{G}_T = \cup_{t\in[0,T]}(\Gamma(t) \times \{t\})$, which can either be parametrized by $\tilde{X}$ or X, we have

$$\partial_{t,X}^\bullet f - v \cdot \nabla_\Gamma f = \partial_{t,X}^\bullet f - v_T \cdot \nabla_\Gamma f = \partial_{t,X}^\square f = \partial_{t,\tilde{X}}^\bullet f, \tag{1.10}$$

where v_T denotes the tangential part of v, $\partial_{t,X}^\square$ denotes the normal time derivative defined in [12, Section 2.4]. The last equality in (1.10) holds since the velocity field of $\tilde{X}$, regarded as a vector valued function on $\mathcal{G}_T$, is exactly the normal part of the velocity field of X, see also [12, p. 18, Remark 29].

For Willmore flow, by using the evolution equations of n and H found in [41], we have the following closed system:

$$\partial_t X = v \circ X, \tag{1.11a}$$

$$v \cdot n = V, \tag{1.11b}$$

$$\kappa n = \Delta_{\Gamma[X]} v, \tag{1.11c}$$

$$V = \Delta_{\Gamma[X]} H + Q, \tag{1.11d}$$

$$\partial_t^\bullet H - v \cdot \nabla_{\Gamma[X]} H = -\Delta_{\Gamma[X]} V - |A|^2 V, \tag{1.11e}$$

$$\begin{aligned}\partial_t^\bullet n - v \cdot \nabla_{\Gamma[X]} n = & -\Delta_{\Gamma[X]} z + (HA - A^2)\, z + |\nabla_{\Gamma[X]} H|^2 n \\ & - 2\big(\nabla_{\Gamma[X]} \cdot (A \nabla_{\Gamma[X]} H)\big)\, n - A^2 \nabla_{\Gamma[X]} H - \nabla_{\Gamma[X]} Q,\end{aligned} \tag{1.11f}$$

$$z = \Delta_{\Gamma[X]} n + |A|^2 n, \tag{1.11g}$$

where $A = \nabla_{\Gamma[X]} n$, $Q = -\frac{1}{2}H^3 + |A|^2 H$, and $|A|^2 = |\nabla_{\Gamma[X]} n|^2$. The above new system simply replaces the velocity equation $v = Vn$ in [41] by (1.11b)–(1.11c). Setting $Q = 0$ in (1.11) would yield a closed system for surface diffusion flow.

In the evolving surface FEM, the systems (1.9) and (1.11) can be rewritten into matrix-vector forms as in [40–42, 44], and the stability estimates for the equations of n and H have already been established in [40, 41]. The stability analysis for the velocity in (1.9b)–(1.9c) is the main contribution of this article. This is obtained by choosing test functions associated to the tangential projections of some proper functions. By combining the stability estimates of the velocity equations (i.e., Theorem 3.2) and the equations of n and H, we obtain optimal-order error estimates of the evolving surface FEMs for finite elements of degree $\geqslant 2$ for both mean curvature flow and Willmore flow; see Theorems 2.1–2.2. Extensive numerical experiments are presented to illustrate the convergence of the proposed method and the performance of the artificial tangential velocity for improving the mesh quality.

The rest of this article is organized as follows. In Section 2, we introduce the basic notations and propose the modified systems of equations with artificial tangential velocity for mean curvature flow and Willmore flow. The continuous problems are then spatially semi-discretized in the framework of evolving surface FEM and the matrix-vector formulations. Then we present the main convergence results of the spatially semi-discretized evolving surface FEMs. In Sections 3 and 4, we prove the convergence of the evolving surface FEMs for mean curvature flow and Willmore flow, respectively. In Section 5, we present numerical results to support the theoretical analysis in this article.

2 The numerical method and main results

2.1 Basic notations for an evolving surface

Given a smooth surface $\Gamma \subset \mathbb{R}^3$, the surface gradient for a scalar function $u : \Gamma \to \mathbb{R}$ is a column vector denoted by $\nabla_\Gamma u$. In the case of a vector-valued function $u = (u_1, u_2, u_3)^\top : \Gamma \to \mathbb{R}^3$, we use the following conventional notations:

$$Du = \begin{pmatrix} (\nabla_\Gamma u_1)^\top \\ (\nabla_\Gamma u_2)^\top \\ (\nabla_\Gamma u_3)^\top \end{pmatrix} \quad \text{and} \quad \nabla_\Gamma u = (Du)^\top = (\nabla_\Gamma u_1, \nabla_\Gamma u_2, \nabla_\Gamma u_3).$$

The mean curvature of Γ is defined as the trace of the extended Weingarten mapping $A = \nabla_\Gamma n$, which is expressed as

$$H = \mathrm{tr}(\nabla_\Gamma n),$$

where n denotes the unit exterior normal vector of Γ.

The evolving surface is described by the flow map $X(\cdot, t) : \Gamma^0 \to \mathbb{R}^3$, $t \in [0, T]$, which is a diffeomorphism from a given initial surface Γ^0 to the current surface

$$\Gamma(t) = \Gamma[X(\cdot, t)] = \{X(p, t) : p \in \Gamma^0\}.$$

For any fixed $p \in \Gamma^0$, the set of points $\{X(p,t) : t \in [0,T]\}$ is a trajectory starting from p. The velocity of the surface at the point $X(p,t) \in \Gamma[X(\cdot,t)]$ along the trajectory is

$$v(X(p,t),t) = \partial_t X(p,t).$$

Throughout this article, we denote by C and h_0 two generic positive constants which are different at different occurrences, possibly depending on the norms of the exact solution and T, but are independent of the mesh size h.

2.2 The evolving surface FEM

We assume that the given closed smooth initial surface $\Gamma^0 \subset \mathbb{R}^3$ is partitioned into an admissible family of shape-regular and quasi-uniform triangulations $\mathcal{T}_h$ with mesh size h; see [30] for the notion of admissible family of triangulations. Let $\mathbf{x}^0 = (p_1, \cdots, p_N) \in \mathbb{R}^{3N}$ be the vector that collects all nodes $p_j \in \mathbb{R}^3$, $j = 1, \ldots, N$ in the triangulation of Γ^0 by finite elements of degree k, as defined in [23]. The nodal vector $\mathbf{x}^0$ determines an approximate surface $\Gamma_h[\mathbf{x}^0]$ that interpolates the surface Γ^0 at the nodes.

We evolve the vector $\mathbf{x}^0$ in time and denote its position at time t by $\mathbf{x}(t) = (x_1(t), \cdots, x_N(t))$, which determines a surface $\Gamma_h[\mathbf{x}(t)]$ by piecewise polynomial interpolation on the plane reference triangle. There exists a unique finite element function $X_h(\cdot,t)$ of piecewise polynomial degree k defined on $\Gamma_h[\mathbf{x}^0]$ satisfying

$$X_h(p_j,t) = x_j(t) \quad \text{for} \quad j = 1, \ldots, N.$$

This is the discrete flow map, which maps the discrete initial surface $\Gamma_h[\mathbf{x}^0]$ to $\Gamma_h[\mathbf{x}(t)]$.

If $w(\cdot,t)$ is a function defined on $\Gamma_h[\mathbf{x}(t)]$ for $t \in [0,T]$, then the material derivative $\partial^\bullet_{t,h} w$ on $\Gamma_h[\mathbf{x}(t)]$ with respect to the discrete flow map X_h is defined by

$$\partial^\bullet_{t,h} w(x,t) = \frac{\mathrm{d}}{\mathrm{d}t} w(X_h(p,t),t) \quad \text{for } x = X_h(p,t) \in \Gamma_h[\mathbf{x}(t)].$$

The finite element basis functions on $\Gamma_h[\mathbf{x}]$ are denoted by $\phi_j[\mathbf{x}]$, $j = 1, \ldots, N$, which satisfy the following identities:

$$\phi_j[\mathbf{x}](x_i) = \delta_{ij}, \qquad i,j = 1, \ldots, N.$$

The pullback of $\phi_j[\mathbf{x}]$ from any curved triangle on $\Gamma_h[\mathbf{x}]$ to the reference plane triangle is a polynomial of degree k. It is known that $\phi_j[\mathbf{x}(t)]$ satisfies the following transport property (see [30]):

$$\partial^\bullet_{t,h} \phi_j[\mathbf{x}(t)] = 0 \quad \text{on } \Gamma_h[\mathbf{x}(t)], \;\; j = 1, \ldots, N. \tag{2.1}$$

The finite element space on the surface $\Gamma_h[\mathbf{x}]$ is defined as

$$S_h[\mathbf{x}] = S_h(\Gamma_h[\mathbf{x}]) := \operatorname{span}\left\{ \sum_{j=1}^N c_j \phi_j[\mathbf{x}] : c_j \in \mathbb{R} \right\}.$$

The evolving surface FEM for (1.9) is to find $X_h(\cdot,t) \in S_h[\mathbf{x}^0]^3$ and
$(v_h(\cdot,t), \kappa_h(\cdot,t), n_h(\cdot,t), H_h(\cdot,t)) \in S_h[\mathbf{x}(t)]^3 \times S_h[\mathbf{x}(t)] \times S_h[\mathbf{x}(t)]^3 \times S_h[\mathbf{x}(t)]$,
such that

$$\partial_t X_h = v_h \circ X_h, \tag{2.2a}$$

$$\int_{\Gamma_h[\mathbf{x}]} v_h \cdot n_h \chi_\kappa = - \int_{\Gamma_h[\mathbf{x}]} H_h \chi_\kappa, \tag{2.2b}$$

$$\int_{\Gamma_h[\mathbf{x}]} \kappa_h n_h \cdot \chi_v + \int_{\Gamma_h[\mathbf{x}]} \nabla_{\Gamma_h[\mathbf{x}]} v_h \cdot \nabla_{\Gamma_h[\mathbf{x}]} \chi_v = 0, \tag{2.2c}$$

$$\begin{aligned} \int_{\Gamma_h[\mathbf{x}]} \partial^\bullet_{t,h} n_h \cdot \chi_n + \int_{\Gamma_h[\mathbf{x}]} \nabla_{\Gamma_h[\mathbf{x}]} n_h \cdot \nabla_{\Gamma_h[\mathbf{x}]} \chi_n \\ = \int_{\Gamma_h[\mathbf{x}]} \big(|A_h|^2 n_h + v_h \cdot \nabla_{\Gamma_h[\mathbf{x}]} n_h\big) \cdot \chi_n, \end{aligned} \tag{2.2d}$$

$$\begin{aligned} \int_{\Gamma_h[\mathbf{x}]} \partial^\bullet_{t,h} H_h \chi_H + \int_{\Gamma_h[\mathbf{x}]} \nabla_{\Gamma_h[\mathbf{x}]} H_h \cdot \nabla_{\Gamma_h[\mathbf{x}]} \chi_H \\ = \int_{\Gamma_h[\mathbf{x}]} \big(|A_h|^2 H_h + v_h \cdot \nabla_{\Gamma_h[\mathbf{x}]} H_h\big) \chi_H, \end{aligned} \tag{2.2e}$$

hold for all test functions

$$(\chi_v, \chi_\kappa, \chi_n, \chi_H) \in S_h[\mathbf{x}(t)]^3 \times S_h[\mathbf{x}(t)] \times S_h[\mathbf{x}(t)]^3 \times S_h[\mathbf{x}(t)],$$

where $A_h = \nabla_{\Gamma_h[\mathbf{x}]} n_h$ is the discretized Weingarten map. The initial value for the system (2.2) can be chosen as follows: $X_h(\cdot,0) = \mathrm{id}$ on $\Gamma_h[\mathbf{x}^0]$; $n_h(\cdot,0)$ and $H_h(\cdot,0)$ are chosen as the Lagrangian interpolations of $n(\cdot,0)$ and $H(\cdot,0)$, respectively, or any other approximations such that

$$\|n_h - I_h n\|_{L^2(\Gamma_h[\mathbf{x}^*])} + h\|n_h - I_h n\|_{H^1(\Gamma_h[\mathbf{x}^*])} \le Ch^{k+1}, \tag{2.3a}$$

$$\|H_h - I_h H\|_{L^2(\Gamma_h[\mathbf{x}^*])} + h\|H_h - I_h H\|_{H^1(\Gamma_h[\mathbf{x}^*])} \le Ch^{k+1}. \tag{2.3b}$$

Remark 2.1 We define a discrete Laplacian–Beltrami operator $\Delta_{h,\Gamma_h[\mathbf{x}]} : S_h[\mathbf{x}] \to S_h[\mathbf{x}]$ via duality by

$$(\Delta_{h,\Gamma_h[\mathbf{x}]} v_h, w_h) = -(\nabla_{\Gamma_h[\mathbf{x}]} v_h, \nabla_{\Gamma_h[\mathbf{x}]} w_h) \quad \forall w_h \in S_h[\mathbf{x}].$$

Let $P_{\Gamma_h[\mathbf{x}]} : L^2(\Gamma_h[\mathbf{x}]) \to S_h[\mathbf{x}]$ be the L^2-orthogonal projection onto the finite element space. Then, replacing the test function χ_κ in (2.2b) by $-\Delta_{h,\Gamma_h[\mathbf{x}]}\chi_\kappa$, we obtain

$$\begin{aligned} &\int_{\Gamma_h[\mathbf{x}]} \nabla_{\Gamma_h[\mathbf{x}]}(v_h \cdot n_h) \cdot \nabla_{\Gamma_h[\mathbf{x}]} \chi_\kappa \\ &= - \int_{\Gamma_h[\mathbf{x}]} \nabla_{\Gamma_h[\mathbf{x}]} H_h \cdot \nabla_{\Gamma_h[\mathbf{x}]} \chi_\kappa \\ &\quad + \int_{\Gamma_h[\mathbf{x}]} \nabla_{\Gamma_h[\mathbf{x}]}(v_h \cdot n_h - P_{\Gamma_h[\mathbf{x}]}(v_h \cdot n_h)) \cdot \nabla_{\Gamma_h[\mathbf{x}]} \chi_\kappa. \end{aligned} \tag{2.4}$$

Equation (2.4) is derived from (2.2b) and will be used only in the error analysis.

Similarly, the evolving surface FEM for the reformulated equations of Willmore flow in (1.11) is to find $X_h(\cdot,t) \in S_h[\mathbf{x}^0]^3$ and

$$
\begin{aligned}
&(v_h(\cdot,t), \kappa_h(\cdot,t), V_h(\cdot,t), H_h(\cdot,t), n_h(\cdot,t), z_h(\cdot,t)) \\
&\in S_h[\mathbf{x}(t)]^3 \times S_h[\mathbf{x}(t)] \times S_h[\mathbf{x}(t)] \times S_h[\mathbf{x}(t)] \times S_h[\mathbf{x}(t)]^3 \times S_h[\mathbf{x}(t)]^3,
\end{aligned}
$$

such that

$$
\partial_t X_h = v_h \circ X_h, \tag{2.5a}
$$

$$
\int_{\Gamma_h[\mathbf{x}]} v_h \cdot n_h \chi_\kappa = \int_{\Gamma_h[\mathbf{x}]} V_h \chi_\kappa, \tag{2.5b}
$$

$$
\int_{\Gamma_h[\mathbf{x}]} \kappa_h n_h \cdot \chi_v + \int_{\Gamma_h[\mathbf{x}]} \nabla_{\Gamma_h[\mathbf{x}]} v_h \cdot \nabla_{\Gamma_h[\mathbf{x}]} \chi_v = 0, \tag{2.5c}
$$

$$
\int_{\Gamma_h[\mathbf{x}]} V_h \chi_V + \int_{\Gamma_h[\mathbf{x}]} \nabla_{\Gamma_h[\mathbf{x}]} H_h \cdot \nabla_{\Gamma_h[\mathbf{x}]} \chi_V = \int_{\Gamma_h[\mathbf{x}]} Q_h \chi_V, \tag{2.5d}
$$

$$
\begin{aligned}
&\int_{\Gamma_h[\mathbf{x}]} \partial^\bullet_{t,h} H_h \, \chi_H - \int_{\Gamma_h[\mathbf{x}]} \nabla_{\Gamma_h[\mathbf{x}]} V_h \cdot \nabla_{\Gamma_h[\mathbf{x}]} \chi_H \\
&= \int_{\Gamma_h[\mathbf{x}]} (v_h \cdot \nabla_{\Gamma_h[\mathbf{x}]} H_h - |A_h|^2 \, V_h) \, \chi_H,
\end{aligned} \tag{2.5e}
$$

$$
\begin{aligned}
&\int_{\Gamma_h[\mathbf{x}]} \partial^\bullet_{t,h} n_h \cdot \chi_n - \int_{\Gamma_h[\mathbf{x}]} \nabla_{\Gamma_h[\mathbf{x}]} z_h \cdot \nabla_{\Gamma_h[\mathbf{x}]} \chi_n = \int_{\Gamma_h[\mathbf{x}]} (v_h \cdot \nabla_{\Gamma_h[\mathbf{x}]} n_h) \cdot \chi_n \\
&\quad + \int_{\Gamma_h[\mathbf{x}]} (H_h A_h - A_h^2) z_h \cdot \chi_n + 2 \int_{\Gamma_h[\mathbf{x}]} (A_h \nabla_{\Gamma_h[\mathbf{x}]} H_h) \cdot (\nabla_{\Gamma_h[\mathbf{x}]} \chi_n \, n_h) \\
&\quad + \int_{\Gamma_h[\mathbf{x}]} \big(|\nabla_{\Gamma_h[\mathbf{x}]} H_h|^2 n_h + A_h^2 \nabla_{\Gamma_h[\mathbf{x}]} H_h \big) \cdot \chi_n \\
&\quad + \int_{\Gamma_h[\mathbf{x}]} Q_h \, \nabla_{\Gamma_h[\mathbf{x}]} \cdot \chi_n - \int_{\Gamma_h[\mathbf{x}]} Q_h H_h \, n_h \cdot \chi_n,
\end{aligned} \tag{2.5f}
$$

$$
\int_{\Gamma_h[\mathbf{x}]} z_h \cdot \chi_z + \int_{\Gamma_h[\mathbf{x}]} \nabla_{\Gamma_h[\mathbf{x}]} n_h \cdot \nabla_{\Gamma_h[\mathbf{x}]} \chi_z = \int_{\Gamma_h[\mathbf{x}]} |A_h|^2 n_h \cdot \chi_z, \tag{2.5g}
$$

hold for all test functions

$$
(\chi_v, \chi_\kappa, \chi_V, \chi_H, \chi_n, \chi_z) \in S_h[\mathbf{x}(t)]^3 \times S_h[\mathbf{x}(t)] \times S_h[\mathbf{x}(t)] \times S_h[\mathbf{x}(t)] \times S_h[\mathbf{x}(t)]^3 \times S_h[\mathbf{x}(t)]^3.
$$

In above, (2.5f) is derived from (1.11f) by integration by part, more details can be found in [41, P 603].

2.3 Matrix-vector formulation

Associated to the finite element space $S_h[\mathbf{x}]$ on the surface $\Gamma_h[\mathbf{x}]$, we define the mass matrix $\mathbf{M}(\mathbf{x}) \in \mathbb{R}^{N\times N}$ and stiffness matrix $\mathbf{A}(\mathbf{x}) \in \mathbb{R}^{N\times N}$ by

$$\mathbf{M}_{ij}(\mathbf{x}) = \int_{\Gamma_h[\mathbf{x}]} \phi_i[\mathbf{x}]\phi_j[\mathbf{x}] \quad \text{and} \quad \mathbf{A}_{ij}(\mathbf{x}) = \int_{\Gamma_h[\mathbf{x}]} \nabla_{\Gamma_h[\mathbf{x}]}\phi_i[\mathbf{x}] \cdot \nabla_{\Gamma_h[\mathbf{x}]}\phi_j[\mathbf{x}],$$

for $i,j = 1,\dots,N$. Let $\mathbf{K}(\mathbf{x}) = \mathbf{M}(\mathbf{x}) + \mathbf{A}(\mathbf{x})$ and

$$\mathbf{M}^{[d]}(\mathbf{x}) = \mathbf{M}(\mathbf{x}) \otimes I_d \quad \text{and} \quad \mathbf{A}^{[d]}(\mathbf{x}) = \mathbf{A}(\mathbf{x}) \otimes I_d,$$

where I_d is the $d\times d$ identity matrix. We denote by $\mathbf{v}$, $\mathbf{n}$ and $\mathbf{H}$ the vectors which collect the nodal values of v_h, n_h and H_h, respectively.

Let $\mathbf{B}(\mathbf{x},\mathbf{n}), \mathbf{D}(\mathbf{x},\mathbf{n}) \in \mathbb{R}^{N\times 3N}$ be matrices associated to the left-hand side of (2.2b) and (2.4), respectively, defined by

$$\begin{aligned}
\mathbf{B}_{i,3(j-1)+m}(\mathbf{x},\mathbf{n}) &= \int_{\Gamma_h[\mathbf{x}]} \phi_i[\mathbf{x}]\phi_j[\mathbf{x}](n_h)_m, \\
\mathbf{D}_{i,3(j-1)+m}(\mathbf{x},\mathbf{n}) &= \int_{\Gamma_h[\mathbf{x}]} \nabla_{\Gamma_h[\mathbf{x}]}(\phi_j[\mathbf{x}](n_h)_m) \cdot \nabla_{\Gamma_h[\mathbf{x}]}\phi_i[\mathbf{x}],
\end{aligned}$$

where $i,j = 1,\dots,N$, $m = 1,2,3$ and $(n_h)_m$ is the m-th component of $n_h \in \mathbb{R}^3$.

Let $\mathbf{f}_1(\mathbf{x},\mathbf{n},\mathbf{v}) \in \mathbb{R}^{3N}$ and $\mathbf{f}_2(\mathbf{x},\mathbf{n},\mathbf{v},\mathbf{H}) \in \mathbb{R}^N$ be the nonlinear terms associated to the right-hand side of (2.2d) and (2.2e), respectively, defined by

$$\mathbf{f}_1(\mathbf{x},\mathbf{n},\mathbf{v})_{3(j-1)+m} = \int_{\Gamma_h[\mathbf{x}]} (v_h \cdot \nabla_{\Gamma_h[\mathbf{x}]} n_h)_m \phi_j + \int_{\Gamma_h[\mathbf{x}]} |\nabla_{\Gamma_h[\mathbf{x}]} n_h|^2 (n_h)_m \phi_j, \tag{2.6}$$

$$\mathbf{f}_2(\mathbf{x},\mathbf{n},\mathbf{v},\mathbf{H})_j = \int_{\Gamma_h[\mathbf{x}]} v_h \cdot \nabla_{\Gamma_h[\mathbf{x}]} H_h \phi_j + \int_{\Gamma_h[\mathbf{x}]} |\nabla_{\Gamma_h[\mathbf{x}]} n_h|^2 H_h \phi_j. \tag{2.7}$$

Let $\boldsymbol{\rho}(\mathbf{x},\mathbf{n},\mathbf{v}) \in \mathbb{R}^N$ be the nodal vector satisfying the following relation:

$$\boldsymbol{\rho}(\mathbf{x},\mathbf{n},\mathbf{v}) \cdot \boldsymbol{\chi}_{\boldsymbol{\kappa}} := \int_{\Gamma_h[\mathbf{x}]} \nabla_{\Gamma_h[\mathbf{x}]}[v_h \cdot n_h - P_{\Gamma_h[\mathbf{x}]}(v_h \cdot n_h)] \cdot \nabla_{\Gamma_h[\mathbf{x}]} \chi_\kappa \quad \forall \boldsymbol{\chi}_{\boldsymbol{\kappa}} \in \mathbb{R}^N, \tag{2.8}$$

where $\chi_\kappa \in S_h[\mathbf{x}]$ is the finite element function associated to the nodal vector $\boldsymbol{\chi}_{\boldsymbol{\kappa}}$.

By introducing $\mathbf{u} := (\mathbf{n},\mathbf{H})^\top$, the spatially semidiscrete evolving surface FEM in (2.2) can be rewritten into the matrix-vector form:

$$\dot{\mathbf{x}} = \mathbf{v}, \tag{2.9a}$$

$$\mathbf{B}(\mathbf{x},\mathbf{n})\mathbf{v} = -\mathbf{M}(\mathbf{x})\mathbf{H}, \tag{2.9b}$$

$$\mathbf{B}(\mathbf{x},\mathbf{n})^\top \boldsymbol{\kappa} + \mathbf{A}^{[3]}(\mathbf{x})\mathbf{v} = \mathbf{0}, \tag{2.9c}$$

$$\mathbf{M}^{[4]}(\mathbf{x})\dot{\mathbf{u}} + \mathbf{A}^{[4]}(\mathbf{x})\mathbf{u} = \mathbf{f}(\mathbf{x},\mathbf{u},\mathbf{v}), \tag{2.9d}$$

where

$$\mathbf{f}(\mathbf{x},\mathbf{u},\mathbf{v}) = \begin{pmatrix} \mathbf{f}_1(\mathbf{x},\mathbf{n},\mathbf{v}) \\ \mathbf{f}_2(\mathbf{x},\mathbf{n},\mathbf{v},\mathbf{H}) \end{pmatrix} \in \mathbb{R}^{3N+N}. \tag{2.10}$$

Similarly, equation (2.4) can be written as

$$\mathbf{D}(\mathbf{x},\mathbf{n})\mathbf{v} = -\mathbf{A}(\mathbf{x})\mathbf{H} + \boldsymbol{\rho}(\mathbf{x},\mathbf{n},\mathbf{v}). \tag{2.11}$$

The equations in (2.9) can be used for computation, while equation (2.11) is only used in the error analysis. In the sequel, the superscript in the mass and stiffness matrices will be omitted.

Similarly, by using the following notation introduced in [41]:

$$\mathbf{u} = \begin{pmatrix} \mathbf{H} \\ \mathbf{n} \end{pmatrix} \in \mathbb{R}^{4N}, \quad \mathbf{w} = \begin{pmatrix} \mathbf{V} \\ \mathbf{z} \end{pmatrix} \in \mathbb{R}^{4N},$$

the evolving surface FEM in (2.5) for Willmore flow can be written into the following matrix-vector form:

$$\dot{\mathbf{x}} = \mathbf{v}, \tag{2.12a}$$

$$\mathbf{B}(\mathbf{x},\mathbf{n})\mathbf{v} = \mathbf{M}(\mathbf{x})\mathbf{V}, \tag{2.12b}$$

$$\mathbf{B}(\mathbf{x},\mathbf{n})^\top \boldsymbol{\kappa} + \mathbf{A}^{[3]}(\mathbf{x})\mathbf{v} = \mathbf{0}, \tag{2.12c}$$

$$\mathbf{M}^{[4]}(\mathbf{x})\dot{\mathbf{u}} - \mathbf{A}^{[4]}(\mathbf{x})\mathbf{w} = \mathbf{F}(\mathbf{x},\mathbf{u})\mathbf{w} + \mathbf{f}^{\mathrm{W}}(\mathbf{x},\mathbf{u},\mathbf{v}), \tag{2.12d}$$

$$\mathbf{M}^{[4]}(\mathbf{x})\mathbf{w} + \mathbf{A}^{[4]}(\mathbf{x})\mathbf{u} = \mathbf{g}(\mathbf{x},\mathbf{u}), \tag{2.13}$$

where $\mathbf{F}(\mathbf{x},\mathbf{u})\mathbf{w}$, $\mathbf{f}^{\mathrm{W}}(\mathbf{x},\mathbf{u},\mathbf{v})$ and $\mathbf{g}(\mathbf{x},\mathbf{u})$ are some nonlinear functions of $\mathbf{x}$ and $\mathbf{u}$ associated to the right-hand side of (2.5). Compared with the matrix-vector formulation in [41, equation (3.5)], the only difference in (2.12d)-(2.13) is an additional dependence on velocity of $\mathbf{f}^{\mathrm{W}}$. Similarly as [41], (2.13) is further modified as

$$\mathbf{M}^{[4]}(\mathbf{x})\mathbf{w} + \mathbf{A}^{[4]}(\mathbf{x})\mathbf{u} = \mathbf{g}(\mathbf{x},\mathbf{u}) + \boldsymbol{\vartheta}, \tag{2.12e}$$

with

$$\boldsymbol{\vartheta} = \mathbf{M}^{[4]}(\mathbf{x}^0)(\bar{\mathbf{w}}^*(0) - \bar{\mathbf{w}}(0)),$$

so that the initial value becomes $\mathbf{w}(0) = \bar{\mathbf{w}}^*(0)$, where $\bar{\mathbf{w}}(0)$ is the vector obtained from (2.13) at time $t = 0$, and $\bar{\mathbf{w}}^*(0)$ denotes the vector which consists of the values of the exact solution $w(0) = (V(0), z(0))^\top$ at the nodes.

2.4 Lifts

In order to compare the numerical solution defined on the approximate surface $\Gamma_h[\mathbf{x}]$ with the solution defined on the exact surface $\Gamma[X(\cdot,t)]$, we need to lift a function from $\Gamma_h[\mathbf{x}]$ to $\Gamma[X(\cdot,t)]$.

Let $\mathbf{x}^*(t)$ be the nodes on the exact surface $\Gamma[X(\cdot,t)]$ as the image of $\mathbf{x}^0$ under the flow map. From [42, Lemma 7.1] or [23, (2.15)-(2.16)] we know that, there exists a sufficiently small $h_0 > 0$ such that for $h \le h_0$ and $t \in [0,T]$, any point $x \in \Gamma_h[\mathbf{x}^*(t)]$ can be lifted to $\Gamma[X(\cdot,t)]$ as x^ℓ. This lift operator from $x \in \Gamma_h[\mathbf{x}^*(t)]$ to $x^\ell \in \Gamma[X(\cdot,t)]$ is one-to-one and onto. Correspondingly, any function w on $\Gamma_h[\mathbf{x}^*]$ can be lifted to a function w^ℓ on Γ, defined as follows:

$$w^\ell(x^\ell) = w(x) \quad \forall\, x \in \Gamma_h[\mathbf{x}^*(t)].$$

Moreover, there exists a constant $C > 0$ such that the following estimates hold uniformly for h and t,

$$\begin{aligned} C^{-1}\left\|\varphi_h\right\|_{L^2(\Gamma_h[\mathbf{x}^*])} &\le \left\|\varphi_h^\ell\right\|_{L^2(\Gamma[X])} \le C\left\|\varphi_h\right\|_{L^2(\Gamma_h[\mathbf{x}^*])} \\ C^{-1}\left\|\nabla_{\Gamma_h[\mathbf{x}^*]}\varphi_h\right\|_{L^2(\Gamma_h[\mathbf{x}^*])} &\le \left\|\nabla_{\Gamma[X]}\varphi_h^\ell\right\|_{L^2(\Gamma[X])} \le C\left\|\nabla_{\Gamma_h[\mathbf{x}^*]}\varphi_h\right\|_{L^2(\Gamma_h[\mathbf{x}^*])} \end{aligned} \tag{2.14}$$

for all $\varphi_h \in L^2(\Gamma_h[\mathbf{x}^*])$ and $\varphi_h \in H^1(\Gamma_h[\mathbf{x}^*])$. For any given finite element function $w_h \in S_h[\mathbf{x}]$ on the approximate surface $\Gamma_h[\mathbf{x}]$, we denote its nodal vector by $\mathbf{w}$, which collects all the values of w_h at the nodes of $\Gamma_h[\mathbf{x}]$. The finite element function on the interpolated surface $\Gamma_h[\mathbf{x}^*]$ with the same nodal vector $\mathbf{w}$ is denoted by $\hat{w}_h$. The function $\hat{w}_h$ can be further lifted to $\Gamma[X]$ as $(\hat{w}_h)^\ell$. The lift from $S_h[\mathbf{x}]$ to $\Gamma[X]$ is denoted by $w_h^L = (\hat{w}_h)^\ell$.

2.5 Convergence of the method

The main theoretical results in this article are the following two theorems.

Theorem 2.1 *Suppose that the exact solution (X, v, κ, n, H) of the mean curvature flow (1.9) is sufficiently smooth for $t \in [0,T]$, and the flow map $X(\cdot,t) : \Gamma^0 \to \Gamma(t)$ is a diffeomorphism for $t \in [0,T]$. Then there exists a constant $h_0 > 0$ such that for all initial triangular partition with mesh size $h \le h_0$, the solutions to the evolving surface FEM in (2.2) with finite elements degree $k \geqslant 2$ satisfy the following error bounds,*

$$\begin{aligned} &\|X_h^\ell(\cdot,t) - X(\cdot,t)\|_{H^1(\Gamma^0)^3} \le Ch^k, && \|v_h^L(\cdot,t) - v(\cdot,t)\|_{H^1(\Gamma(t))^3} \le Ch^k, \\ &\|H_h^L(\cdot,t) - H(\cdot,t)\|_{H^1(\Gamma(t))} \le Ch^k, && \|n_h^L(\cdot,t) - n(\cdot,t)\|_{H^1(\Gamma(t))^3} \le Ch^k, \end{aligned}$$

where the constant C is independent of h and $t \in [0,T]$, but may depend on T.

Sufficient regularity assumptions are the following: we assume with bounds that are uniform in time, $X(\cdot,t) \in H^{k+1}(\Gamma^0)$, $v(\cdot,t) \in H^{k+1}(\Gamma(X(\cdot,t)))^3$ and for $u = (n, H)$, we require $u(\cdot,t), \partial^\bullet u(\cdot,t) \in W^{k+1,\infty}(\Gamma(X(\cdot,t)))^4$.

Theorem 2.2 *Suppose that the exact solution $(X, v, \kappa, V, H, n, z)$ of the Willmore flow (1.11) is sufficiently smooth for $t \in [0,T]$, and the flow map $X(\cdot,t) : \Gamma^0 \to \Gamma(t)$ is a diffeomorphism for $t \in [0,T]$. Then there exists a constant $h_0 > 0$ such that for all initial triangular partition with mesh size $h \le h_0$, the* *solutions to the modified evolving surface FEM in (2.12) with finite elements degree $k \geqslant 2$ satisfy the following error bounds,*

$$
\begin{aligned}
&\|X_h^\ell(\cdot,t) - X(\cdot,t)\|_{H^1(\Gamma^0)^3} \le Ch^k, \quad &&\|v_h^L(\cdot,t) - v(\cdot,t)\|_{H^1(\Gamma(t))^3} \le Ch^k,\\
&\|V_h^L(\cdot,t) - V(\cdot,t)\|_{H^1(\Gamma(t))} \le Ch^k, \quad &&\|H_h^L(\cdot,t) - H(\cdot,t)\|_{H^1(\Gamma(t))} \le Ch^k,\\
&\|n_h^L(\cdot,t) - n(\cdot,t)\|_{H^1(\Gamma(t))^3} \le Ch^k, \quad &&\|z_h^L(\cdot,t) - z(\cdot,t)\|_{H^1(\Gamma(t))^3} \le Ch^k,
\end{aligned}
$$

where the constant C is independent of h and $t \in [0,T]$, but may depend on T.

Sufficient regularity assumptions are the following: we assume, with bounds that are uniform in time, $X(\cdot,t) \in H^{k+1}(\Gamma^0)$, $v(\cdot,t) \in H^{k+1}(\Gamma(X(\cdot,t)))^3$ and for $u = (n,H)$, we have $u(\cdot,t), \partial^\bullet u(\cdot,t), \partial^{(2)} u \in W^{k+1,\infty}(\Gamma(X(\cdot,t)))^4$ for $w = (V,z)$, we have $w, \partial^\bullet w \in W^{k+1,\infty}(\Gamma(X(\cdot,t)))^4$.

The rest of this article is devoted to the proof of Theorems 2.1 and 2.2.

3 Proof of Theorem 2.1

3.1 Error equations and defects

Let $X_h^*(\cdot,t)$ be the Lagrange interpolation of $X(\cdot,t)$ onto the approximate initial surface $\Gamma_h[\mathbf{x}^0]$, and let $\mathbf{x}^*(t)$ be the nodal vector associated to the finite element function $X_h^*(\cdot,t)$, i.e., the vector which collects the values of $X_h^*(\cdot,t)$ at the nodes on $\Gamma_h[\mathbf{x}^0]$. Then $\Gamma_h[\mathbf{x}^*]$ is the interpolated surface which interpolates the exact surface $\Gamma[X(\cdot,t)]$ at the nodes. Let $\boldsymbol{\kappa}^*$ be the nodal vector associated to the Lagrange interpolation $\kappa_h^* \in S_h[\mathbf{x}^*]$ of the exact solution κ on the surface $\Gamma[X(\cdot,t)]$.

Let $u_h^* \in S_h[\mathbf{x}^*]^4$ and $v_h^* \in S_h[\mathbf{x}^*]^3$ be the Ritz projections of u and v, respectively, defined by

$$
\begin{aligned}
&\int_{\Gamma_h[\mathbf{x}^*]} \nabla_{\Gamma_h[\mathbf{x}^*]} u_h^* \cdot \nabla_{\Gamma_h[\mathbf{x}^*]} \varphi_h + \int_{\Gamma_h[\mathbf{x}^*]} u_h^* \cdot \varphi_h \\
&\qquad = \int_{\Gamma[X]} \nabla_{\Gamma[X]} u \cdot \nabla_{\Gamma[X]} \varphi_h^\ell + \int_{\Gamma[X]} u \cdot \varphi_h^\ell, \qquad (3.1)\\
&\int_{\Gamma_h[\mathbf{x}^*]} \nabla_{\Gamma_h[\mathbf{x}^*]} v_h^* \cdot \nabla_{\Gamma_h[\mathbf{x}^*]} \psi_h + \int_{\Gamma_h[\mathbf{x}^*]} v_h^* \cdot \psi_h \\
&\qquad = \int_{\Gamma[X]} \nabla_{\Gamma[X]} v \cdot \nabla_{\Gamma[X]} \psi_h^\ell + \int_{\Gamma[X]} v \cdot \psi_h^\ell, \qquad (3.2)
\end{aligned}
$$

for any $\varphi_h \in S_h[\mathbf{x}^*]^4$ and $\psi_h \in S_h[\mathbf{x}^*]^3$, and let $\mathbf{u}^*$ and $\mathbf{v}^*$ be the nodal vectors associated to the finite element functions u_h^* and v_h^*. It is known that the Ritz projection has the same order of accuracy as the interpolation, but has an advantage for error analysis by cancelling a critical term in the defects; see [39, 40].

Theorem 3.1 ([39, Theorem 6.3]) *If $u \in H^{k+1}(\Gamma(t))^m$ for $t \in [0,T]$, with $m \geqslant 1$, then there exists a sufficiently small $h_0 > 0$ such that for all $h \leq h_0$ the following estimate holds:*

$$\big\|u_h^{*,\ell} - u\big\|_{L^2(\Gamma(t))} + h\big\|u_h^{*,\ell} - u\big\|_{H^1(\Gamma(t))} \leq Ch^{k+1}\|u\|_{H^{k+1}(\Gamma(t))}, \tag{3.3}$$

where $u_h^{*,\ell}$ is the lift of u_h^* onto the exact surface $\Gamma(t) = \Gamma[(X(\cdot,t)]$.

Remark 3.1 The maximum-norm error bound of Ritz projection can be obtained by using Theorem 3.1 and an inverse inequality as follows. Combining (3.3) and the interpolation error bound in [23, Proposition 2.7] by the triangle inequality, we obtain

$$\|u_h^{*,\ell} - (I_h u)^\ell\|_{L^2(\Gamma(t))} \leq Ch^{k+1},$$

where $I_h : C(\Gamma[X(\cdot,t)]) \to \Gamma_h[\mathbf{x}^*]$ denotes the Lagrange interpolation operator (the pullback of $I_h u$ from a curved triangle on $\Gamma_h[\mathbf{x}^*]$ to the reference triangle is a polynomial of degree k). By using the equivalence relation in (2.14), we obtain

$$\|u_h^* - I_h u\|_{L^2(\Gamma_h[\mathbf{x}^*])} \leq Ch^{k+1}.$$

Applying the inverse inequality yields

$$\|u_h^* - I_h u\|_{W_h^{k,\infty}(\Gamma_h[\mathbf{x}^*])} \leq C, \tag{3.4}$$

which leads to the boundedness of $\|u_h^*\|_{W_h^{k,\infty}(\Gamma_h[\mathbf{x}^*])}$. By using the inverse inequality and triangle inequality, one can derive the following L^∞ bound of the Ritz projection error:

$$\begin{aligned}\|u_h^{*,\ell} - u\|_{L^\infty(\Gamma(t))} &\leq Ch^{-1}\|u_h^{*,\ell} - (I_h u)^\ell\|_{L^2(\Gamma(t))} + \|u - (I_h u)^\ell\|_{L^\infty(\Gamma(t))}\\ &\leq Ch^k. \end{aligned} \tag{3.5}$$

□

The defects are defined by plugging the functions X_h^*, v_h^*, κ_h^* and u_h^* into (2.2). In particular, we define the defects $d_v \in S_h[\mathbf{x}^*]$, $d_\kappa \in S_h[\mathbf{x}^*]^3$ and $d_u \in S_h[\mathbf{x}^*]^4$ as the finite element functions which satisfy the following relations:

$$\int_{\Gamma_h[\mathbf{x}^*]} (v_h^* \cdot n_h^*)\chi_\kappa = -\int_{\Gamma_h[\mathbf{x}^*]} H_h^*\chi_\kappa + \int_{\Gamma_h[\mathbf{x}^*]} d_v\chi_\kappa, \tag{3.6}$$

$$\int_{\Gamma_h[\mathbf{x}^*]} \kappa_h^* n_h^* \cdot \chi_v + \int_{\Gamma_h[\mathbf{x}^*]} \nabla_{\Gamma_h[\mathbf{x}^*]} v_h^* \cdot \nabla_{\Gamma_h[\mathbf{x}^*]}\chi_v = \int_{\Gamma_h[\mathbf{x}^*]} d_\kappa\chi_v, \tag{3.7}$$

and

$$\begin{aligned}&\int_{\Gamma_h[\mathbf{x}^*]} \partial_{t,h}^\bullet u_h^* \cdot \chi_u + \int_{\Gamma_h[\mathbf{x}^*]} \nabla_{\Gamma_h[\mathbf{x}^*]} u_h^* \cdot \nabla_{\Gamma_h[\mathbf{x}^*]}\chi_u\\ &= \int_{\Gamma_h[\mathbf{x}^*]} \left(|\nabla_{\Gamma_h[\mathbf{x}^*]} n_h^*|^2 u_h^* + v_h^* \cdot \nabla_{\Gamma_h[\mathbf{x}^*]} u_h^*\right)\chi_u + \int_{\Gamma_h[\mathbf{x}^*]} d_u\chi_u. \end{aligned} \tag{3.8}$$

The matrix-vector formulation of (3.6)–(3.8) can be written as

$$\dot{\mathbf{x}}^* = \mathbf{v}^*, \tag{3.9a}$$
$$\mathbf{B}(\mathbf{x}^*,\mathbf{n}^*)\mathbf{v}^* = -\mathbf{M}(\mathbf{x}^*)\mathbf{H}^* + \mathbf{M}(\mathbf{x}^*)\mathbf{d}_{\mathbf{v}}, \tag{3.9b}$$
$$\mathbf{B}(\mathbf{x}^*,\mathbf{n}^*)^\top \boldsymbol{\kappa}^* + \mathbf{A}(\mathbf{x}^*)\mathbf{v}^* = \mathbf{M}(\mathbf{x}^*)\mathbf{d}_{\boldsymbol{\kappa}}, \tag{3.9c}$$
$$\mathbf{M}\left(\mathbf{x}^*\right)\dot{\mathbf{u}}^* + \mathbf{A}\left(\mathbf{x}^*\right)\mathbf{u}^* = \mathbf{f}\left(\mathbf{x}^*,\mathbf{u}^*,\mathbf{v}^*\right) + \mathbf{M}\left(\mathbf{x}^*\right)\mathbf{d}_{\mathbf{u}}. \tag{3.9d}$$

Then, subtracting (3.9) from (2.9), we obtain the following equations for the error functions $\mathbf{e}_{\mathbf{x}} = \mathbf{x} - \mathbf{x}^*$, $\mathbf{e}_{\mathbf{v}} = \mathbf{v} - \mathbf{v}^*$, $\mathbf{e}_{\boldsymbol{\kappa}} = \boldsymbol{\kappa} - \boldsymbol{\kappa}^*$ and $\mathbf{e}_{\mathbf{u}} = \mathbf{u} - \mathbf{u}^*$:

$$\dot{\mathbf{e}}_{\mathbf{x}} = \mathbf{e}_{\mathbf{v}}, \tag{3.10a}$$
$$\begin{aligned}\mathbf{B}(\mathbf{x}^*,\mathbf{n}^*)\mathbf{e}_{\mathbf{v}} = {} & (\mathbf{B}(\mathbf{x}^*,\mathbf{n}^*) - \mathbf{B}(\mathbf{x},\mathbf{n}))\mathbf{v} \\ & - \mathbf{M}(\mathbf{x}^*)\mathbf{e}_{\mathbf{H}} + (\mathbf{M}(\mathbf{x}^*) - \mathbf{M}(\mathbf{x}))\mathbf{H} - \mathbf{M}(\mathbf{x}^*)\mathbf{d}_{\mathbf{v}},\end{aligned} \tag{3.10b}$$

$$\begin{aligned}\mathbf{B}(\mathbf{x}^*,\mathbf{n}^*)^\top \mathbf{e}_{\boldsymbol{\kappa}} + \mathbf{A}(\mathbf{x}^*)\mathbf{e}_{\mathbf{v}} = {} & (\mathbf{B}(\mathbf{x}^*,\mathbf{n}^*)^\top - \mathbf{B}(\mathbf{x},\mathbf{n})^\top)\boldsymbol{\kappa} \\ & + (\mathbf{A}(\mathbf{x}^*) - \mathbf{A}(\mathbf{x}))\mathbf{v} - \mathbf{M}(\mathbf{x}^*)\mathbf{d}_{\boldsymbol{\kappa}},\end{aligned} \tag{3.10c}$$
$$\begin{aligned}\mathbf{M}(\mathbf{x})\dot{\mathbf{e}}_{\mathbf{u}} + \mathbf{A}(\mathbf{x})\mathbf{e}_{\mathbf{u}} = {} & -\left(\mathbf{M}(\mathbf{x}) - \mathbf{M}\left(\mathbf{x}^*\right)\right)\dot{\mathbf{u}}^* - \left(\mathbf{A}(\mathbf{x}) - \mathbf{A}\left(\mathbf{x}^*\right)\right)\mathbf{u}^* \\ & + \left(\mathbf{f}(\mathbf{x},\mathbf{u},\mathbf{v}) - \mathbf{f}\left(\mathbf{x}^*,\mathbf{u}^*,\mathbf{v}^*\right)\right) - \mathbf{M}\left(\mathbf{x}^*\right)\mathbf{d}_{\mathbf{u}}.\end{aligned} \tag{3.10d}$$

Similarly, the error equation corresponding to (2.11) is given by

$$\begin{aligned}\mathbf{D}(\mathbf{x}^*,\mathbf{n}^*)\mathbf{e}_{\mathbf{v}} = {} & (\mathbf{D}(\mathbf{x}^*,\mathbf{n}^*) - \mathbf{D}(\mathbf{x},\mathbf{n}))\mathbf{v} - \mathbf{A}(\mathbf{x}^*)\mathbf{e}_{\mathbf{H}} + (\mathbf{A}(\mathbf{x}^*) - \mathbf{A}(\mathbf{x}))\mathbf{H} \\ & - \big(\boldsymbol{\rho}(\mathbf{x}^*,\mathbf{n}^*,\mathbf{v}^*) - \boldsymbol{\rho}(\mathbf{x},\mathbf{n},\mathbf{v}) + \mathbf{M}(\mathbf{x}^*)\widetilde{\mathbf{d}}_{\mathbf{v}}\big),\end{aligned} \tag{3.11}$$

where $\widetilde{\mathbf{d}}_{\mathbf{v}}$ is the nodal vector associated to the finite element function $\tilde{d}_v \in S_h[\mathbf{x}^*]$, which is defined by substituting v_h^*, n_h^* and $\mathbf{x}^*$ into (2.4), i.e.,

$$\begin{aligned}&\int_{\Gamma_h[\mathbf{x}^*]} \nabla_{\Gamma_h[\mathbf{x}^*]}(v_h^* \cdot n_h^*) \cdot \nabla_{\Gamma_h[\mathbf{x}^*]}\chi_\kappa \\ &= \int_{\Gamma_h[\mathbf{x}^*]} \nabla_{\Gamma_h[\mathbf{x}^*]}[v_h^* \cdot n_h^* - P_{\Gamma_h[\mathbf{x}^*]}(v_h^* \cdot n_h^*)] \cdot \nabla_{\Gamma_h[\mathbf{x}^*]}\chi_\kappa \\ &\quad - \int_{\Gamma_h[\mathbf{x}^*]} \nabla_{\Gamma_h[\mathbf{x}^*]}H_h^* \cdot \nabla_{\Gamma_h[\mathbf{x}^*]}\chi_\kappa + \int_{\Gamma_h[\mathbf{x}^*]} \tilde{d}_v\chi_\kappa.\end{aligned} \tag{3.12}$$

3.2 Estimates for the bilinear forms

With the help of the mass matrix and stiffness matrix defined in Section 2.3, we can represent the L^2 and H^1 norms of a scalar function $H_h \in S_h[\mathbf{x}]$ by vector norms of the corresponding nodal vector $\mathbf{H}$, i.e.,

$$\begin{aligned}\|\mathbf{H}\|^2_{\mathbf{M}(\mathbf{x})} &= \mathbf{H}^\top\mathbf{M}(\mathbf{x})\mathbf{H} = \|H_h\|^2_{L^2(\Gamma_h[\mathbf{x}])}\,, \\ \|\mathbf{H}\|^2_{\mathbf{A}(\mathbf{x})} &= \mathbf{H}^\top\mathbf{A}(\mathbf{x})\mathbf{H} = \left\|\nabla_{\Gamma_h[\mathbf{x}]}H_h\right\|^2_{L^2(\Gamma_h[\mathbf{x}])}\,, \\ \|\mathbf{H}\|^2_{\mathbf{K}(\mathbf{x})} &= \mathbf{H}^\top\mathbf{K}(\mathbf{x})\mathbf{H} = \|H_h\|^2_{H^1(\Gamma_h[\mathbf{x}])}\,,\end{aligned}$$

where $\mathbf{K}(\mathbf{x}) = \mathbf{M}(\mathbf{x}) + \mathbf{A}(\mathbf{x})$. To measure the defect function $\tilde{d}_v \in S_h[\mathbf{x}^*]$, we need to use the discrete H^{-1} norm defined as follows (cf. [42]):

$$\|\tilde{d}_v\|_{H_h^{-1}(\Gamma_h[\mathbf{x}^*])} = \sup_{0\neq\varphi_h\in S_h[\mathbf{x}^*]} \frac{\int_{\Gamma_h[\mathbf{x}^*]} \tilde{d}_v \cdot \varphi_h}{\|\varphi_h\|_{H^1(\Gamma[\mathbf{x}^*])}},$$

which can also be expressed in terms of the nodal vector $\widetilde{\mathbf{d}}_{\mathbf{v}}$ as

$$\|\widetilde{\mathbf{d}}_{\mathbf{v}}\|_{\star,\mathbf{x}^*} := \widetilde{\mathbf{d}}_{\mathbf{v}}^{\top} \mathbf{M}(\mathbf{x}^*)\mathbf{K}(\mathbf{x}^*)^{-1}\mathbf{M}(\mathbf{x}^*)\widetilde{\mathbf{d}}_{\mathbf{v}}.$$

In previous articles [40, 42], some technical results concerning the norm equivalence of $\|\cdot\|_{\mathbf{M}}$ and $\|\cdot\|_{\mathbf{A}}$ on different finite element surfaces were discussed. In this section, we extend those results to two matrices depending on the normal vectors, i.e, $\mathbf{B}(\mathbf{x},\mathbf{n})$ and $\mathbf{D}(\mathbf{x},\mathbf{n})$.

For $\mathbf{e}_{\mathbf{x}} = \mathbf{x} - \mathbf{x}^*$, we consider the following intermediate surfaces between $\Gamma_h[\mathbf{x}^*]$ and $\Gamma_h[\mathbf{x}]$:

$$\Gamma_h^\theta = \Gamma_h[\mathbf{x}^* + \theta\mathbf{e}_{\mathbf{x}}], \quad \theta \in [0,1]. \tag{3.13}$$

The finite element functions on the intermediate surface Γ_h^θ with nodal vectors $\mathbf{e}_{\mathbf{x}}, \mathbf{e}_{\mathbf{n}}, \mathbf{z}$ and $\mathbf{w}$ are denoted by e_x^θ, e_n^θ, z_h^θ and w_h^θ, respectively. Let $n_h^{*,\theta}$ be the finite element function on Γ_h^θ associated to the nodal vector $\mathbf{n}^*$, and define

$$n_h^\theta = n_h^{*,\theta} + \theta e_n^\theta \in S_h[\mathbf{x}^* + \theta\mathbf{e}_{\mathbf{x}}],$$

which connects the Ritz projection $n_h^0 = n_h^* \in S_h[\mathbf{x}^*]^3$ to the numerical solution $n_h^1 = n_h \in S_h[\mathbf{x}]^3$. Similarly, we define $v_h^\theta = v_h^{*,\theta} + \theta e_v^\theta$.

Lemma 3.1 *The following identities hold:*

$$(\mathbf{M}(\mathbf{x})-\mathbf{M}(\mathbf{x}^*))\mathbf{z}\cdot\mathbf{w}=\int_0^1\int_{\Gamma_h^\theta} w_h^\theta(\nabla_{\Gamma_h^\theta}\cdot e_x^\theta)z_h^\theta, \tag{3.14}$$

$$(\mathbf{A}(\mathbf{x})-\mathbf{A}(\mathbf{x}^*))\mathbf{z}\cdot\mathbf{w}=\int_0^1\int_{\Gamma_h^\theta} \nabla_{\Gamma_h^\theta}w_h^\theta\cdot\left(D_{\Gamma_h^\theta}e_x^\theta\right)\nabla_{\Gamma_h^\theta}z_h^\theta, \tag{3.15}$$

$$(\mathbf{B}(\mathbf{x},\mathbf{n})-\mathbf{B}(\mathbf{x}^*,\mathbf{n}^*))\mathbf{z}\cdot\mathbf{w}=\int_0^1\int_{\Gamma_h^\theta} z_h^\theta\cdot e_n^\theta w_h^\theta+z_h^\theta\cdot(n_h^{*,\theta}+\theta e_n^\theta)w_h^\theta\nabla_{\Gamma_h^\theta}\cdot e_x^\theta, \tag{3.16}$$

$$\begin{aligned}&(\mathbf{D}(\mathbf{x},\mathbf{n})-\mathbf{D}(\mathbf{x}^*,\mathbf{n}^*))\mathbf{z}\cdot\mathbf{w}\\ &=\int_0^1\int_{\Gamma_h^\theta}\nabla_{\Gamma_h^\theta}(z_h^\theta\cdot e_n^\theta)\cdot\nabla_{\Gamma_h^\theta}w_h^\theta+D_{\Gamma_h^\theta}e_x^\theta\nabla_{\Gamma_h^\theta}(z_h^\theta\cdot n_h^\theta)\cdot\nabla_{\Gamma_h^\theta}w_h^\theta,\end{aligned} \tag{3.17}$$

$$\begin{aligned}&(\boldsymbol{\rho}(\mathbf{x},\mathbf{n},\mathbf{v})-\boldsymbol{\rho}(\mathbf{x}^*,\mathbf{n}^*,\mathbf{v}^*))\cdot\mathbf{w}\\ &=\int_0^1\int_{\Gamma_h^\theta}\nabla_{\Gamma_h^\theta}[e_v^\theta\cdot n_h^\theta-P_{\Gamma_h^\theta}(e_v^\theta\cdot n_h^\theta)]\cdot\nabla_{\Gamma_h^\theta}w_h^\theta\\ &\quad+\int_{\Gamma_h^\theta}\nabla_{\Gamma_h^\theta}[v_h^\theta\cdot e_n^\theta-P_{\Gamma_h^\theta}(v_h^\theta\cdot e_n^\theta)]\cdot\nabla_{\Gamma_h^\theta}w_h^\theta\\ &\quad-\int_{\Gamma_h^\theta}\nabla_{\Gamma_h^\theta}P_{\Gamma_h^\theta}[(v_h^\theta\cdot n_h^\theta-P_{\Gamma_h^\theta}(v_h^\theta\cdot n_h^\theta))(\nabla_{\Gamma_h^\theta}\cdot e_x^\theta)]\cdot\nabla_{\Gamma_h^\theta}w_h^\theta\\ &\quad+\int_{\Gamma_h^\theta}D_{\Gamma_h^\theta}e_x^\theta\nabla_{\Gamma_h^\theta}[v_h^\theta\cdot n_h^\theta-P_{\Gamma_h^\theta}(v_h^\theta\cdot n_h^\theta)]\cdot\nabla_{\Gamma_h^\theta}w_h^\theta,\end{aligned} \tag{3.18}$$

where $D_{\Gamma_h^\theta}e_x^\theta=\operatorname{tr}(E^\theta)I_3-\left(E^\theta+(E^\theta)^\top\right)$ *and* $E^\theta=\nabla_{\Gamma_h^\theta}e_x^\theta\in\mathbb{R}^{3\times3}$.

Proof Identities (3.14)–(3.15) have been proved in [40, Lemma 7.1]. Hence, we focus on the proof of (3.16)–(3.17). By using the intermediate surfaces Γ_h^θ defined in (3.13), we have

$$(\mathbf{B}(\mathbf{x},\mathbf{n})-\mathbf{B}(\mathbf{x}^*,\mathbf{n}^*))\mathbf{z}\cdot\mathbf{w}=\int_{\Gamma_h^\theta}(z_h^\theta\cdot n_h^\theta)w_h^\theta\Big|_{\theta=0}^{\theta=1}=\int_0^1\frac{\mathrm{d}}{\mathrm{d}\theta}\int_{\Gamma_h^\theta}(z_h^\theta\cdot n_h^\theta)w_h^\theta\mathrm{d}\theta.$$

By using the Leibniz rule of differentiation, see [32, Lemma 3.1] and the transport property of w_h^θ, z_h^θ and $n_h^{*,\theta}$, we obtain

$$\begin{aligned}\frac{\mathrm{d}}{\mathrm{d}\theta}\int_{\Gamma_h^\theta}(z_h^\theta\cdot n_h^\theta)w_h^\theta&=\int_{\Gamma_h^\theta}(z_h^\theta\cdot n_h^\theta)\partial_\theta^\bullet w_h^\theta+\int_{\Gamma_h^\theta}\partial_\theta^\bullet(z_h^\theta\cdot n_h^\theta)w_h^\theta\\ &\quad+\int_{\Gamma_h^\theta}\left[(z_h^\theta\cdot n_h^\theta)w_h^\theta\right]\nabla_{\Gamma_h^\theta}\cdot e_x^\theta\\ &=\int_{\Gamma_h^\theta}z_h^\theta\cdot e_n^\theta w_h^\theta+\int_{\Gamma_h^\theta}z_h^\theta\cdot(n_h^{*,\theta}+\theta e_n^\theta)w_h^\theta\nabla_{\Gamma_h^\theta}\cdot e_x^\theta.\end{aligned}$$

This proves (3.16). Similarly,

$$(\mathbf{D}(\mathbf{x},\mathbf{n})-\mathbf{D}(\mathbf{x}^*,\mathbf{n}^*))\mathbf{z}\cdot\mathbf{w}=\int_{\Gamma_h^\theta}\nabla_{\Gamma_h^\theta}(z_h^\theta\cdot n_h^\theta)\nabla_{\Gamma_h^\theta}w_h^\theta\Big|_{\theta=0}^{\theta=1}$$
$$=\int_0^1\frac{\mathrm{d}}{\mathrm{d}\theta}\int_{\Gamma_h^\theta}\nabla_{\Gamma_h^\theta}(z_h^\theta\cdot n_h^\theta)\cdot\nabla_{\Gamma_h^\theta}w_h^\theta\mathrm{d}\theta,$$

where the integrand satisfies

$$\begin{aligned}&\frac{\mathrm{d}}{\mathrm{d}\theta}\int_{\Gamma_h^\theta}\nabla_{\Gamma_h^\theta}(z_h^\theta\cdot n_h^\theta)\cdot\nabla_{\Gamma_h^\theta}w_h^\theta\\&=\int_{\Gamma_h^\theta}\partial_\theta^\bullet\nabla_{\Gamma_h^\theta}(z_h^\theta\cdot n_h^\theta)\cdot\nabla_{\Gamma_h^\theta}w_h^\theta+\nabla_{\Gamma_h^\theta}(z_h^\theta\cdot n_h^\theta)\cdot\partial_\theta^\bullet\nabla_{\Gamma_h^\theta}w_h^\theta\\&\quad+\nabla_{\Gamma_h^\theta}(z_h^\theta\cdot n_h^\theta)\cdot\nabla_{\Gamma_h^\theta}w_h^\theta\nabla_{\Gamma_h^\theta}\cdot e_x^\theta.\end{aligned}$$

To interchange the material derivative and the surface gradient, we use the following formula, see [32, Lemma 2.6]:

$$\begin{aligned}&\partial_\theta^\bullet\nabla_{\Gamma_h^\theta}(z_h^\theta\cdot n_h^\theta)\\&=\nabla_{\Gamma_h^\theta}\partial_\theta^\bullet(z_h^\theta\cdot n_h^\theta)-(\nabla_{\Gamma_h^\theta}v_{\Gamma_h^\theta}-n_{\Gamma_h^\theta}(n_{\Gamma_h^\theta})^\top(\nabla_{\Gamma_h^\theta}v_{\Gamma_h^\theta})^\top)\nabla_{\Gamma_h^\theta}(z_h^\theta\cdot n_h^\theta),\end{aligned}\tag{3.19}$$

where $v_{\Gamma_h^\theta}$ and $n_{\Gamma_h^\theta}$ denote the velocity (as θ changes) and normal vector of the intermediate surface Γ_h^θ. Since Γ_h^θ moves with velocity e_x^θ as θ increases, it follows that $v_{\Gamma_h^\theta}=e_x^\theta$ and therefore

$$\begin{aligned}&\frac{\mathrm{d}}{\mathrm{d}\theta}\int_{\Gamma_h^\theta}\nabla_{\Gamma_h^\theta}(z_h^\theta\cdot n_h^\theta)\cdot\nabla_{\Gamma_h^\theta}w_h^\theta\\&=\int_{\Gamma_h^\theta}\nabla_{\Gamma_h^\theta}(z_h^\theta\cdot e_n^\theta)\cdot\nabla_{\Gamma_h^\theta}w_h^\theta+D_{\Gamma_h^\theta}e_x^\theta\nabla_{\Gamma_h^\theta}(z_h^\theta\cdot n_h^\theta)\cdot\nabla_{\Gamma_h^\theta}w_h^\theta.\end{aligned}$$

This proves (3.17).

The proof of (3.18) is similar. By using (3.17), we have

$$\begin{aligned}&(\boldsymbol{\rho}(\mathbf{x},\mathbf{n},\mathbf{v})-\boldsymbol{\rho}(\mathbf{x}^*,\mathbf{n}^*,\mathbf{v}^*))\cdot\mathbf{w}\\&=\int_0^1\frac{\mathrm{d}}{\mathrm{d}\theta}\int_{\Gamma_h^\theta}\nabla_{\Gamma_h^\theta}[v_h^\theta\cdot n_h^\theta-P_{\Gamma_h^\theta}(v_h^\theta\cdot n_h^\theta)]\cdot\nabla_{\Gamma_h^\theta}w_h^\theta\\&=\int_0^1\int_{\Gamma_h^\theta}\nabla_{\Gamma_h^\theta}[e_v^\theta\cdot n_h^\theta-P_{\Gamma_h^\theta}(e_v^\theta\cdot n_h^\theta)]\cdot\nabla_{\Gamma_h^\theta}w_h^\theta\\&\quad+\int_{\Gamma_h^\theta}\nabla_{\Gamma_h^\theta}[v_h^\theta\cdot e_n^\theta-P_{\Gamma_h^\theta}(v_h^\theta\cdot e_n^\theta)]\cdot\nabla_{\Gamma_h^\theta}w_h^\theta\\&\quad+\int_{\Gamma_h^\theta}\nabla_{\Gamma_h^\theta}[P_{\Gamma_h^\theta}\partial_\theta^\bullet(v_h^\theta\cdot n_h^\theta)-\partial_\theta^\bullet P_{\Gamma_h^\theta}(v_h^\theta\cdot n_h^\theta)]\cdot\nabla_{\Gamma_h^\theta}w_h^\theta\\&\quad+\int_{\Gamma_h^\theta}D_{\Gamma_h^\theta}e_x^\theta\nabla_{\Gamma_h^\theta}[v_h^\theta\cdot n_h^\theta-P_{\Gamma_h^\theta}(v_h^\theta\cdot n_h^\theta)]\cdot\nabla_{\Gamma_h^\theta}w_h^\theta,\end{aligned}\tag{3.20}$$

where the term $\partial_\theta^\bullet P_{\Gamma_h^\theta}(v_h^\theta \cdot n_h^\theta)$ can be more explicitly expressed by differentiating the following identity for the L^2 projection:

$$\int_{\Gamma_h^\theta} P_{\Gamma_h^\theta} z^\theta w_h^\theta = \int_{\Gamma_h^\theta} z^\theta w_h^\theta,$$

which implies that

$$\int_{\Gamma_h^\theta} \partial_\theta^\bullet (P_{\Gamma_h^\theta} z^\theta)\, w_h^\theta = \int_{\Gamma_h^\theta} \partial_\theta^\bullet z^\theta\, w_h^\theta + \int_{\Gamma_h^\theta} (z^\theta - P_{\Gamma_h^\theta} z^\theta) w_h^\theta (\nabla_{\Gamma_h^\theta} \cdot e_x^\theta),$$

and therefore

$$\partial_\theta^\bullet (P_{\Gamma_h^\theta} z^\theta) = P_{\Gamma_h^\theta} \partial_\theta^\bullet z^\theta + P_{\Gamma_h^\theta} [(z^\theta - P_{\Gamma_h^\theta} z^\theta)(\nabla_{\Gamma_h^\theta} \cdot e_x^\theta)]. \tag{3.21}$$

Substituting (3.21) into (3.20) yields the desired result in (3.18). □

The following result has been established in [42, Lemma 4.3] and [40, Lemma 7.2].

Lemma 3.2 *Suppose that* $\|\nabla_{\Gamma_h[\mathbf{x}^*]} e_x^0\|_{L^\infty(\Gamma_h[\mathbf{x}^*])} \le 1/2$, *then for* $0 \le \theta \le 1$ *and* $1 \le p \le \infty$, w_h^θ *on* Γ_h^θ *is bounded by*

$$\|w_h^\theta\|_{L^p(\Gamma_h^\theta)} \le c_p \|w_h^0\|_{L^p(\Gamma_h[\mathbf{x}^*])}, \tag{3.22}$$

$$\|\nabla_{\Gamma_h^\theta} w_h^\theta\|_{L^p(\Gamma_h^\theta)} \le c_p \|\nabla_{\Gamma_h[\mathbf{x}^*]} w_h^0\|_{L^p(\Gamma_h[\mathbf{x}^*])}, \tag{3.23}$$

where c_p *is a constant independent of* θ *and* h *and* $c_\infty = 2$.

Remark 3.2 If $\|\nabla_{\Gamma_h[\mathbf{x}^*]} e_x^0\|_{L^\infty(\Gamma_h[\mathbf{x}^*])} \le 1/4$, we have $\|\nabla_{\Gamma_h^\theta} e_x^\theta\|_{L^\infty(\Gamma_h^\theta)} \le 1/2$ for any $\theta \in [0,1]$, and

$$\begin{aligned} &\text{The norms } \|\cdot\|_{\mathbf{M}(\mathbf{x}^*+\theta\mathbf{e}_\mathbf{x})} \text{ are h-uniformly equivalent for } \theta \in [0,1], \\ &\text{The norms } \|\cdot\|_{\mathbf{A}(\mathbf{x}^*+\theta\mathbf{e}_\mathbf{x})} \text{ are h-uniformly equivalent for } \theta \in [0,1]. \end{aligned} \tag{3.24}$$

Then, by Lemma 3.1 and (3.24), we obtain

$$(\mathbf{M}(\mathbf{x}^*) - \mathbf{M}(\mathbf{x}))\mathbf{z} \cdot \mathbf{w} \le C \|\mathbf{w}\|_{\mathbf{M}(\mathbf{x}^*)} \|\mathbf{e}_\mathbf{x}\|_{\mathbf{A}(\mathbf{x}^*)} \|z_h^0\|_{L^\infty(\Gamma_h[\mathbf{x}^*])}, \tag{3.25}$$

$$(\mathbf{A}(\mathbf{x}^*) - \mathbf{A}(\mathbf{x}))\mathbf{z} \cdot \mathbf{w} \le C \|\mathbf{w}\|_{\mathbf{A}(\mathbf{x}^*)} \|\mathbf{e}_\mathbf{x}\|_{\mathbf{A}(\mathbf{x}^*)} \|\nabla_{\Gamma_h[\mathbf{x}^*]} z_h^0\|_{L^\infty(\Gamma_h[\mathbf{x}^*])}, \tag{3.26}$$

$$(\mathbf{A}(\mathbf{x}^*) - \mathbf{A}(\mathbf{x}))\mathbf{z} \cdot \mathbf{w} \le C \|e_x\|_{W^{1,\infty}(\Gamma_h[\mathbf{x}^*])} \|\mathbf{z}\|_{\mathbf{A}(\mathbf{x}^*)} \|\mathbf{w}\|_{\mathbf{A}(\mathbf{x}^*)}. \tag{3.27}$$

Remark 3.3 The equivalence relations (3.22)–(3.23) are not limited to the space of finite element functions. Given three nodal vectors $\mathbf{w} \in \mathbb{R}^N$ and $\mathbf{z}, \boldsymbol{\chi} \in \mathbb{R}^{3N}$, the associated finite element functions are denoted as $w_h^\theta \in S_h^\theta = S_h[\mathbf{x}^* + \theta \mathbf{e}_\mathbf{x}]$ and $z_h^\theta, \chi_h^\theta \in (S_h^\theta)^3$. Under the assumption of Remark 3.2, we have

$$\begin{aligned} &\|z_h^\theta \cdot \chi_h^\theta - w_h^\theta\|_{L^2(\Gamma_h^\theta)}^2 - \|z_h^0 \cdot \chi_h^0 - w_h^0\|_{L^2(\Gamma_h[\mathbf{x}^*])}^2 \\ &= \int_0^\theta \partial_\tau^\bullet \int_{\Gamma_h^\tau} (z_h^\tau \cdot u_h^\tau - w_h^\tau)^2 \mathrm{d}\tau \\ &= \int_0^\theta \int_{\Gamma_h^\tau} (z_h^\tau \cdot u_h^\tau - w_h^\tau)^2 \nabla_{\Gamma_h^\tau} \cdot e_x^\tau \mathrm{d}\tau \\ &\le C \int_0^\theta \|z_h^\tau \cdot u_h^\tau - w_h^\tau\|_{L^2(\Gamma_h^\tau)}^2. \end{aligned}$$

By Gronwall's inequality, we conclude that

$$\|z_h^\theta \cdot \chi_h^\theta - w_h^\theta\|^2_{L^2(\Gamma_h^\theta)} \le C\|z_h^0 \cdot \chi_h^0 - w_h^0\|^2_{L^2(\Gamma_h[\mathbf{x}^*])}. \tag{3.28}$$

An analogous inequality can also be obtained for the H^1 seminorm, i.e.,

$$\|\nabla_{\Gamma_h[\mathbf{x}]}(z_h^1 \cdot \chi_h^1 - w_h^1)\|^2_{L^2(\Gamma_h[\mathbf{x}])} \le C\|\nabla_{\Gamma_h[\mathbf{x}^*]}(z_h^0 \cdot \chi_h^0 - w_h^0)\|^2_{L^2(\Gamma_h[\mathbf{x}^*])}. \tag{3.29}$$

Furthermore, this equivalence also holds for the multiplication of more elements, such as

$$\|(z_h^1 \cdot \chi_h^1)w_h^1\|^2_{L^2(\Gamma_h[\mathbf{x}])} \le C\|(z_h^0 \cdot \chi_h^0)w_h^0\|^2_{L^2(\Gamma_h[\mathbf{x}^*])}.$$

By (3.16)–(3.17) and Lemma 3.2, we immediately obtain the following lemma.

Lemma 3.3 *Assume that the following two conditions hold:*

(A) $\|\nabla_{\Gamma_h[\mathbf{x}^*]} e_x^0\|_{L^\infty(\Gamma_h[\mathbf{x}^*])} \le 1/4$.
(B) z_h^0, $n_h^{*,0}$, e_n^0, $v_h^{*,0}$ *are bounded in* $W^{1,\infty}(\Gamma_h[\mathbf{x}^*])$ *(uniformly with respect to* h*).*

Then the following inequalities hold for $\mathbf{z} \in \mathbb{R}^{3N}$ *and* $\mathbf{w} \in \mathbb{R}^N$*:*

$$(\mathbf{B}(\mathbf{x}^*, \mathbf{n}^*) - \mathbf{B}(\mathbf{x}, \mathbf{n}))\mathbf{z} \cdot \mathbf{w} \le C(\|\mathbf{e_n}\|_{\mathbf{M}(\mathbf{x}^*)} + \|\mathbf{e_x}\|_{\mathbf{A}(\mathbf{x}^*)})\|\mathbf{w}\|_{\mathbf{M}(\mathbf{x}^*)}, \tag{3.30}$$

$$(\mathbf{D}(\mathbf{x}^*, \mathbf{n}^*) - \mathbf{D}(\mathbf{x}, \mathbf{n}))\mathbf{z} \cdot \mathbf{w} \le C\left(\|\mathbf{e_n}\|_{\mathbf{K}(\mathbf{x}^*)} + \|\mathbf{e_x}\|_{\mathbf{A}(\mathbf{x}^*)}\right)\|\mathbf{w}\|_{\mathbf{A}(\mathbf{x}^*)}, \tag{3.31}$$

$$\begin{aligned}&(\boldsymbol{\rho}(\mathbf{x}, \mathbf{n}, \mathbf{v}) - \boldsymbol{\rho}(\mathbf{x}^*, \mathbf{n}^*, \mathbf{v}^*)) \cdot \mathbf{w} \\ &\le C(h\|\mathbf{e_v}\|_{\mathbf{K}(\mathbf{x}^*)} + h\|\mathbf{e_n}\|_{\mathbf{K}(\mathbf{x}^*)} + \|\mathbf{e_x}\|_{\mathbf{A}(\mathbf{x}^*)})\|\mathbf{w}\|_{\mathbf{A}(\mathbf{x}^*)}.\end{aligned} \tag{3.32}$$

If Assumption (B) is changed to

(C) $\|n_h^{*,0}\|_{W^{1,\infty}(\Gamma[\mathbf{x}^*])}$ *has a upper bound independent of* h*, and there exists* $\alpha > 0$ *such that*

$$\max\{\|e_x^0\|_{W^{1,\infty}(\Gamma_h[\mathbf{x}^*])}, \|e_n^0\|_{W^{1,\infty}(\Gamma_h[\mathbf{x}^*])}\} \le h^\alpha,$$

then the following results hold:

$$(\mathbf{B}(\mathbf{x}^*, \mathbf{n}^*) - \mathbf{B}(\mathbf{x}, \mathbf{n}))\mathbf{z} \cdot \mathbf{w} \le Ch^\alpha\|\mathbf{z}\|_{\mathbf{M}(\mathbf{x}^*)}\|\mathbf{w}\|_{\mathbf{M}(\mathbf{x}^*)}, \tag{3.33}$$

$$(\mathbf{D}(\mathbf{x}^*, \mathbf{n}^*) - \mathbf{D}(\mathbf{x}, \mathbf{n}))\mathbf{z} \cdot \mathbf{w} \le Ch^\alpha\|\mathbf{z}\|_{\mathbf{K}(\mathbf{x}^*)}\|\mathbf{w}\|_{\mathbf{A}(\mathbf{x}^*)}. \tag{3.34}$$

Proof We first prove (3.33)-(3.34) under the assumptions (A) and (C). From (3.16) we see that

$$\begin{aligned}(\mathbf{B}(\mathbf{x}, \mathbf{n}) - \mathbf{B}(\mathbf{x}^*, \mathbf{n}^*))\mathbf{z} \cdot \mathbf{w} &= \int_0^1 \int_{\Gamma_h^\theta} z_h^\theta \cdot e_n^\theta w_h^\theta + z_h^\theta \cdot (n_h^{*,\theta} + \theta e_n^\theta) w_h^\theta \nabla_{\Gamma_h^\theta} \cdot e_x^\theta \\ &\le \|z_h^\theta\|_{L^2(\Gamma_h^\theta)}\|w_h^\theta\|_{L^2(\Gamma_h^\theta)}\|e_n^\theta\|_{L^\infty(\Gamma_h^\theta)} \\ &\quad + \|z_h^\theta\|_{L^2(\Gamma_h^\theta)}\|w_h^\theta\|_{L^2(\Gamma_h^\theta)}\|\nabla_{\Gamma_h^\theta} e_x^\theta\|_{L^\infty(\Gamma_h^\theta)}(\|n_h^{*,\theta}\|_{L^\infty(\Gamma_h^\theta)} + \|e_n^\theta\|_{L^\infty(\Gamma_h^\theta)}) \\ &\le Ch^\alpha\|\mathbf{z}\|_{\mathbf{M}(\mathbf{x}^*)}\|\mathbf{w}\|_{\mathbf{M}(\mathbf{x}^*)}.\end{aligned}$$

Similarly, (3.17) implies that

$$
\begin{aligned}
&(\mathbf{D}(\mathbf{x},\mathbf{n}) - \mathbf{D}(\mathbf{x}^*,\mathbf{n}^*))\mathbf{z}\cdot\mathbf{w} \\
&= \int_0^1 \int_{\Gamma_h^\theta} \nabla_{\Gamma_h^\theta}(z_h^\theta \cdot e_n^\theta)\cdot\nabla_{\Gamma_h^\theta} w_h^\theta + D_{\Gamma_h^\theta} e_x^\theta \nabla_{\Gamma_h^\theta}(z_h^\theta\cdot n_h^\theta)\cdot\nabla_{\Gamma_h^\theta} w_h^\theta \\
&\le Ch^\alpha \|\mathbf{z}\|_{\mathbf{K}(\mathbf{x}^*)}\|\mathbf{w}\|_{\mathbf{A}(\mathbf{x}^*)}.
\end{aligned}
$$

For (3.30)-(3.31) under conditions (A) and (B), the proof is similar and therefore omitted. For (3.32), we apply the Hölder inequality to the integrand of (3.18) and obtain

$$
\begin{aligned}
&(\boldsymbol{\rho}(\mathbf{x},\mathbf{n},\mathbf{v}) - \boldsymbol{\rho}(\mathbf{x}^*,\mathbf{n}^*,\mathbf{v}^*))\cdot\mathbf{w} \\
&\le \int_0^1 \Big\{ \|\nabla_{\Gamma_h^\theta}[e_v^\theta\cdot n_h^\theta - P_{\Gamma_h^\theta}(e_v^\theta\cdot n_h^\theta)]\|_{L^2(\Gamma_h^\theta)}\|\nabla_{\Gamma_h^\theta} w_h^\theta\|_{L^2(\Gamma_h^\theta)} && (3.35)\\
&\quad + \|\nabla_{\Gamma_h^\theta}[e_v^\theta\cdot e_n^\theta - P_{\Gamma_h^\theta}(e_v^\theta\cdot e_n^\theta)]\|_{L^2(\Gamma_h^\theta)}\|\nabla_{\Gamma_h^\theta} w_h^\theta\|_{L^2(\Gamma_h^\theta)} && (3.36)\\
&\quad + \|\nabla_{\Gamma_h^\theta}[e_n^\theta\cdot v_h^{*,\theta} - P_{\Gamma_h^\theta}(e_n^\theta\cdot v_h^{*,\theta})]\|_{L^2(\Gamma_h^\theta)}\|\nabla_{\Gamma_h^\theta} w_h^\theta\|_{L^2(\Gamma_h^\theta)} && (3.37)\\
&\quad + Ch^{-1}\|(v_h^\theta\cdot n_h^\theta - P_{\Gamma_h^\theta}(v_h^\theta\cdot n_h^\theta))(\nabla_{\Gamma_h^\theta}\cdot e_x^\theta)\|_{L^2(\Gamma_h^\theta)}\|\nabla_{\Gamma_h^\theta} w_h^\theta\|_{L^2(\Gamma_h^\theta)} && (3.38)\\
&\quad + C\|D_{\Gamma_h^\theta} e_x^\theta \nabla_{\Gamma_h^\theta}[v_h^\theta\cdot n_h^\theta - P_{\Gamma_h^\theta}(v_h^\theta\cdot n_h^\theta)]\|_{L^2(\Gamma_h^\theta)}\|\nabla_{\Gamma_h^\theta} w_h^\theta\|_{L^2(\Gamma_h^\theta)}\Big\}\,\mathrm{d}\theta. && (3.39)
\end{aligned}
$$

By using (A.2), we obtain

$$
(3.35)+(3.36)+(3.37) \le Ch(\|\mathbf{e_v}\|_{\mathbf{K}(\mathbf{x}^*)} + \|\mathbf{e_n}\|_{\mathbf{K}(\mathbf{x}^*)})\|\mathbf{w}\|_{\mathbf{A}(\mathbf{x}^*)},
$$

where the boundedness of n_h^θ, e_n^θ and $v_h^{*,\theta}$ are guaranteed by the norm equivalence (3.24) and condition (B). For (3.38), we have

$$
\begin{aligned}
&\|(v_h^\theta\cdot n_h^\theta - P_{\Gamma_h^\theta}(v_h^\theta\cdot n_h^\theta))(\nabla_{\Gamma_h^\theta}\cdot e_x^\theta)\|_{L^2(\Gamma_h^\theta)} \\
&\le \|(v_h^{*,\theta}\cdot n_h^\theta - P_{\Gamma_h^\theta}(v_h^{*,\theta}\cdot n_h^\theta))(\nabla_{\Gamma_h^\theta}\cdot e_x^\theta)\|_{L^2(\Gamma_h^\theta)} \\
&\quad + \|(e_v^\theta\cdot n_h^\theta - P_{\Gamma_h^\theta}(e_v^\theta\cdot n_h^\theta))(\nabla_{\Gamma_h^\theta}\cdot e_x^\theta)\|_{L^2(\Gamma_h^\theta)} \\
&\le C\|v_h^{*,\theta}\cdot n_h^\theta - P_{\Gamma_h^\theta}(v_h^{*,\theta}\cdot n_h^\theta)\|_{L^\infty(\Gamma_h^\theta)}\|\nabla_{\Gamma_h^\theta} e_x^\theta\|_{L^2(\Gamma_h^\theta)} \\
&\quad + C\|e_v^\theta\cdot n_h^\theta - P_{\Gamma_h^\theta}(e_v^\theta\cdot n_h^\theta)\|_{L^2(\Gamma_h^\theta)} \\
&\le Ch\|\mathbf{e_x}\|_{\mathbf{A}(\mathbf{x}^*)} + Ch^2\|\mathbf{e_v}\|_{\mathbf{K}(\mathbf{x}^*)},
\end{aligned}
$$

where the L^∞ error of the first term in the last two line is analyzed by inserting a Lagrange interpolation and using [23, Proposition 2.7] and (A.4), i.e.,

$$\begin{aligned}
&\|v_h^{*,\theta}\cdot n_h^\theta - P_{\Gamma_h^\theta}(v_h^{*,\theta}\cdot n_h^\theta)\|_{L^\infty(\Gamma_h^\theta)} \\
&\le \|v_h^{*,\theta}\cdot n_h^\theta - I_{\Gamma_h^\theta}(v_h^{*,\theta}\cdot n_h^\theta)\|_{L^\infty(\Gamma_h^\theta)} \\
&\quad + h^{-1}\|I_{\Gamma_h^\theta}(v_h^{*,\theta}\cdot n_h^\theta) - P_{\Gamma_h^\theta}(v_h^{*,\theta}\cdot n_h^\theta)\|_{L^2(\Gamma_h^\theta)} \\
&\le \|v_h^{*,\theta}\cdot n_h^\theta - I_{\Gamma_h^\theta}(v_h^{*,\theta}\cdot n_h^\theta)\|_{L^\infty(\Gamma_h^\theta)} \\
&\quad + h^{-1}\|v_h^{*,\theta}\cdot n_h^\theta - I_{\Gamma_h^\theta}(v_h^{*,\theta}\cdot n_h^\theta)\|_{L^2(\Gamma_h^\theta)} \\
&\le Ch\|v_h^{*,0}\|_{W^{1,\infty}(\Gamma_h[\mathbf{x}^*])}\|n_h^{*,0} + e_n^0\|_{W^{1,\infty}(\Gamma_h[\mathbf{x}^*])}.
\end{aligned}$$

For (3.39), by inverse inequality and (A), we obtain

$$\begin{aligned}
&\|D_{\Gamma_h^\theta} e_x^\theta \nabla_{\Gamma_h^\theta}[v_h^\theta\cdot n_h^\theta - P_{\Gamma_h^\theta}(v_h^\theta\cdot n_h^\theta)]\|_{L^2(\Gamma_h^\theta)} \\
&\le \|\nabla_{\Gamma_h^\theta}[v_h^{*,\theta}\cdot n_h^\theta - P_{\Gamma_h^\theta}(v_h^{*,\theta}\cdot n_h^\theta)]\|_{L^\infty(\Gamma_h^\theta)}\|D_{\Gamma_h^\theta} e_x^\theta\|_{L^2(\Gamma_h^\theta)} \\
&\quad + C\|\nabla_{\Gamma_h^\theta}[e_v^\theta\cdot n_h^\theta - P_{\Gamma_h^\theta}(e_v^\theta\cdot n_h^\theta)]\|_{L^2(\Gamma_h^\theta)} \\
&\le C\|\mathbf{e_x}\|_{\mathbf{A}(\mathbf{x}^*)} + Ch\|\mathbf{e_v}\|_{\mathbf{K}(\mathbf{x}^*)}.
\end{aligned}$$

Combining the above results, (3.32) is proved. □

3.3 Poincaré inequality for vector fields on the interpolated surface

In this subsection, we prove a variant of the Poincaré inequality which controls the L^2 norm of a velocity vector field by the L^2 norm of its tangential gradient and normal component (without using the tangential component). The key ingredient is that the normal vector of a closed smooth surface cannot be a constant vector field.

Lemma 3.4 *Under the assumptions of Theorem 2.1, there exist positive constants h_0 and C (independent of h and $t \in [0,T]$) such that the following inequality holds for $h \le h_0$:*

$$\int_{\Gamma_h[\mathbf{x}^*]} |v_h|^2 \le C\bigg(\int_{\Gamma_h[\mathbf{x}^*]} |\nabla_{\Gamma_h[\mathbf{x}^*]} v_h|^2 + \int_{\Gamma_h[\mathbf{x}^*]} |v_h\cdot n_h^*|^2\bigg) \quad \forall\, v_h \in H^1(\Gamma_h[\mathbf{x}^*])^3,$$

where $n_h^* \in S_h[\mathbf{x}^*]^3$ is the interpolation of the exact normal vector n defined on Γ.

Proof Let $h_0 > 0$ be the constant discussed in Section 2.4 to ensure the existence of lift mapping from the interpolated surface $\Gamma[\mathbf{x}^*]$ to the smooth surface Γ for $h \le h_0$ and $t \in [0,T]$. It suffices to prove the following result:

$$\int_{\Gamma_h[\mathbf{x}^*]} |v_h|^2 \le C\bigg(\int_{\Gamma_h[\mathbf{x}^*]} |\nabla_{\Gamma_h[\mathbf{x}^*]} v_h|^2 + \int_{\Gamma} |v_h^\ell\cdot n|^2\bigg) \quad \forall\, v_h \in H^1(\Gamma_h[\mathbf{x}^*])^3, \tag{3.40}$$

where v_h^ℓ is the lift of v_h onto the smooth surface Γ. If (3.40) holds then, by using the norm equivalence of lift in (2.14), we have

$$
\begin{aligned}
&\int_{\Gamma_h[\mathbf{x}^*]} |v_h|^2 \\
&\le C\bigg(\int_{\Gamma_h[\mathbf{x}^*]} |\nabla_{\Gamma_h[\mathbf{x}^*]} v_h|^2 + \int_\Gamma |v_h^\ell \cdot n_h^{*,\ell}|^2 + \int_\Gamma |v_h^\ell \cdot (n - n_h^{*,\ell})|^2 \bigg) \\
&\le C\bigg(\int_{\Gamma_h[\mathbf{x}^*]} |\nabla_{\Gamma_h[\mathbf{x}^*]} v_h|^2 + \int_{\Gamma_h[\mathbf{x}^*]} |v_h \cdot n_h^*|^2 + \|n - n_h^{*,\ell}\|_{L^\infty(\Gamma)} \int_{\Gamma_h[\mathbf{x}^*]} |v_h|^2 \bigg) \\
&\le C\bigg(\int_{\Gamma_h[\mathbf{x}^*]} |\nabla_{\Gamma_h[\mathbf{x}^*]} v_h|^2 + \int_{\Gamma_h[\mathbf{x}^*]} |v_h \cdot n_h^*|^2 \bigg) + Ch \int_{\Gamma_h[\mathbf{x}^*]} |v_h|^2 .
\end{aligned}
$$

For sufficiently small h (adjust the constant h_0 and require $h \le h_0$), the last term can be absorbed by the left-hand side. This proves the desired result of Lemma 3.4.

The proof of (3.40) is by contradiction. Suppose that (3.40) does not hold. Then there exists a sequence of interpolated surfaces $\Gamma_m^* = \Gamma_{h_m}[\mathbf{x}_m^*(t_m)]$ of $\Gamma(t_m)$ and functions $v_m \in H^1(\Gamma_m^*)^3$ such that

$$
\int_{\Gamma_m^*} |v_m|^2 = 1, \tag{3.41}
$$

$$
\int_{\Gamma_m^*} |\nabla_{\Gamma_m^*} v_m|^2 + \int_{\Gamma(t_m)} |v_m^\ell \cdot n_m|^2 \le \frac{1}{m}, \tag{3.42}
$$

where $n_m = n_{\Gamma(t_m)}$ is the unit exterior normal vector field on $\Gamma(t_m)$.

From the compactness of $[0, T]$, there exists a subsequence of $\{t_m\}$ with limit t_∞, which is still denoted as $\{t_m\}$ for the simplicity of notation. Since $\Gamma(t)$ is smooth and compact, $\Gamma(t_m) \to \Gamma(t_\infty)$ uniformly. With the help of the flow mapping $X(\cdot, t)$, we introduce a diffeomorphism $f_m : \Gamma(t_\infty) \to \Gamma(t_m)$ by

$$
f_m(X(p, t_\infty)) = X(p, t_m), \quad \forall p \in \Gamma(0).
$$

By lifting v_m from Γ_m^* to $\Gamma(t_m)$ and then pulling it back to $\Gamma(t_\infty)$ by f_m, we conclude from (3.41)–(3.42) and (2.14) that there exist positive constants C_1, C_2 and C_3 such that

$$
C_1 \le \int_{\Gamma(t_\infty)} |v_m^\ell \circ f_m|^2 \le C_2, \tag{3.43}
$$

$$
\int_{\Gamma(t_\infty)} |\nabla_{\Gamma(t_\infty)} (v_m^\ell \circ f_m)|^2 + \int_{\Gamma(t_\infty)} |(v_m^\ell \cdot n_m) \circ f_m|^2 \le \frac{C_3}{m}. \tag{3.44}
$$

Thus, $v_m^\ell \circ f_m$ is bounded in $H^1(\Gamma(t_\infty))^3$, which is compactly embedded into $L^2(\Gamma(t_\infty))^3$. Therefore, there exists a subsequence convergent to v_∞ in $L^2(\Gamma(t_\infty))^3$, which is still denoted as $v_m^\ell \circ f_m$. Moreover, (3.43) implies that $\int_{\Gamma(t_\infty)} |v_\infty|^2 \ne 0$. Since $\Gamma(t_\infty)$ is connected and

$$
\int_{\Gamma(t_\infty)} |\nabla_{\Gamma(t_\infty)} (v_m^\ell \circ f_m)|^2 \to 0 \quad \text{as} \quad m \to \infty,
$$

the function v_∞ can only be a nonzero constant vector.

Since the flow map $X(\cdot, t_m)$ converges to $X(\cdot, t_\infty)$ uniformly together with its derivatives, it follows that

$$\|n_m \circ f_m - n_\infty\|_{L^\infty(\Gamma(t_\infty))} \to 0, \quad m \to \infty,$$

where n_∞ is the unit exterior normal vector field on $\Gamma(t_\infty)$. From (3.44) we obtain

$$\frac{1}{2}\int_{\Gamma(t_\infty)} |(v_m^\ell \circ f_m) \cdot n_\infty|^2 \le \frac{C_3}{m} + \int_{\Gamma(t_\infty)} |(v_m^\ell \circ f_m) \cdot (n_\infty - n_m \circ f_m)|^2.$$

By passing to the limit $m \to 0$, we obtain $\int_{\Gamma(t_\infty)} |v_\infty \cdot n_\infty|^2 = 0$, which implies that $v_\infty \cdot n_\infty \equiv 0$ on $\Gamma(t_\infty)$. However, since v_∞ is a nonzero constant vector, the normal vector n_∞ cannot be perpendicular to v_∞ on every point of $\Gamma(t_\infty)$. This leads to a contradiction. □

3.4 Estimates for the normal and tangential projections

Let $u_h^* = (n_h^*, H_h^*)$ be the Ritz projection of u defined in (3.1). We introduce an operator P_τ^* which approximates the orthogonal projection along n_h^* by

$$P_\tau^* v_h := v_h - (v_h \cdot n_h^*) n_h^*,$$

for any finite element function $v_h \in S_h[\mathbf{x}^*]^3$ associated with the nodal vector $\mathbf{v} \in \mathbb{R}^{3N}$. Since n_h^* is not normalized, P_τ^* is not an exact projection. Let $P_{\Gamma_h[\mathbf{x}^*]} : L^2(\Gamma_h[\mathbf{x}^*]) \to S_h[\mathbf{x}^*]$ be the L^2-orthogonal projection, which can also be applied to a vector-valued function component-wisely. Thus $P_{\Gamma_h[\mathbf{x}^*]} P_\tau^*$ is a linear operator from $S_h[\mathbf{x}^*]^3$ into itself. Then we can define two matrices $\mathbf{P}_n(\mathbf{x}^*, \mathbf{n}^*) \in \mathbb{R}^{N\times 3N}$ and $\mathbf{P}_\tau(\mathbf{x}^*, \mathbf{n}^*) \in \mathbb{R}^{3N\times 3N}$ by requiring

$$\mathbf{P}_n(\mathbf{x}^*, \mathbf{n}^*)\mathbf{v} = \overrightarrow{P_{\Gamma_h[\mathbf{x}^*]}(v_h \cdot n_h^*)}, \quad \mathbf{P}_\tau(\mathbf{x}^*, \mathbf{n}^*)\mathbf{v} = \overrightarrow{P_{\Gamma_h[\mathbf{x}^*]} P_\tau^* v_h}, \tag{3.45}$$

where the nodal vector associated to a finite element function w_h is denoted as $\overrightarrow{w_h}$. These operators can also be defined on the numerical surface $\Gamma_h[\mathbf{x}]$ with slightly modified notations, i.e.,

$$\begin{aligned}
&\mathbf{P}_n(\mathbf{x}, \mathbf{n})\mathbf{v} := \overrightarrow{P_{\Gamma_h[\mathbf{x}]}(v_h^1 \cdot n_h)}, \quad \mathbf{P}_\tau(\mathbf{x}, \mathbf{n})\mathbf{v} := \overrightarrow{P_{\Gamma_h[\mathbf{x}]} P_\tau v_h^1}, \\
&P_\tau v_h^1 := v_h^1 - (v_h^1 \cdot n_h) n_h,
\end{aligned}$$

where $v_h^1 \in S_h[\mathbf{x}]^3$ is the finite element function with nodal vector $\mathbf{v} \in \mathbb{R}^{3N}$, and n_h is the numerical normal vector field computed in (2.2) (or equivalently, the finite element function in $S_h[\mathbf{x}]^3$ with nodal vector $\mathbf{n}$).

Lemma 3.5 *Suppose that* $\|n_h\|_{W^{1,\infty}(\Gamma_h[\mathbf{x}])}$ *and* $\|n_h^*\|_{W^{1,\infty}(\Gamma_h[\mathbf{x}^*])}$ *are bounded, with an upper bound independent of* h. *Then the following estimates hold:*

$$\|\mathbf{P}_n(\mathbf{x}^*,\mathbf{n}^*)\mathbf{e_v}\|_{\mathbf{A}(\mathbf{x}^*)} + \|\mathbf{P}_\tau(\mathbf{x}^*,\mathbf{n}^*)\mathbf{e_v}\|_{\mathbf{A}(\mathbf{x}^*)} \le C\|\mathbf{e_v}\|_{\mathbf{K}(\mathbf{x}^*)},$$
$$\|\mathbf{P}_n(\mathbf{x}^*,\mathbf{n}^*)\mathbf{e_v}\|_{\mathbf{M}(\mathbf{x}^*)} + \|\mathbf{P}_\tau(\mathbf{x}^*,\mathbf{n}^*)\mathbf{e_v}\|_{\mathbf{M}(\mathbf{x}^*)} \le C\|\mathbf{e_v}\|_{\mathbf{M}(\mathbf{x}^*)}.$$

Moreover,

$$\begin{aligned}&\|\mathbf{e_v} - \mathbf{P}_\tau(\mathbf{x},\mathbf{n})\mathbf{e_v}\|_{\mathbf{A}(\mathbf{x})}\\ &\le C\left(\|e_v\cdot n_h^*\|_{H^1(\Gamma_h[\mathbf{x}^*])} + \|e_v\|_{H^1(\Gamma_h[\mathbf{x}^*])}(\|e_n\|_{W^{1,\infty}(\Gamma_h[\mathbf{x}^*])} + h)\right),\end{aligned}$$

where e_v *and* e_n *are finite element functions on* $\Gamma_h[\mathbf{x}^*]$ *with nodal vectors* $\mathbf{e_v}$ *and* $\mathbf{e_n}$*, respectively.*

Proof From Remark 3.1 we know that the Ritz projection n_h^* of n is bounded in $W^{1,\infty}$ norm. By using estimate (A.2) in Appendix, we obtain

$$\begin{aligned}&\|\nabla_{\Gamma_h[\mathbf{x}^*]}(e_v\cdot n_h^* - P_{\Gamma_h[\mathbf{x}^*]}(e_v\cdot n_h^*))\|_{L^2(\Gamma_h[\mathbf{x}^*])}\\ &\le Ch\|e_v\|_{H^1(\Gamma_h[\mathbf{x}^*])}\|n_h^*\|_{W^{1,\infty}(\Gamma_h[\mathbf{x}^*])}.\end{aligned} \tag{3.46}$$

Then, using the definition in (3.45), the estimate in (3.46), and the triangle inequality, we have

$$\begin{aligned}&\|\mathbf{P}_n(\mathbf{x}^*,\mathbf{n}^*)\mathbf{e_v}\|_{\mathbf{A}(\mathbf{x}^*)}\\ &= \|\nabla_{\Gamma_h[\mathbf{x}^*]}P_{\Gamma_h[\mathbf{x}^*]}(e_v\cdot n_h^*)\|_{L^2(\Gamma_h[\mathbf{x}^*])}\\ &\le \|\nabla_{\Gamma_h[\mathbf{x}^*]}(e_v\cdot n_h^*)\|_{L^2(\Gamma_h[\mathbf{x}^*])} + \|\nabla_{\Gamma_h[\mathbf{x}^*]}(e_v\cdot n_h^* - P_{\Gamma_h[\mathbf{x}^*]}(e_v\cdot n_h^*))\|_{L^2(\Gamma_h[\mathbf{x}^*])}\\ &\le C\|e_v\|_{H^1(\Gamma_h[\mathbf{x}^*])} + Ch\|e_v\|_{H^1(\Gamma_h[\mathbf{x}^*])}\\ &\le C\|\mathbf{e_v}\|_{\mathbf{K}(\mathbf{x}^*)}.\end{aligned}$$

Similarly, estimates (A.1) and (A.3) in Appendix imply that

$$\|e_v\cdot n_h^* - P_{\Gamma_h[\mathbf{x}^*]}(e_v\cdot n_h^*)\|_{L^2(\Gamma_h[\mathbf{x}^*])} \le Ch^2\|e_v\|_{H^1(\Gamma_h[\mathbf{x}^*])}, \tag{3.47}$$

and

$$\begin{aligned}&\left\|\nabla_{\Gamma_h[\mathbf{x}^*]}\left(P_{\Gamma_h[\mathbf{x}^*]}P_\tau^* e_v - P_\tau^* e_v\right)\right\|_{L^2(\Gamma_h[\mathbf{x}^*])}\\ &= \left\|\nabla_{\Gamma_h[\mathbf{x}^*]}\Big((e_v\cdot n_h^*)n_h^* - P_{\Gamma_h[\mathbf{x}^*]}((e_v\cdot n_h^*)n_h^*)\Big)\right\|_{L^2(\Gamma_h[\mathbf{x}^*])}\\ &\le Ch\|e_v\|_{H^1(\Gamma_h[\mathbf{x}^*])}\|n_h^*\|^2_{W^{1,\infty}(\Gamma_h[\mathbf{x}^*])}.\end{aligned} \tag{3.48}$$

In view of the definition in (3.45), by using the triangle inequality and the inequality above, we have

$$\begin{aligned}&\|\mathbf{P}_\tau(\mathbf{x}^*,\mathbf{n}^*)\mathbf{e_v}\|_{\mathbf{A}(\mathbf{x}^*)}\\ &= \|\nabla_{\Gamma_h[\mathbf{x}^*]}(P_{\Gamma_h[\mathbf{x}^*]}P_\tau^* e_v)\|_{L^2(\Gamma_h[\mathbf{x}^*])}\\ &\le \|\nabla_{\Gamma_h[\mathbf{x}^*]}(P_{\Gamma_h[\mathbf{x}^*]}P_\tau^* e_v - P_\tau^* e_v)\|_{L^2(\Gamma_h[\mathbf{x}^*])} + \|\nabla_{\Gamma_h[\mathbf{x}^*]}(P_\tau^* e_v)\|_{L^2(\Gamma_h[\mathbf{x}^*])}\\ &\le Ch\|e_v\|_{H^1(\Gamma_h[\mathbf{x}^*])} + C\|e_v\|_{H^1(\Gamma_h[\mathbf{x}^*])}\\ &\le C\|\mathbf{e_v}\|_{\mathbf{K}(\mathbf{x}^*)}.\end{aligned}$$

This proves the first result of Lemma 3.5.

From the best approximate property of the L^2 projection, we obtain the following estimates in $\mathbf{M}(\mathbf{x}^*)$ norm:

$$\begin{aligned}\|\mathbf{P}_n(\mathbf{x}^*,\mathbf{n}^*)\mathbf{e}_\mathbf{v}\|_{\mathbf{M}(\mathbf{x}^*)} &= \|P_{\Gamma_h[\mathbf{x}^*]}(e_v\cdot n_h^*)\|_{L^2(\Gamma_h[\mathbf{x}^*])}\\ &\le \|e_v\cdot n_h^*\|_{L^2(\Gamma_h[\mathbf{x}^*])} \le C\|\mathbf{e}_\mathbf{v}\|_{\mathbf{M}(\mathbf{x}^*)},\\ \|\mathbf{P}_\tau(\mathbf{x}^*,\mathbf{n}^*)\mathbf{e}_\mathbf{v}\|_{\mathbf{M}(\mathbf{x}^*)} &= \|P_{\Gamma_h[\mathbf{x}^*]}(e_v-(e_v\cdot n_h^*)n_h^*)\|_{L^2(\Gamma_h[\mathbf{x}^*])} \le C\|\mathbf{e}_\mathbf{v}\|_{\mathbf{M}(\mathbf{x}^*)}.\end{aligned}$$

This proves the second result of Lemma 3.5.

Next, by utilizing the interpolation on $\Gamma_h[\mathbf{x}]$ as a bridge, we prove (3.46) which is concerned with the L^2 projection on $\Gamma_h[\mathbf{x}]$. We distinguish the interpolation operators on $\Gamma_h[\mathbf{x}]$ and $\Gamma_h[\mathbf{x}^*]$ by $I_{\Gamma_h[\mathbf{x}]}$ and $I_{\Gamma_h[\mathbf{x}^*]}$, respectively. Corresponding to the nodal vectors $\mathbf{e}_\mathbf{v}$, $\mathbf{n}=\mathbf{n}^*+\mathbf{e}_\mathbf{n}$ and $\mathbf{e}_\mathbf{n}$, we denote by e_v^0, n_h^0 and e_n^0 the associated finite element functions on $\Gamma_h[\mathbf{x}^*]$, and by e_v^1, n_h^1 and e_n^1 the associated functions on $\Gamma_h[\mathbf{x}]$. The key ingredient is

$$\overrightarrow{I_{\Gamma_h[\mathbf{x}]}((e_v^1\cdot n_h^1)n_h^1)} = \overrightarrow{I_{\Gamma_h[\mathbf{x}^*]}((e_v^0\cdot n_h^0)n_h^0)},$$

which allows us to apply the generalized norm equivalence (Remark 3.3) in the following estimation,

$$\begin{aligned}&\|\nabla_{\Gamma_h[\mathbf{x}]}\left((e_v^1\cdot n_h^1)n_h^1 - P_{\Gamma_h[\mathbf{x}]}[(e_v^1\cdot n_h^1)n_h^1]\right)\|_{L^2(\Gamma_h[\mathbf{x}])}\\ &\le \|\nabla_{\Gamma_h[\mathbf{x}]}((e_v^1\cdot n_h^1)n_h^1 - I_{\Gamma_h[\mathbf{x}]}((e_v^1\cdot n_h^1)n_h^1))\|_{L^2(\Gamma_h[\mathbf{x}])}\\ &\quad + Ch^{-1}\|I_{\Gamma_h[\mathbf{x}]}((e_v^1\cdot n_h^1)n_h^1) - (e_v^1\cdot n_h^1)n_h^1\|_{L^2(\Gamma_h[\mathbf{x}])}\\ &\le C\big\|\nabla_{\Gamma_h[\mathbf{x}^*]}\big((e_v^0\cdot n_h^0)n_h^0 - I_{\Gamma_h[\mathbf{x}^*]}((e_v^0\cdot n_h^0)n_h^0)\big)\big\|_{L^2(\Gamma_h[\mathbf{x}^*])}\\ &\quad + Ch^{-1}\big\|I_{\Gamma_h[\mathbf{x}^*]}((e_v^0\cdot n_h^0)n_h^0) - (e_v^0\cdot n_h^0)n_h^0\big\|_{L^2(\Gamma_h[\mathbf{x}^*])}.\end{aligned}\tag{3.49}$$

Then (3.46) can be proved as follows:

$$\begin{aligned}&\|\mathbf{e}_\mathbf{v}-\mathbf{P}_\tau(\mathbf{x},\mathbf{n})\mathbf{e}_\mathbf{v}\|_{\mathbf{A}(\mathbf{x})}\\ &= \|\nabla_{\Gamma_h[\mathbf{x}]}(e_v^1 - P_{\Gamma_h[\mathbf{x}]}P_\tau e_v^1)\|_{L^2(\Gamma_h[\mathbf{x}])}\\ &\le \|\nabla_{\Gamma_h[\mathbf{x}]}(e_v^1 - P_\tau e_v^1)\|_{L^2(\Gamma_h[\mathbf{x}])} + \|\nabla_{\Gamma_h[\mathbf{x}]}(P_\tau e_v^1 - P_{\Gamma_h[\mathbf{x}]}P_\tau e_v^1)\|_{L^2(\Gamma_h[\mathbf{x}])},\end{aligned}$$

where the first term can be estimated by the norm equivalence in Remark 3.3, i.e.,

$$\begin{aligned}\|\nabla_{\Gamma_h[\mathbf{x}]}(e_v^1 - P_\tau e_v^1)\|_{L^2(\Gamma_h[\mathbf{x}])} &= \|\nabla_{\Gamma_h[\mathbf{x}]}((e_v^1\cdot n_h^1)n_h^1)\|_{L^2(\Gamma_h[\mathbf{x}])}\\ &\le C\|\nabla_{\Gamma_h[\mathbf{x}^*]}((e_v^0\cdot n_h^0)n_h^0)\|_{L^2(\Gamma_h[\mathbf{x}^*])}\\ &\le C\|e_v^0\cdot n_h^0\|_{H^1(\Gamma_h[\mathbf{x}^*])}\|n_h^0\|_{W^{1,\infty}(\Gamma_h[\mathbf{x}^*])}\\ &\le C\left(\|e_v^0\cdot n_h^*\|_{H^1(\Gamma_h[\mathbf{x}^*])} + \|e_v^0\cdot e_n^0\|_{H^1(\Gamma_h[\mathbf{x}^*])}\right),\end{aligned}$$

and the second term can be estimated by (3.49) and (A.5), i.e.,

$$
\begin{aligned}
&\|\nabla_{\Gamma_h[\mathbf{x}]}(P_\tau e_v^1 - P_{\Gamma_h[\mathbf{x}]}P_\tau e_v^1)\|_{L^2(\Gamma_h[\mathbf{x}])} \\
&= \|\nabla_{\Gamma_h[\mathbf{x}]}\left((e_v^1\cdot n_h^1)n_h^1 - P_{\Gamma_h[\mathbf{x}]}((e_v^1\cdot n_h^1)n_h^1)\right)\|_{L^2(\Gamma_h[\mathbf{x}])} \\
&\le C\big\|\nabla_{\Gamma_h[\mathbf{x}^*]}\big((e_v^0\cdot n_h^0)n_h^0 - I_{\Gamma_h[\mathbf{x}^*]}((e_v^0\cdot n_h^0)n_h^0)\big)\big\|_{L^2(\Gamma_h[\mathbf{x}^*])} \\
&\quad + Ch^{-1}\big\|I_{\Gamma_h[\mathbf{x}^*]}((e_v^0\cdot n_h^0)n_h^0) - (e_v^0\cdot n_h^0)n_h^0\big\|_{L^2(\Gamma_h[\mathbf{x}^*])} \\
&\le Ch\|e_v^0\|_{H^1(\Gamma_h[\mathbf{x}^*])}.
\end{aligned} \tag{3.50}
$$

Therefore, we obtain

$$
\begin{aligned}
&\|\mathbf{e_v} - \mathbf{P}_\tau(\mathbf{x},\mathbf{n})\mathbf{e_v}\|_{\mathbf{A}(\mathbf{x})} \\
&\le C\left(\|e_v^0\cdot n_h^*\|_{H^1(\Gamma_h[\mathbf{x}^*])} + \|e_v^0\|_{H^1(\Gamma_h[\mathbf{x}^*])}(\|e_n^0\|_{W^{1,\infty}(\Gamma_h[\mathbf{x}^*])} + h)\right).
\end{aligned}
$$

This proves the last result of Lemma 3.5. □

3.5 Stability estimates

In this section, we present stability estimates for the error system (3.10). The stability estimates for the equations of $\mathbf{e_x}$ and $\mathbf{e_u}$ in (3.10) have already been established in [40, inequality (7.33) and p. 824], i.e., under the assumption that

$$
\|e_x\|_{W^{1,\infty}(\Gamma_h[\mathbf{x}^*])} \le h^{(k-1)/2}, \tag{3.51a}
$$

$$
\|e_u\|_{W^{1,\infty}(\Gamma_h[\mathbf{x}^*])} \le h^{(k-1)/2}, \tag{3.51b}
$$

$$
\|e_u\|_{L^{\infty}(\Gamma_h[\mathbf{x}^*])} \le h^{(k+1)/2}, \tag{3.51c}
$$

hold for $t\in[0,t_*]$, the solutions of (3.10a) and (3.10d) satisfy the following estimates for $t\in[0,t_*]$:

$$
\|\mathbf{e_x}(t)\|^2_{\mathbf{K}(\mathbf{x}^*(t))} \le C\int_0^t \|\mathbf{e_v}(s)\|^2_{\mathbf{K}(\mathbf{x}^*(s))}\,\mathrm{d}s + C\int_0^t \|\mathbf{e_x}(s)\|^2_{\mathbf{K}(\mathbf{x}^*(s))}\,\mathrm{d}s, \tag{3.52}
$$

$$
\begin{aligned}
\|\mathbf{e_u}(t)\|^2_{\mathbf{K}(\mathbf{x}^*(t))} \le{}& C\int_0^t \left(\|\mathbf{e_v}(s)\|^2_{\mathbf{K}(\mathbf{x}^*(s))} + \|\mathbf{e_u}(s)\|^2_{\mathbf{K}(\mathbf{x}^*(s))}\right)\mathrm{d}s \\
&+ C\int_0^t \|\mathbf{e_x}(s)\|^2_{\mathbf{K}(\mathbf{x}^*(s))}\,\mathrm{d}s + C\,\|\mathbf{e_x}(t)\|^2_{\mathbf{K}(\mathbf{x}^*(t))} \\
&+ C\,\|\mathbf{e_u}(0)\|^2_{\mathbf{K}(\mathbf{x}^*(0))} + C\int_0^t \|\mathbf{d_u}(s)\|^2_{\mathbf{M}(\mathbf{x}^*(s))}\,\mathrm{d}s.
\end{aligned} \tag{3.53}
$$

Remark 3.4 Equation (3.10d) and the equation considered in [40] have only minor difference (i.e., the error from a low-order term $v_h\cdot\nabla_{\Gamma_h[\mathbf{x}]}u_h$), which does not affect the stability estimate.

The stability estimates for the equations of $\mathbf{e_v}$ and $\mathbf{e}_\kappa$ in (3.10b)–(3.10c) are the main results of this subsection, which are presented in Theorem 3.2.

Theorem 3.2 *Suppose that $k \geqslant 2$ and (3.51) holds. Then there exists a constant $h_0 > 0$ such that for $h \leq h_0$ the solutions of (3.10b)–(3.10c) satisfy the following estimates*:

$$\begin{aligned}&\|\mathbf{e_v}\|_{\mathbf{K}(\mathbf{x}^*)}\\ &\leq C(\|\mathbf{e_x}\|_{\mathbf{A}(\mathbf{x}^*)} + \|\mathbf{e_u}\|_{\mathbf{K}(\mathbf{x}^*)} + \|\mathbf{d_v}\|_{\mathbf{M}(\mathbf{x}^*)} + \|\widetilde{\mathbf{d}}_\mathbf{v}\|_{\star,\mathbf{x}^*} + \|\mathbf{d}_{\boldsymbol{\kappa}}\|_{\mathbf{M}(\mathbf{x}^*)}), \quad (3.54)\\ &\|\mathbf{e}_{\boldsymbol{\kappa}}\|_{\mathbf{M}(\mathbf{x}^*)}\\ &\leq C(\|\mathbf{e_u}\|_{\mathbf{M}(\mathbf{x}^*)} + h^{-1}\|\mathbf{e_x}\|_{\mathbf{A}(\mathbf{x}^*)} + h^{-1}\|\mathbf{e_v}\|_{\mathbf{A}(\mathbf{x}^*)} + \|\mathbf{d}_{\boldsymbol{\kappa}}\|_{\mathbf{M}(\mathbf{x}^*)}). \quad (3.55)\end{aligned}$$

Proof Since $k \geqslant 2$ and (3.51) holds, it follows that

$$\|n_h^0\|_{W^{1,\infty}(\Gamma_h[\mathbf{x}^*])} \leq C \quad \text{and} \quad \|H_h^0\|_{W^{1,\infty}(\Gamma_h[\mathbf{x}^*])} \leq C, \tag{3.56}$$

and

$$\|e_n\|_{L^\infty(\Gamma_h[\mathbf{x}^*])} \leq h^{1.5}. \tag{3.57}$$

By applying Lemma 3.4 to the finite element function $e_v \in S_h[\mathbf{x}^*]^3$ associated with $\mathbf{e_v}$, we have

$$\|\mathbf{e_v}\|_{\mathbf{K}(\mathbf{x}^*)} \leq C\left(\|\mathbf{e_v}\|_{\mathbf{A}(\mathbf{x}^*)} + \|e_v \cdot n_h^*\|_{L^2(\Gamma_h[\mathbf{x}^*])}\right). \tag{3.58}$$

In the following, we present estimates for $\|e_v \cdot n_h^*\|_{L^2(\Gamma_h[\mathbf{x}^*])}$ and $\|\mathbf{e_v}\|_{\mathbf{A}(\mathbf{x}^*)}$, separately. The latter requires us to obtain estimates for $\|e_v \cdot n_h^*\|_{H^1(\Gamma_h[\mathbf{x}^*])}$ and $\|\mathbf{e}_{\boldsymbol{\kappa}}\|_{\mathbf{M}(\mathbf{x}^*)}$.

(a) *Estimation of $\|e_v \cdot n_h^*\|_{L^2(\Gamma_h[\mathbf{x}^*])}$*. Testing (3.10b) by $\mathbf{P}_n(\mathbf{x}^*, \mathbf{n}^*)\mathbf{e_v}$ and using the relation

$$\begin{aligned}&\mathbf{B}(\mathbf{x}^*, \mathbf{n}^*)\mathbf{e_v} \cdot \mathbf{P}_n(\mathbf{x}^*, \mathbf{n}^*)\mathbf{e_v}\\ &= \int_{\Gamma_h[\mathbf{x}^*]} (e_v \cdot n_h^*)\, P_{\Gamma_h[\mathbf{x}^*]}(e_v \cdot n_h^*)\\ &= \int_{\Gamma_h[\mathbf{x}^*]} |e_v \cdot n_h^*|^2 + \int_{\Gamma_h[\mathbf{x}^*]} e_v \cdot n_h^*\, (P_{\Gamma_h[\mathbf{x}^*]}(e_v \cdot n_h^*) - e_v \cdot n_h^*),\end{aligned}$$

we obtain

$$\begin{aligned}\|e_v \cdot n_h^*\|^2_{L^2(\Gamma_h[\mathbf{x}^*])} &= \int_{\Gamma_h[\mathbf{x}^*]} e_v \cdot n_h^*\, (e_v \cdot n_h^* - P_{\Gamma_h[\mathbf{x}^*]}(e_v \cdot n_h^*))\\ &\quad + (\mathbf{M}(\mathbf{x}^*) - \mathbf{M}(\mathbf{x}))\mathbf{H} \cdot \mathbf{P}_n(\mathbf{x}^*, \mathbf{n}^*)\mathbf{e_v}\\ &\quad + (\mathbf{B}(\mathbf{x}^*, \mathbf{n}^*) - \mathbf{B}(\mathbf{x}, \mathbf{n}))\mathbf{v} \cdot \mathbf{P}_n(\mathbf{x}^*, \mathbf{n}^*)\mathbf{e_v}\\ &\quad - \mathbf{M}(\mathbf{x}^*)\mathbf{e_H} \cdot \mathbf{P}_n(\mathbf{x}^*, \mathbf{n}^*)\mathbf{e_v}\\ &\quad - \mathbf{M}(\mathbf{x}^*)\mathbf{d_v} \cdot \mathbf{P}_n(\mathbf{x}^*, \mathbf{n}^*)\mathbf{e_v}\\ &=: J_1 + J_2 + J_3 + J_4 + J_5.\end{aligned} \tag{3.59}$$

The first term in (3.59) can be estimated by the Cauchy-Schwarz inequality and (3.47), i.e.,

$$J_1 \le Ch^2 \|e_v \cdot n_h^*\|_{L^2(\Gamma_h[\mathbf{x}^*])} \|\mathbf{e_v}\|_{\mathbf{K}(\mathbf{x}^*)}.$$

Since $\|H_h^0\|_{W^{1,\infty}(\Gamma_h[\mathbf{x}^*])}$ is bounded, as shown in (3.56), the second term in (3.59) can be estimated directly using (3.25), i.e.,

$$J_2 \le C\|\mathbf{e_x}\|_{\mathbf{A}(\mathbf{x}^*)} \|\mathbf{P}_n(\mathbf{x}^*, \mathbf{n}^*)\mathbf{e_v}\|_{\mathbf{M}(\mathbf{x}^*)}.$$

The third term in (3.59) can be decomposed into two terms through $\mathbf{v} = \mathbf{v}^* + \mathbf{e_v}$ and then estimated by using (3.30) and (3.33) with $\alpha = (k-1)/2$, respectively, i.e.,

$$\begin{aligned} J_3 &= (\mathbf{B}(\mathbf{x}^*, \mathbf{n}^*) - \mathbf{B}(\mathbf{x}, \mathbf{n}))(\mathbf{v}^* + \mathbf{e_v}) \cdot \mathbf{P}_n(\mathbf{x}^*, \mathbf{n}^*)\mathbf{e_v} \\ &\le C(\|\mathbf{e_n}\|_{\mathbf{M}(\mathbf{x}^*)} + \|\mathbf{e_x}\|_{\mathbf{A}(\mathbf{x}^*)} + h^{(k-1)/2}\|\mathbf{e_v}\|_{\mathbf{M}(\mathbf{x}^*)})\|\mathbf{P}_n(\mathbf{x}^*, \mathbf{n}^*)\mathbf{e_v}\|_{\mathbf{M}(\mathbf{x}^*)}. \end{aligned} \tag{3.60}$$

Substituting the following estimate into (3.59)–(3.60),

$$\|\mathbf{P}_n(\mathbf{x}^*, \mathbf{n}^*)\mathbf{e_v}\|_{\mathbf{M}(\mathbf{x}^*)} = \|P_{\Gamma_h[\mathbf{x}^*]}(e_v \cdot n_h^*)\|_{L^2(\Gamma_h[\mathbf{x}^*])} \le \|e_v \cdot n_h^*\|_{L^2(\Gamma_h[\mathbf{x}^*])},$$

we obtain

$$\begin{aligned} \|e_v \cdot n_h^*\|_{L^2(\Gamma_h[\mathbf{x}^*])} &\le C(\|\mathbf{e_u}\|_{\mathbf{M}(\mathbf{x}^*)} + \|\mathbf{e_x}\|_{\mathbf{A}(\mathbf{x}^*)} + \|\mathbf{d_v}\|_{\mathbf{M}(\mathbf{x}^*)}) \\ &\quad + C(h^{(k-1)/2}\|\mathbf{e_v}\|_{\mathbf{M}(\mathbf{x}^*)} + h^2\|\mathbf{e_v}\|_{\mathbf{K}(\mathbf{x}^*)}). \end{aligned} \tag{3.61}$$

By substituting (3.61) into (3.58), we find that the two terms $h^{(k-1)/2}\|\mathbf{e_v}\|_{\mathbf{M}(\mathbf{x}^*)} + h^2\|\mathbf{e_v}\|_{\mathbf{K}(\mathbf{x}^*)}$ can be absorbed by the left-hand side of (3.58). Therefore, we obtain

$$\|\mathbf{e_v}\|_{\mathbf{K}(\mathbf{x}^*)} \le C\big(\|\mathbf{e_v}\|_{\mathbf{A}(\mathbf{x}^*)} + \|\mathbf{e_u}\|_{\mathbf{M}(\mathbf{x}^*)} + \|\mathbf{e_x}\|_{\mathbf{A}(\mathbf{x}^*)} + \|\mathbf{d_v}\|_{\mathbf{M}(\mathbf{x}^*)}\big). \tag{3.62}$$

(b) *Estimation of* $\|e_v \cdot n_h^*\|_{H^1(\Gamma_h[\mathbf{x}^*])}$. In order to obtain an H^1-seminorm estimate for $e_v \cdot n_h^*$, we test (3.11) by $\mathbf{P}_n(\mathbf{x}^*, \mathbf{n}^*)\mathbf{e_v}$. By using the relation

$$\begin{aligned} &\mathbf{D}(\mathbf{x}^*, \mathbf{n}^*)\mathbf{e_v} \cdot \mathbf{P}_n(\mathbf{x}^*, \mathbf{n}^*)\mathbf{e_v} \\ &= \int_{\Gamma_h[\mathbf{x}^*]} \nabla_{\Gamma_h[\mathbf{x}^*]}(e_v \cdot n_h^*) \cdot \nabla_{\Gamma_h[\mathbf{x}^*]} P_{\Gamma_h[\mathbf{x}^*]}(e_v \cdot n_h^*) \\ &= \int_{\Gamma_h[\mathbf{x}^*]} |\nabla_{\Gamma_h[\mathbf{x}^*]}(e_v \cdot n_h^*)|^2 \\ &\quad + \int_{\Gamma_h[\mathbf{x}^*]} \nabla_{\Gamma_h[\mathbf{x}^*]}(e_v \cdot n_h^*) \cdot \nabla_{\Gamma_h[\mathbf{x}^*]}\big(P_{\Gamma_h[\mathbf{x}^*]}(e_v \cdot n_h^*) - e_v \cdot n_h^*\big), \end{aligned}$$

we obtain

$$
\begin{aligned}
&\|\nabla_{\Gamma_h[\mathbf{x}^*]}(e_v\cdot n_h^*)\|^2_{L^2(\Gamma_h[\mathbf{x}^*])}\\
&=\int_{\Gamma_h[\mathbf{x}^*]}\nabla_{\Gamma_h[\mathbf{x}^*]}(e_v\cdot n_h^*)\cdot\nabla_{\Gamma_h[\mathbf{x}^*]}\big(e_v\cdot n_h^*-P_{\Gamma_h[\mathbf{x}^*]}(e_v\cdot n_h^*)\big)\\
&\quad+(\mathbf{D}(\mathbf{x}^*,\mathbf{n}^*)-\mathbf{D}(\mathbf{x},\mathbf{n}))\mathbf{v}\cdot\mathbf{P}_n(\mathbf{x}^*,\mathbf{n}^*)\mathbf{e_v}\\
&\quad+(\mathbf{A}(\mathbf{x}^*)-\mathbf{A}(\mathbf{x}))\mathbf{H}\cdot\mathbf{P}_n(\mathbf{x}^*,\mathbf{n}^*)\mathbf{e_v}\\
&\quad+\big(\boldsymbol{\rho}(\mathbf{x},\mathbf{n},\mathbf{v})-\boldsymbol{\rho}(\mathbf{x}^*,\mathbf{n}^*,\mathbf{v}^*)\big)\cdot\mathbf{P}_n(\mathbf{x}^*,\mathbf{n}^*)\mathbf{e_v}\\
&\quad-\mathbf{A}(\mathbf{x}^*)\mathbf{e_H}\cdot\mathbf{P}_n(\mathbf{x}^*,\mathbf{n}^*)\mathbf{e_v}\\
&\quad-\mathbf{M}(\mathbf{x}^*)\widetilde{\mathbf{d}}_\mathbf{v}\cdot\mathbf{P}_n(\mathbf{x}^*,\mathbf{n}^*)\mathbf{e_v}\\
&=:J_1^*+J_2^*+J_3^*+J_4^*+J_5^*+J_6^*. \qquad (3.63)
\end{aligned}
$$

The first term in (3.63) can be estimated directly by applying (3.46), i.e.,

$$|J_1^*|\le Ch\|\mathbf{e_v}\|^2_{\mathbf{K}(\mathbf{x}^*)}.$$

The second term in (3.63) can be decomposed into two terms through $\mathbf{v}=\mathbf{v}^*+\mathbf{e_v}$ and then estimated by using (3.31) and (3.34) with $\alpha=(k-1)/2$, respectively, i.e.,

$$|J_2^*|\le C\left(\|\mathbf{e_n}\|_{\mathbf{K}(\mathbf{x}^*)}+\|\mathbf{e_x}\|_{\mathbf{A}(\mathbf{x}^*)}+h^{(k-1)/2}\|\mathbf{e_v}\|_{\mathbf{K}(\mathbf{x}^*)}\right)\|\mathbf{e_v}\|_{\mathbf{K}(\mathbf{x}^*)}.$$

Since $\|H_h^0\|_{W^{1,\infty}(\Gamma_h[\mathbf{x}^*])}$ is bounded, the third term in (3.63) can be estimated by using (3.26), i.e.,

$$|J_3^*|\le C\|\mathbf{e_x}\|_{\mathbf{A}(\mathbf{x}^*)}\|\mathbf{e_v}\|_{\mathbf{K}(\mathbf{x}^*)}.$$

The fourth term in (3.63) can be estimated by applying (3.32), i.e.,

$$
\begin{aligned}
|J_4^*|&\le C(h\|\mathbf{e_v}\|_{\mathbf{K}(\mathbf{x}^*)}+h\|\mathbf{e_n}\|_{\mathbf{K}(\mathbf{x}^*)}+\|\mathbf{e_x}\|_{\mathbf{A}(\mathbf{x}^*)})\|\mathbf{P}_n(\mathbf{x}^*,\mathbf{n}^*)\mathbf{e_v}\|_{\mathbf{A}(\mathbf{x}^*)}\\
&\le C(h\|\mathbf{e_v}\|_{\mathbf{K}(\mathbf{x}^*)}+h\|\mathbf{e_n}\|_{\mathbf{K}(\mathbf{x}^*)}+\|\mathbf{e_x}\|_{\mathbf{A}(\mathbf{x}^*)})\|\mathbf{e_v}\|_{\mathbf{K}(\mathbf{x}^*)}.
\end{aligned}
$$

The last two terms in (3.63) can be estimated directly, i.e.,

$$|J_5^*|+|J_6^*|\le C(\|\mathbf{e_H}\|_{\mathbf{A}(\mathbf{x}^*)}+\|\widetilde{\mathbf{d}}_\mathbf{v}\|_{\star,\mathbf{x}^*})\|\mathbf{e_v}\|_{\mathbf{K}(\mathbf{x}^*)}.$$

Then, substituting the estimates of $|J_1^*|$, $|J_2^*|$, $|J_3^*|$, $|J_4^*|$, $|J_5^*|$ and $|J_6^*|$ into (3.63), we obtain

$$
\begin{aligned}
&\|\nabla_{\Gamma_h[\mathbf{x}^*]}(e_v\cdot n_h^*)\|^2_{L^2(\Gamma_h[\mathbf{x}^*])}\\
&\le C(\|\mathbf{e_x}\|_{\mathbf{A}(\mathbf{x}^*)}+\|\mathbf{e_u}\|_{\mathbf{K}(\mathbf{x}^*)}+\|\widetilde{\mathbf{d}}_\mathbf{v}\|_{\star,\mathbf{x}^*})\|\mathbf{e_v}\|_{\mathbf{K}(\mathbf{x}^*)}+Ch^{\frac12}\|\mathbf{e_v}\|^2_{\mathbf{K}(\mathbf{x}^*)}\\
&\le C\epsilon^{-1}(\|\mathbf{e_x}\|_{\mathbf{A}(\mathbf{x}^*)}+\|\mathbf{e_u}\|_{\mathbf{K}(\mathbf{x}^*)}+\|\widetilde{\mathbf{d}}_\mathbf{v}\|_{\star,\mathbf{x}^*})^2+(\epsilon+Ch^{\frac12})\|\mathbf{e_v}\|^2_{\mathbf{K}(\mathbf{x}^*)}, \qquad (3.64)
\end{aligned}
$$

where $\epsilon\in(0,1)$ can be arbitrary. This can be combined with (3.61) to yield an estimate for the full H^1 norm:

$$
\begin{aligned}
\|e_v\cdot n_h^*\|^2_{H^1(\Gamma_h[\mathbf{x}^*])}\le C\epsilon^{-1}(\|\mathbf{e_x}\|_{\mathbf{A}(\mathbf{x}^*)}+\|\mathbf{e_u}\|_{\mathbf{K}(\mathbf{x}^*)}+\|\mathbf{d_v}\|_{\mathbf{M}(\mathbf{x}^*)}+\|\widetilde{\mathbf{d}}_\mathbf{v}\|_{\star,\mathbf{x}^*})^2\\
+(\epsilon+Ch^{\frac12})\|\mathbf{e_v}\|^2_{\mathbf{K}(\mathbf{x}^*)}, \qquad (3.65)
\end{aligned}
$$

where $\epsilon \in (0,1)$ can be arbitrary.

(c) *Estimation of* $\|\mathbf{e}_{\boldsymbol{\kappa}}\|_{\mathbf{M}(\mathbf{x}^*)}$. Testing (3.10c) with the nodal vector $\mathbf{e}_{\boldsymbol{\kappa},\mathbf{n}} = \overrightarrow{P_{\Gamma_h[\mathbf{x}^*]}(e_\kappa n_h^*)}$ and using the relation,

$$\begin{aligned}\mathbf{B}(\mathbf{x}^*,\mathbf{n}^*)^\top \mathbf{e}_{\boldsymbol{\kappa}} \cdot \mathbf{e}_{\boldsymbol{\kappa},\mathbf{n}} &= \int_{\Gamma_h[\mathbf{x}^*]} e_\kappa n_h^* \cdot P_{\Gamma_h[\mathbf{x}^*]}(e_\kappa n_h^*) \\ &= \int_{\Gamma_h[\mathbf{x}^*]} |e_\kappa n_h^*|^2 + \int_{\Gamma_h[\mathbf{x}^*]} e_\kappa n_h^* \cdot \big(P_{\Gamma_h[\mathbf{x}^*]}(e_\kappa n_h^*) - e_\kappa n_h^*\big),\end{aligned}$$

we obtain

$$\begin{aligned}\|e_\kappa n_h^*\|^2_{L^2(\Gamma_h[\mathbf{x}^*])} = &\int_{\Gamma_h[\mathbf{x}^*]} (e_\kappa n_h^*) \cdot (e_\kappa n_h^* - P_{\Gamma_h[\mathbf{x}^*]}(e_\kappa n_h^*)) \\ &+ (\mathbf{B}(\mathbf{x}^*,\mathbf{n}^*)^\top - \mathbf{B}(\mathbf{x},\mathbf{n})^\top)\boldsymbol{\kappa} \cdot \mathbf{e}_{\boldsymbol{\kappa},\mathbf{n}} \\ &+ (\mathbf{A}(\mathbf{x}^*) - \mathbf{A}(\mathbf{x}))\mathbf{v} \cdot \mathbf{e}_{\boldsymbol{\kappa},\mathbf{n}} \\ &- \mathbf{A}(\mathbf{x}^*)\mathbf{e}_{\mathbf{v}} \cdot \mathbf{e}_{\boldsymbol{\kappa},\mathbf{n}} \\ &- \mathbf{M}(\mathbf{x}^*)\mathbf{d}_{\boldsymbol{\kappa}} \cdot \mathbf{e}_{\boldsymbol{\kappa},\mathbf{n}} \\ =: &\, J_1^\# + J_2^\# + J_3^\# + J_4^\# + J_5^\#. \end{aligned} \tag{3.66}$$

From (3.5) and (2.14) we know that

$$\begin{aligned}\||n_h^*|^2 - 1\|_{L^\infty(\Gamma_h[\mathbf{x}^*])} &= \|(n_h^* - n^{-\ell}) \cdot (n_h^* + n^{-\ell})\|_{L^\infty(\Gamma_h[\mathbf{x}^*])} \\ &= C\|(n_h^{*,\ell} - n)\|_{L^\infty(\Gamma(t))}\|(n_h^{*,\ell} + n)\|_{L^\infty(\Gamma(t))} \le Ch^2. \end{aligned} \tag{3.67}$$

In above, $n^{-\ell}$ denotes the normal extension of n from Γ to $\Gamma_h[\mathbf{x}^*]$, which can be regarded as the inverse of the lift from $\Gamma_h[\mathbf{x}^*]$ to Γ. Thus, by choosing h_0 sufficiently small, $|n_h^*|^2$ has positive lower bound in $L^\infty(\Gamma_h[\mathbf{x}^*])$ independent of h. Then $\|\mathbf{e}_{\boldsymbol{\kappa}}\|_{\mathbf{M}(\mathbf{x}^*)}$ is equivalent to $\|e_\kappa n_h^*\|_{L^2(\Gamma_h[\mathbf{x}^*])}$. By using estimate (A.1) in Appendix with an additional inverse inequality, we have

$$\begin{aligned}J_1^\# &\le \|e_\kappa n_h^*\|_{L^2(\Gamma_h[\mathbf{x}^*])}\|e_\kappa n_h^* - P_{\Gamma_h[\mathbf{x}^*]}(e_\kappa n_h^*)\|_{L^2(\Gamma_h[\mathbf{x}^*])} \\ &\le \|e_\kappa n_h^*\|_{L^2(\Gamma_h[\mathbf{x}^*])} Ch\|\mathbf{e}_{\boldsymbol{\kappa}}\|_{\mathbf{M}(\mathbf{x}^*)} \\ &\le Ch\|e_\kappa n_h^*\|^2_{L^2(\Gamma_h[\mathbf{x}^*])}.\end{aligned}$$

By using (3.30) and (3.33), we obtain

$$\begin{aligned}J_2^\# =&(\mathbf{B}(\mathbf{x}^*,\mathbf{n}^*) - \mathbf{B}(\mathbf{x},\mathbf{n}))\mathbf{e}_{\boldsymbol{\kappa},\mathbf{n}} \cdot (\boldsymbol{\kappa}^* + \mathbf{e}_{\boldsymbol{\kappa}}) \\ \le& C\left(\|\mathbf{e}_{\mathbf{n}}\|_{\mathbf{M}(\mathbf{x}^*)} + \|\mathbf{e}_{\mathbf{x}}\|_{\mathbf{A}(\mathbf{x}^*)} + h^{(k-1)/2}\|\mathbf{e}_{\boldsymbol{\kappa}}\|_{\mathbf{M}(\mathbf{x}^*)}\right)\|e_\kappa n_h^*\|_{L^2(\Gamma_h[\mathbf{x}^*])}.\end{aligned}$$

Similarly as the proof of Lemma 3.5, for the nodal vector $\mathbf{e}_{\boldsymbol{\kappa},\mathbf{n}} = \overrightarrow{P_{\Gamma_h[\mathbf{x}^*]}(e_\kappa n_h^*)}$ we have

$$
\begin{aligned}
&\|\mathbf{e}_{\boldsymbol{\kappa},\mathbf{n}}\|_{\mathbf{A}(\mathbf{x}^*)} \\
&= \|\nabla_{\Gamma_h[\mathbf{x}^*]} P_{\Gamma_h[\mathbf{x}^*]}(e_\kappa n_h^*)\|_{L^2(\Gamma_h[\mathbf{x}^*])} \\
&\le \|\nabla_{\Gamma_h[\mathbf{x}^*]}(e_\kappa n_h^* - P_{\Gamma_h[\mathbf{x}^*]}(e_\kappa n_h^*))\|_{L^2(\Gamma_h[\mathbf{x}^*])} + \|\nabla_{\Gamma_h[\mathbf{x}^*]}(e_\kappa n_h^*)\|_{L^2(\Gamma_h[\mathbf{x}^*])} \\
&\le Ch\|\mathbf{e}_{\boldsymbol{\kappa}}\|_{\mathbf{K}(\mathbf{x}^*)}\|n_h^*\|_{W^{1,\infty}(\Gamma_h[\mathbf{x}^*])} + C\|\mathbf{e}_{\boldsymbol{\kappa}}\|_{\mathbf{K}(\mathbf{x}^*)}\|n_h^*\|_{W^{1,\infty}(\Gamma_h[\mathbf{x}^*])} \\
&\le Ch^{-1}\|\mathbf{e}_{\boldsymbol{\kappa}}\|_{\mathbf{M}(\mathbf{x}^*)} \qquad \text{(inverse inequality)} \\
&\le Ch^{-1}\|e_\kappa n_h^*\|_{L^2(\Gamma_h[\mathbf{x}^*])}.
\end{aligned}
$$

Then, by using (3.26)–(3.27) and the inequality above, we obtain

$$
\begin{aligned}
J_3^{\#} &= (\mathbf{A}(\mathbf{x}^*) - \mathbf{A}(\mathbf{x}))(\mathbf{v}^* + \mathbf{e}_\mathbf{v}) \cdot \mathbf{e}_{\boldsymbol{\kappa},\mathbf{n}} \\
&\le C\left(\|\mathbf{e}_\mathbf{x}\|_{\mathbf{A}(\mathbf{x}^*)} + h^{(k-1)/2}\|\mathbf{e}_\mathbf{v}\|_{\mathbf{A}(\mathbf{x}^*)}\right)\|\mathbf{e}_{\boldsymbol{\kappa},\mathbf{n}}\|_{\mathbf{A}(\mathbf{x}^*)} \\
&\le Ch^{-1}\left(\|\mathbf{e}_\mathbf{x}\|_{\mathbf{A}(\mathbf{x}^*)} + h^{(k-1)/2}\|\mathbf{e}_\mathbf{v}\|_{\mathbf{A}(\mathbf{x}^*)}\right)\|e_\kappa n_h^*\|_{L^2(\Gamma_h[\mathbf{x}^*])}.
\end{aligned}
$$

The last two terms in (3.66) can be estimated as follows:

$$
\begin{aligned}
J_4^{\#} + J_5^{\#} &\le C\|\mathbf{e}_\mathbf{v}\|_{\mathbf{A}(\mathbf{x}^*)}\|\mathbf{e}_{\boldsymbol{\kappa},\mathbf{n}}\|_{\mathbf{A}(\mathbf{x}^*)} + C\|\mathbf{d}_{\boldsymbol{\kappa}}\|_{\mathbf{M}(\mathbf{x}^*)}\|\mathbf{e}_{\boldsymbol{\kappa},\mathbf{n}}\|_{\mathbf{M}(\mathbf{x}^*)} \\
&\le Ch^{-1}\|\mathbf{e}_\mathbf{v}\|_{\mathbf{A}(\mathbf{x}^*)}\|e_\kappa n_h^*\|_{L^2(\Gamma_h[\mathbf{x}^*])} + C\|\mathbf{d}_{\boldsymbol{\kappa}}\|_{\mathbf{M}(\mathbf{x}^*)}\|e_\kappa n_h^*\|_{L^2(\Gamma_h[\mathbf{x}^*])}.
\end{aligned}
$$

Substituting the estimates of $J_1^{\#}$, $J_2^{\#}$, $J_3^{\#}$, $J_4^{\#}$ and $J_5^{\#}$ into (3.66), we obtain

$$
\begin{aligned}
&\|e_\kappa n_h^*\|_{L^2(\Gamma_h[\mathbf{x}^*])}^2 \\
&\le C\left(\|\mathbf{e}_\mathbf{n}\|_{\mathbf{M}(\mathbf{x}^*)} + h^{-1}\|\mathbf{e}_\mathbf{x}\|_{\mathbf{A}(\mathbf{x}^*)} + h^{-1}\|\mathbf{e}_\mathbf{v}\|_{\mathbf{A}(\mathbf{x}^*)}\right)\|e_\kappa n_h^*\|_{L^2(\Gamma_h[\mathbf{x}^*])} \\
&\quad + Ch^{\frac{1}{2}}\|\mathbf{e}_{\boldsymbol{\kappa}}\|_{\mathbf{M}(\mathbf{x}^*)}\|e_\kappa n_h^*\|_{L^2(\Gamma_h[\mathbf{x}^*])} + C\|\mathbf{d}_{\boldsymbol{\kappa}}\|_{\mathbf{M}(\mathbf{x}^*)}\|e_\kappa n_h^*\|_{L^2(\Gamma_h[\mathbf{x}^*])}.
\end{aligned}
$$

Since $\|\mathbf{e}_{\boldsymbol{\kappa}}\|_{\mathbf{M}(\mathbf{x}^*)} \sim \|e_\kappa n_h^*\|_{L^2(\Gamma_h[\mathbf{x}^*])}$, for sufficiently small h the term

$$
h^{\frac{1}{2}}\|\mathbf{e}_{\boldsymbol{\kappa}}\|_{\mathbf{M}(\mathbf{x}^*)}\|e_\kappa n_h^*\|_{L^2(\Gamma_h[\mathbf{x}^*])}
$$

on the right-hand side of the above inequality can be absorbed by the left-hand side. Therefore, the following inequality holds:

$$
\begin{aligned}
&\|\mathbf{e}_{\boldsymbol{\kappa}}\|_{\mathbf{M}(\mathbf{x}^*)} \\
&\le C(\|\mathbf{e}_\mathbf{u}\|_{\mathbf{M}(\mathbf{x}^*)} + h^{-1}\|\mathbf{e}_\mathbf{x}\|_{\mathbf{A}(\mathbf{x}^*)} + h^{-1}\|\mathbf{e}_\mathbf{v}\|_{\mathbf{A}(\mathbf{x}^*)} + \|\mathbf{d}_{\boldsymbol{\kappa}}\|_{\mathbf{M}(\mathbf{x}^*)}).
\end{aligned} \tag{3.68}
$$

(d) *Estimation of* $\|\mathbf{e}_\mathbf{v}\|_{\mathbf{A}(\mathbf{x}^*)}$. We reformulate (3.10c) as

$$
\begin{aligned}
\mathbf{B}(\mathbf{x},\mathbf{n})^\top \mathbf{e}_{\boldsymbol{\kappa}} + \mathbf{A}(\mathbf{x})\mathbf{e}_\mathbf{v} = (&\mathbf{B}(\mathbf{x}^*,\mathbf{n}^*)^\top - \mathbf{B}(\mathbf{x},\mathbf{n})^\top)\boldsymbol{\kappa}^* \\
&+ (\mathbf{A}(\mathbf{x}^*) - \mathbf{A}(\mathbf{x}))\mathbf{v}^* - \mathbf{M}(\mathbf{x}^*)\mathbf{d}_{\boldsymbol{\kappa}},
\end{aligned}
$$

and test the above equation by $\mathbf{P}_\tau(\mathbf{x},\mathbf{n})\mathbf{e_v} = \overrightarrow{P_{\Gamma_h[\mathbf{x}]}P_\tau e_v^1}$, where e_v^1 is the finite element function on $\Gamma_h[\mathbf{x}]$ with nodal vector $\mathbf{e_v}$. Then we obtain

$$\begin{aligned}\|\mathbf{e_v}\|_{\mathbf{A}(\mathbf{x})}^2 &= \mathbf{A}(\mathbf{x})\mathbf{e_v}\cdot(\mathbf{e_v}-\mathbf{P}_\tau(\mathbf{x},\mathbf{n})\mathbf{e_v})\\ &\quad -\mathbf{B}(\mathbf{x},\mathbf{n})^\top\mathbf{e}_{\boldsymbol{\kappa}}\cdot\mathbf{P}_\tau(\mathbf{x},\mathbf{n})\mathbf{e_v}\\ &\quad +(\mathbf{B}(\mathbf{x}^*,\mathbf{n}^*)^\top-\mathbf{B}(\mathbf{x},\mathbf{n})^\top)\boldsymbol{\kappa}^*\cdot\mathbf{P}_\tau(\mathbf{x},\mathbf{n})\mathbf{e_v}\\ &\quad +(\mathbf{A}(\mathbf{x}^*)-\mathbf{A}(\mathbf{x}))\mathbf{v}^*\cdot\mathbf{P}_\tau(\mathbf{x},\mathbf{n})\mathbf{e_v}\\ &\quad -\mathbf{M}(\mathbf{x}^*)\mathbf{d}_{\boldsymbol{\kappa}}\cdot\mathbf{P}_\tau(\mathbf{x},\mathbf{n})\mathbf{e_v}\\ &=: J_1^\star+J_2^\star+J_3^\star+J_4^\star+J_5^\star. \end{aligned}\tag{3.69}$$

By using (3.46), (3.30) and (3.26), we have

$$\begin{aligned} J_1^\star &\le \|\mathbf{e_v}\|_{\mathbf{A}(\mathbf{x})}\|\mathbf{e_v}-\mathbf{P}_\tau(\mathbf{x},\mathbf{n})\mathbf{e_v}\|_{\mathbf{A}(\mathbf{x})}\\ &\le C\|\mathbf{e_v}\|_{\mathbf{A}(\mathbf{x}^*)}\big(\|e_v\cdot n_h^*\|_{H^1(\Gamma_h[\mathbf{x}^*])}+h^{\frac12}\|\mathbf{e_v}\|_{\mathbf{K}(\mathbf{x}^*)}\big), \end{aligned}\tag{3.70}$$

$$J_3^\star \le C\left(\|\mathbf{e_n}\|_{\mathbf{M}(\mathbf{x}^*)}+\|\mathbf{e_x}\|_{\mathbf{A}(\mathbf{x}^*)}\right)\|\mathbf{e_v}\|_{\mathbf{M}(\mathbf{x}^*)},\tag{3.71}$$

$$J_4^\star \le C\|\mathbf{e_x}\|_{\mathbf{A}(\mathbf{x}^*)}\|\mathbf{e_v}\|_{\mathbf{K}(\mathbf{x}^*)},\tag{3.72}$$

$$J_5^\star \le C\|\mathbf{d}_{\boldsymbol{\kappa}}\|_{\mathbf{M}(\mathbf{x}^*)}\|\mathbf{e_v}\|_{\mathbf{M}(\mathbf{x}^*)}.\tag{3.73}$$

Since $P_\tau e_v^1$ is approximately perpendicular to n_h, we decompose $J_2^\star$ into the following two parts:

$$J_2^\star = \int_{\Gamma_h[\mathbf{x}]} e_\kappa^1 n_h^1\cdot(P_\tau e_v^1 - P_{\Gamma_h[\mathbf{x}]}P_\tau e_v^1) - \int_{\Gamma_h[\mathbf{x}]} e_\kappa^1 n_h^1\cdot P_\tau e_v^1.\tag{3.74}$$

The first term in (3.74) can be estimated by using the generalized norm equivalence as in (3.49) and the superconvegence property, i.e.,

$$\begin{aligned}&\int_{\Gamma_h[\mathbf{x}]} e_\kappa^1 n_h^1\cdot(P_\tau e_v^1 - P_{\Gamma_h[\mathbf{x}]}P_\tau e_v^1)\\ &\le \|e_\kappa^1 n_h^1\|_{L^2(\Gamma_h[\mathbf{x}])}\|P_\tau e_v^1 - P_{\Gamma_h[\mathbf{x}]}P_\tau e_v^1\|_{L^2(\Gamma_h[\mathbf{x}])}\\ &\le C\|e_\kappa^1 n_h^1\|_{L^2(\Gamma_h[\mathbf{x}])}\|(e_v\cdot n_h^0)n_h^0 - I_{\Gamma_h[\mathbf{x}^*]}(e_v\cdot n_h^0)n_h^0\|_{L^2(\Gamma_h[\mathbf{x}^*])}\\ &\le Ch^2\|e_\kappa^1 n_h^1\|_{L^2(\Gamma_h[\mathbf{x}])}\|e_v\|_{H^1(\Gamma_h[\mathbf{x}^*])}\\ &\le Ch^2\|\mathbf{e}_{\boldsymbol{\kappa}}\|_{\mathbf{M}(\mathbf{x}^*)}\|\mathbf{e_v}\|_{\mathbf{K}(\mathbf{x}^*)}.\end{aligned}$$

The second term in (3.74) can be estimated as follows:

$$\begin{aligned}&-\int_{\Gamma_h[\mathbf{x}]} e_\kappa^1 n_h^1\cdot P_\tau e_v^1\\ &=\int_{\Gamma_h[\mathbf{x}]}(e_\kappa^1 n_h^1\cdot e_v^1)(|n_h^1|^2-1)\\ &\le C\|e_\kappa n_h^0\|_{L^2(\Gamma_h[\mathbf{x}^*])}\|e_v\|_{L^2(\Gamma_h[\mathbf{x}^*])}\||n_h^1|^2-1\|_{L^\infty(\Gamma_h[\mathbf{x}])}\\ &\le C\|e_\kappa n_h^0\|_{L^2(\Gamma_h[\mathbf{x}^*])}\|e_v\|_{L^2(\Gamma_h[\mathbf{x}^*])}\||n_h^0|^2-1\|_{L^\infty(\Gamma_h[\mathbf{x}^*])}\\ &\le C\|e_\kappa n_h^0\|_{L^2(\Gamma_h[\mathbf{x}^*])}\|e_v\|_{L^2(\Gamma_h[\mathbf{x}^*])}(Ch^2+\|e_n(n_h^0+n_h^*)\|_{L^\infty(\Gamma_h[\mathbf{x}^*])})\\ &\le Ch^{1.5}\|\mathbf{e}_{\boldsymbol{\kappa}}\|_{\mathbf{M}(\mathbf{x}^*)}\|\mathbf{e_v}\|_{\mathbf{M}(\mathbf{x}^*)},\end{aligned}\tag{3.75}$$

where the last two inequalities in (3.75) use (3.67) and (3.57). The two estimates above imply that

$$
\begin{aligned}
J_2^\star &\le Ch^{1.5}\|\mathbf{e}_{\boldsymbol{\kappa}}\|_{\mathbf{M}(\mathbf{x}^*)}\|\mathbf{e}_{\mathbf{v}}\|_{\mathbf{K}(\mathbf{x}^*)} \\
&\le C(h^{1.5}\|\mathbf{e}_{\mathbf{u}}\|_{\mathbf{M}(\mathbf{x}^*)} + h^{0.5}\|\mathbf{e}_{\mathbf{x}}\|_{\mathbf{A}(\mathbf{x}^*)})\|\mathbf{e}_{\mathbf{v}}\|_{\mathbf{K}(\mathbf{x}^*)} \\
&\quad + C(h^{0.5}\|\mathbf{e}_{\mathbf{v}}\|_{\mathbf{A}(\mathbf{x}^*)} + h^{1.5}\|\mathbf{d}_{\boldsymbol{\kappa}}\|_{\mathbf{M}(\mathbf{x}^*)})\|\mathbf{e}_{\mathbf{v}}\|_{\mathbf{K}(\mathbf{x}^*)}, \qquad (3.76)
\end{aligned}
$$

where the last inequality follows from (3.68).

Substituting (3.70)–(3.76) into (3.69) and using (3.65), we obtain

$$
\begin{aligned}
&\|\mathbf{e}_{\mathbf{v}}\|^2_{\mathbf{A}(\mathbf{x}^*)} \\
&\le C\|\mathbf{e}_{\mathbf{v}}\|^2_{\mathbf{A}(\mathbf{x})} \\
&\le C\|e_v\cdot n_h^*\|_{H^1(\Gamma_h[\mathbf{x}^*])}\|\mathbf{e}_{\mathbf{v}}\|_{\mathbf{A}(\mathbf{x}^*)} + Ch^{\frac12}\|\mathbf{e}_{\mathbf{v}}\|^2_{\mathbf{K}(\mathbf{x}^*)} \\
&\quad + C(\|\mathbf{e}_{\mathbf{u}}\|_{\mathbf{M}(\mathbf{x}^*)} + \|\mathbf{e}_{\mathbf{x}}\|_{\mathbf{A}(\mathbf{x}^*)} + \|\mathbf{d}_{\boldsymbol{\kappa}}\|_{\mathbf{M}(\mathbf{x}^*)})\|\mathbf{e}_{\mathbf{v}}\|_{\mathbf{K}(\mathbf{x}^*)} \\
&\le C(\epsilon^{\frac12} + \epsilon^{-\frac12}h^{\frac12})\|\mathbf{e}_{\mathbf{v}}\|^2_{\mathbf{K}(\mathbf{x}^*)} \\
&\quad + C\epsilon^{-\frac32}(\|\mathbf{e}_{\mathbf{u}}\|_{\mathbf{K}(\mathbf{x}^*)} + \|\mathbf{e}_{\mathbf{x}}\|_{\mathbf{A}(\mathbf{x}^*)} + \|\mathbf{d}_{\mathbf{v}}\|_{\mathbf{M}(\mathbf{x}^*)} + \|\widetilde{\mathbf{d}}_{\mathbf{v}}\|_{\star,\mathbf{x}^*} + \|\mathbf{d}_{\boldsymbol{\kappa}}\|_{\mathbf{M}(\mathbf{x}^*)})^2 \\
&\le C(\epsilon^{\frac12} + \epsilon^{-\frac12}h^{\frac12})\|\mathbf{e}_{\mathbf{v}}\|^2_{\mathbf{A}(\mathbf{x}^*)} \\
&\quad + C\epsilon^{-\frac32}(\|\mathbf{e}_{\mathbf{u}}\|_{\mathbf{K}(\mathbf{x}^*)} + \|\mathbf{e}_{\mathbf{x}}\|_{\mathbf{A}(\mathbf{x}^*)} + \|\mathbf{d}_{\mathbf{v}}\|_{\mathbf{M}(\mathbf{x}^*)} + \|\widetilde{\mathbf{d}}_{\mathbf{v}}\|_{\star,\mathbf{x}^*} + \|\mathbf{d}_{\boldsymbol{\kappa}}\|_{\mathbf{M}(\mathbf{x}^*)})^2,
\end{aligned}
$$

where the last inequality uses (3.62). By first choosing a sufficiently small constant ϵ and then choosing sufficiently small h_0 compared to ϵ, the term $C(\epsilon^{\frac12} + \epsilon^{-\frac12}h^{\frac12})\|\mathbf{e}_{\mathbf{v}}\|^2_{\mathbf{A}(\mathbf{x}^*)}$ can be absorbed by the left-hand side of the above inequality. Therefore, we obtain

$$
\|\mathbf{e}_{\mathbf{v}}\|_{\mathbf{A}(\mathbf{x}^*)} \le C(\|\mathbf{e}_{\mathbf{u}}\|_{\mathbf{K}(\mathbf{x}^*)} + \|\mathbf{e}_{\mathbf{x}}\|_{\mathbf{A}(\mathbf{x}^*)} + \|\mathbf{d}_{\mathbf{v}}\|_{\mathbf{M}(\mathbf{x}^*)} + \|\widetilde{\mathbf{d}}_{\mathbf{v}}\|_{\star,\mathbf{x}^*} + \|\mathbf{d}_{\boldsymbol{\kappa}}\|_{\mathbf{M}(\mathbf{x}^*)}). \qquad (3.77)
$$

Then substituting (3.77) into (3.62) yields the desired result of Theorem 3.2. □

3.6 Estimates for the defects (consistency errors)

The following estimates for the geometric perturbation errors were proved in [39, Lemma 5.6] and will be used in estimating the consistency errors, i.e., $\|\mathbf{d}_{\mathbf{v}}\|_{\mathbf{M}(\mathbf{x}^*)}$, $\|\widetilde{\mathbf{d}}_{\mathbf{v}}\|_{\star,\mathbf{x}^*}$ and $\|\mathbf{d}_{\boldsymbol{\kappa}}\|_{\mathbf{M}(\mathbf{x}^*)}$.

Lemma 3.6 *Under the assumptions of Theorem 2.1, there exists a positive constant $h_0 > 0$ such that for $h \le h_0$ the following estimates hold for all*

$w_h, \varphi_h \in S_h[\mathbf{x}^*]$:

$$\left| \int_{\Gamma_h[\mathbf{x}^*]} w_h \varphi_h - \int_{\Gamma[X]} w_h^\ell \varphi_h^\ell \right| \le C h^{k+1} \| w_h^\ell \|_{L^2(\Gamma[X])} \| \varphi_h^\ell \|_{L^2(\Gamma[X])},$$
$$\left| \int_{\Gamma_h[\mathbf{x}^*]} \nabla_{\Gamma_h[\mathbf{x}^*]} w_h \cdot \nabla_{\Gamma_h[\mathbf{x}^*]} \varphi_h - \int_{\Gamma[X]} \nabla_{\Gamma[X]} w_h^\ell \cdot \nabla_{\Gamma[X]} \varphi_h^\ell \right|$$
$$\le C h^{k+1} \| \nabla_{\Gamma[X]} w_h^\ell \|_{L^2(\Gamma[X])} \| \nabla_{\Gamma[X]} \varphi_h^\ell \|_{L^2(\Gamma[X])}.$$

Remark 3.5 In fact, Lemma 3.6 holds for any $w_h, \varphi_h \in H^1(\Gamma_h[\mathbf{x}^*])$. Utilizing $(w_h \cdot n_h)^\ell = w_h^\ell \cdot n_h^\ell$, the results of Lemma 3.6 can also be generalized to the products of three functions:

$$\left| \int_{\Gamma_h[\mathbf{x}^*]} (w_h \cdot n_h) \varphi_h - \int_{\Gamma[X]} (w_h^\ell \cdot n_h^\ell) \varphi_h^\ell \right|$$
$$\le C h^{k+1} \| w_h^\ell \cdot n_h^\ell \|_{L^2(\Gamma[X])} \| \varphi_h^\ell \|_{L^2(\Gamma[X])}, \tag{3.78}$$

and

$$\left| \int_{\Gamma_h[\mathbf{x}^*]} \nabla_{\Gamma_h[\mathbf{x}^*]} (w_h \cdot n_h) \cdot \nabla_{\Gamma_h[\mathbf{x}^*]} \varphi_h - \int_{\Gamma[X]} \nabla_{\Gamma[X]} (w_h^\ell \cdot n_h^\ell) \cdot \nabla_{\Gamma[X]} \varphi_h^\ell \right|$$
$$\le C h^{k+1} \| \nabla_{\Gamma[X]} (w_h^\ell \cdot n_h^\ell) \|_{L^2(\Gamma[X])} \| \nabla_{\Gamma[X]} \varphi_h^\ell \|_{L^2(\Gamma[X])}, \tag{3.79}$$

with $w_h, n_h \in S_h[\mathbf{x}^*]^3$ and $\varphi_h \in S_h[\mathbf{x}^*]$.

The upper bounds for the consistency errors are presented in the following lemma and proved by using Lemma 3.6 and (3.78)–(3.79).

Lemma 3.7 *Under the assumptions of Theorem 2.1, there exist positive constants $h_0 > 0$ and $C > 0$ such that for $h \le h_0$ and $t \in [0, T]$ the defects in (3.10b)–(3.10c) are bounded by*

$$\| \widetilde{\mathbf{d}}_\mathbf{v} \|_{\star, \mathbf{x}^*} = \| \widetilde{d}_v \|_{H_h^{-1}(\Gamma_h[\mathbf{x}^*])} \le C h^k, \quad \| \mathbf{d}_\mathbf{v} \|_{\mathbf{M}(\mathbf{x}^*)} = \| d_v \|_{L^2(\Gamma_h[\mathbf{x}^*])} \le C h^k,$$
$$\| \mathbf{d}_\mathbf{u} \|_{\mathbf{M}(\mathbf{x}^*)} = \| d_u \|_{L^2(\Gamma_h[\mathbf{x}^*])} \le C h^k, \qquad \| \mathbf{d}_{\boldsymbol{\kappa}} \|_{\mathbf{M}(\mathbf{x}^*)} = \| d_\kappa \|_{L^2(\Gamma_h[\mathbf{x}^*])} \le C h^k,$$

where the constant C is independent of h and $t \in [0, T]$.

Proof Subtracting the following equation (satisfied by the exact solution) from (3.12),

$$0 = \int_{\Gamma[X]} \nabla_{\Gamma[X]} (v \cdot n) \cdot \nabla_{\Gamma[X]} \chi_\kappa^\ell + \int_{\Gamma[X]} \nabla_{\Gamma[X]} H \cdot \nabla_{\Gamma[X]} \chi_\kappa^\ell,$$

we obtain

$$\int_{\Gamma_h[\mathbf{x}^*]} \widetilde{d}_v \chi_\kappa = \int_{\Gamma_h[\mathbf{x}^*]} \nabla_{\Gamma_h[\mathbf{x}^*]}(v_h^* \cdot n_h^*) \cdot \nabla_{\Gamma_h[\mathbf{x}^*]}\chi_\kappa \tag{3.80}$$
$$- \int_{\Gamma[X]} \nabla_{\Gamma[X]}(v \cdot n) \cdot \nabla_{\Gamma[X]}\chi_\kappa^\ell$$
$$+ \int_{\Gamma_h[\mathbf{x}^*]} \nabla_{\Gamma_h[\mathbf{x}^*]} H_h^* \cdot \nabla_{\Gamma_h[\mathbf{x}^*]}\chi_\kappa - \int_{\Gamma[X]} \nabla_{\Gamma[X]} H \cdot \nabla_{\Gamma[X]}\chi_\kappa^\ell$$
$$- \int_{\Gamma_h[\mathbf{x}^*]} \nabla_{\Gamma_h[\mathbf{x}^*]}[v_h^* \cdot n_h^* - P_{\Gamma_h[\mathbf{x}^*]}(v_h^* \cdot n_h^*)] \cdot \nabla_{\Gamma_h[\mathbf{x}^*]}\chi_\kappa.$$

By using the geometric perturbation errors in Lemma 3.6 and error estimate for the Ritz projection in (3.3), we obtain

$$\left| \int_{\Gamma_h[\mathbf{x}^*]} \nabla_{\Gamma_h[\mathbf{x}^*]} H_h^* \cdot \nabla_{\Gamma_h[\mathbf{x}^*]}\chi_\kappa - \int_{\Gamma[X]} \nabla_{\Gamma[X]} H \cdot \nabla_{\Gamma[X]}\chi_\kappa^\ell \right|$$
$$\leq \left(Ch^{k+1} + \|\nabla_{\Gamma[X]}(H_h^{*,\ell} - H)\|_{L^2(\Gamma[X])} \right) \|\nabla_{\Gamma[X]}\chi_\kappa^\ell\|_{L^2(\Gamma[X])}$$
$$\leq Ch^k \|\nabla_{\Gamma[X]}\chi_\kappa^\ell\|_{L^2(\Gamma[X])}.$$

The first term on the right-hand side of (3.80) can be estimated similarly by using (3.79). The last term on the right-hand side of (3.80) can be estimated by following the technique of (A.12) and using boundedness of the Ritz projections $\|v_h^*\|_{W_h^{k,\infty}}$ and $\|n_h^*\|_{W_h^{k,\infty}}$, see (3.4). Then we obtain

$$\left| \int_{\Gamma_h[\mathbf{x}^*]} \widetilde{d}_v \chi_\kappa \right| \leq Ch^k \|\chi_\kappa\|_{H^1(\Gamma_h[\mathbf{x}^*])}.$$

This proves that

$$\|\widetilde{\mathbf{d}}_\mathbf{v}\|_{\star,\mathbf{x}^*} \leq Ch^k.$$

Similarly, subtracting the following equation (satisfied by the exact solution) from (3.6),

$$\int_{\Gamma[X]} (v \cdot n)\chi_\kappa^\ell + \int_{\Gamma[X]} H\chi_\kappa^\ell = 0,$$

and then using Lemma 3.6 and (3.78), we have

$$\int_{\Gamma_h[\mathbf{x}^*]} d_v \chi_\kappa$$
$$= \int_{\Gamma_h[\mathbf{x}^*]} (v_h^* \cdot n_h^*)\chi_\kappa - \int_{\Gamma[X]} (v \cdot n)\chi_\kappa^\ell + \int_{\Gamma_h[\mathbf{x}^*]} H_h^* \chi_\kappa - \int_{\Gamma[X]} H\chi_\kappa^\ell$$
$$\leq \left(Ch^{k+1} + \|v_h^{*,\ell} \cdot n_h^{*,\ell} - v \cdot n\|_{L^2(\Gamma[X])} + \|H_h^{*,\ell} - H\|_{L^2(\Gamma[X])} \right) \|\chi_\kappa^\ell\|_{L^2(\Gamma[X])}$$
$$\leq Ch^k \|\chi_\kappa^\ell\|_{L^2(\Gamma[X])}.$$

This proves that

$$\|\mathbf{d_v}\|_{\mathbf{M}(\mathbf{x}^*)} \leq Ch^k.$$

Similarly, subtracting the following equation (satisfied by the exact solution) from (3.7),

$$\int_{\Gamma[X]} \kappa n \cdot \chi_v^\ell + \int_{\Gamma[X]} \nabla_{\Gamma[X]} v \cdot \nabla_{\Gamma[X]} \chi_v^\ell = 0,$$

we obtain

$$\begin{aligned}\int_{\Gamma_h[\mathbf{x}^*]} d_\kappa \chi_v = &\int_{\Gamma_h[\mathbf{x}^*]} \kappa_h^* n_h^* \cdot \chi_v - \int_{\Gamma[X]} \kappa n \cdot \chi_v^\ell \\ &+ \int_{\Gamma_h[\mathbf{x}^*]} \nabla_{\Gamma_h[\mathbf{x}^*]} v_h^* \cdot \nabla_{\Gamma_h[\mathbf{x}^*]} \chi_v - \int_{\Gamma[X]} \nabla_{\Gamma[X]} v \cdot \nabla_{\Gamma[X]} \chi_v^\ell.\end{aligned}$$

Since v_h^* is the Ritz projection of v defined in (3.2), the last line of the above equality equals

$$- \int_{\Gamma_h[\mathbf{x}^*]} v_h^* \cdot \chi_v + \int_{\Gamma[X]} v \cdot \chi_v^\ell . \tag{3.81}$$

This removes the gradient in the consistency error associated to d_κ. Therefore, we obtain

$$\|\mathbf{d}_{\boldsymbol{\kappa}}\|_{\mathbf{M}(\mathbf{x}^*)} \leq Ch^k.$$

The estimate for $\|\mathbf{d_u}\|_{\mathbf{M}(\mathbf{x}^*)}$ is the same as that given in [40, Section 8]. The proof of Lemma 3.7 is complete. □

3.7 Error estimates

If $\mathbf{x}(0)$, $\mathbf{n}(0)$ and $\mathbf{H}(0)$ are obtained from interpolation or other approximation satisfying (2.3), then the following estimates hold at $t = 0$ for sufficiently small h (as a result of the inverse inequality):

$$\|e_x\|_{W^{1,\infty}(\Gamma_h[\mathbf{x}^*])} \leq \frac{1}{2} h^{(k-1)/2}, \tag{3.82a}$$

$$\|e_u\|_{W^{1,\infty}(\Gamma_h[\mathbf{x}^*])} \leq \frac{1}{2} h^{(k-1)/2}, \tag{3.82b}$$

$$\|e_u\|_{L^\infty(\Gamma_h[\mathbf{x}^*])} \leq \frac{1}{2} h^{(k+1)/2}. \tag{3.82c}$$

With the finite element discretization in space, (2.2) is essentially an ordinary differential equation (ODE) which has a unique solution locally in time. If the solution exists and satisfying (3.82) for $t \in [0, t_*)$, then the solution remains bounded as $t \to t_*$ in view of (3.82). As a result, the solution exists and satisfying (3.82) for $t \in [0, t_*]$. We denote by $t_* \in [0, T]$ the maximal value such that the solution exists and satisfying (3.82) for $t \in [0, t_*]$.

If $t_* = T$ then we set $\delta = 0$.

If $t_* < T$ then, by the local existence of solutions to ODEs, the solution continues to exist and satisfying the following estimates in a bigger interval $[0, t_* + \delta]$:

$$
\begin{aligned}
&\|e_x\|_{W^{1,\infty}(\Gamma_h[\mathbf{x}^*])} \le h^{(k-1)/2},\\
&\|e_u\|_{W^{1,\infty}(\Gamma_h[\mathbf{x}^*])} \le h^{(k-1)/2},\\
&\|e_u\|_{L^\infty(\Gamma_h[\mathbf{x}^*])} \le h^{(k+1)/2}.
\end{aligned}
$$

for some number $\delta > 0$ which may depend on h.

In both cases, the stability estimate in Theorem 3.2 and (3.52)–(3.53) hold for $t \in [0, t_* + \delta]$. By substituting (3.54) into (3.52) + $\epsilon\times$(3.53), we obtain the following result for $t \in [0, t_* + \delta]$:

$$
\begin{aligned}
\|\mathbf{e_x}(t)\|_{\mathbf{K}(\mathbf{x}^*(t))}^2 + \epsilon\, \|\mathbf{e_u}(t)\|_{\mathbf{K}(\mathbf{x}^*(t))}^2 \le{}& C \int_0^t \big(\|\mathbf{e_x}(s)\|_{\mathbf{K}(\mathbf{x}^*)}^2 + \|\mathbf{e_u}(s)\|_{\mathbf{K}(\mathbf{x}^*)}^2 \big) \mathrm{d}s \\
&+ C \int_0^t \big(\|\mathbf{d_v}(s)\|_{\mathbf{M}(\mathbf{x}^*)}^2 + \|\widetilde{\mathbf{d}}_{\mathbf{v}}(s)\|_{\star,\mathbf{x}^*}^2\big) \mathrm{d}s \\
&+ C \int_0^t \big(\|\mathbf{d}_{\boldsymbol{\kappa}}(s)\|_{\mathbf{M}(\mathbf{x}^*)}^2 + \|\mathbf{d_u}(s)\|_{\mathbf{M}(\mathbf{x}^*)}^2\big) \mathrm{d}s \\
&+ C\epsilon\, \|\mathbf{e_x}(t)\|_{\mathbf{K}(\mathbf{x}^*(t))}^2 + C\epsilon\, \|\mathbf{e_u}(0)\|_{\mathbf{K}(\mathbf{x}^*(0))}^2 .
\end{aligned}
\tag{3.83}
$$

By choosing a sufficiently small constant ϵ, the term $C\epsilon\, \|\mathbf{e_x}(t)\|_{\mathbf{K}(\mathbf{x}^*(t))}^2$ can be absorbed by the left-hand side. Then we can apply the Gronwall's inequality and use the consistency error bounds in Lemma 3.7. This yields the following error bound:

$$
\|\mathbf{e_x}(t)\|_{\mathbf{K}(\mathbf{x}^*(t))} + \|\mathbf{e_u}(t)\|_{\mathbf{K}(\mathbf{x}^*(t))} \le Ch^k \quad \text{for } t \in [0, t_* + \delta]. \tag{3.84}
$$

Substituting this result into (3.54), we also obtain

$$
\|\mathbf{e_v}(t)\|_{\mathbf{K}(\mathbf{x}^*(t))} \le Ch^k \quad \text{for } t \in [0, t_* + \delta]. \tag{3.85}
$$

Since the two dimensional closed surface $\Gamma(t)$ is compact, it is direct to prove the Sobolev embedding in the borderline case, i.e, $H^1(\Gamma(t)) \subset L^p(\Gamma(t))$ for $2 \le p < \infty$, by following the technique of partition of unity in [36, Theorem 3.5] and [51, Chapter V]. By using the norm equivalence of lift (2.14) and the dependence of Sobolev constant on p analyzed in [52, Lemma 6.4], we obtain

$$
\|e_u\|_{L^p(\Gamma_h[\mathbf{x}^*])} \le C\|e_u^\ell\|_{L^p(\Gamma(t))} \le Cp^{1/2}\|e_u^\ell\|_{H^1(\Gamma(t))} \le Cp^{1/2}\|e_u\|_{H^1(\Gamma_h[\mathbf{x}^*])},
$$

for all $2 \le p < \infty$, where C is a constant independent of p. Combining the inverse inequality as in [52, Lemma 6.4], and choosing $p = \log(1/h)$, we obtain

$$
\begin{aligned}
\|e_u\|_{L^\infty(\Gamma_h[\mathbf{x}^*])} &\le Ch^{-2/p}\|e_u\|_{L^p(\Gamma_h[\mathbf{x}^*])} \le Ch^{-2/p}p^{1/2}\|e_u\|_{H^1(\Gamma_h[\mathbf{x}^*])} \\
&\le C\left(\log(1/h)\right)^{1/2} \|\mathbf{e_u}\|_{\mathbf{K}(\mathbf{x}^*)} \le C\left(\log(1/h)\right)^{1/2} h^k.
\end{aligned}
$$

Thus, there exists a positive constant h_0 (independent of t_* and δ) such that for $h \le h_0$ the above error estimates imply that (3.82) holds for $t \in [0, t_*+\delta]$. Since $t_* \in [0, T]$ is the maximal number such that (3.82) holds for $t \in [0, t_*]$, it follows that $t_* = T$ when $h \le h_0$. Therefore, the error bounds in (3.84)–(3.85) hold for all $t \in [0, T]$. This can be combined with the error estimates for the Ritz projection and the interpolation (see Theorem 3.1 and [23, Proposition 2.7]) to yield the desired results in Theorem 2.1. □

4 Proof of Theorem 2.2

Theorem 2.2 can be proved similarly as Theorem 2.1 by combining the stability results in Theorem 3.2 and [41]. For simplicity, we present the stability estimates under the assumption that the errors in L^∞ and $W^{1,\infty}$ norms are sufficiently small. This can be made rigorous by using the arguments in Section 3.7 with similar assumptions as (3.82).

The error equations for the modified evolving surface FEM in (2.12) can be written into the following matrix-vector form:

$$\dot{\mathbf{e}}_{\mathbf{x}} = \mathbf{e}_{\mathbf{v}}, \tag{4.1a}$$

$$\begin{aligned}\mathbf{B}(\mathbf{x}^*, \mathbf{n}^*)\mathbf{e}_{\mathbf{v}} &= (\mathbf{B}(\mathbf{x}^*, \mathbf{n}^*) - \mathbf{B}(\mathbf{x}, \mathbf{n}))\mathbf{v} \\ &\quad + \mathbf{M}(\mathbf{x}^*)\mathbf{e}_{\mathbf{V}} - (\mathbf{M}(\mathbf{x}^*) - \mathbf{M}(\mathbf{x}))\mathbf{V} - \mathbf{M}(\mathbf{x}^*)\mathbf{d}_{\mathbf{v}},\end{aligned} \tag{4.1b}$$

$$\begin{aligned}\mathbf{B}(\mathbf{x}^*, \mathbf{n}^*)^\top \mathbf{e}_{\boldsymbol{\kappa}} + \mathbf{A}(\mathbf{x}^*)\mathbf{e}_{\mathbf{v}} &= (\mathbf{B}(\mathbf{x}^*, \mathbf{n}^*)^\top - \mathbf{B}(\mathbf{x}, \mathbf{n})^\top)\boldsymbol{\kappa} \\ &\quad + (\mathbf{A}(\mathbf{x}^*) - \mathbf{A}(\mathbf{x}))\mathbf{v} - \mathbf{M}(\mathbf{x}^*)\mathbf{d}_{\boldsymbol{\kappa}},\end{aligned} \tag{4.1c}$$

$$\begin{aligned}\mathbf{M}(\mathbf{x})\dot{\mathbf{e}}_{\mathbf{u}} - \mathbf{A}(\mathbf{x})\mathbf{e}_{\mathbf{w}} = &- \big(\mathbf{M}(\mathbf{x}) - \mathbf{M}(\mathbf{x}^*)\big)\dot{\mathbf{u}}^* + \big(\mathbf{A}(\mathbf{x}) - \mathbf{A}(\mathbf{x}^*)\big)\mathbf{w}^* \\ &+ \big(\mathbf{F}(\mathbf{x}, \mathbf{u})\mathbf{w} - \mathbf{F}(\mathbf{x}^*, \mathbf{u}^*)\mathbf{w}^*\big) \\ &+ \big(\mathbf{f}^{\mathrm{W}}(\mathbf{x}, \mathbf{u}, \mathbf{v}) - \mathbf{f}^{\mathrm{W}}(\mathbf{x}^*, \mathbf{u}^*, \mathbf{v}^*)\big) \\ &- \mathbf{M}(\mathbf{x}^*)\mathbf{d}_{\mathbf{u}},\end{aligned} \tag{4.1d}$$

$$\begin{aligned}\mathbf{M}(\mathbf{x})\mathbf{e}_{\mathbf{w}} + \mathbf{A}(\mathbf{x})\mathbf{e}_{\mathbf{u}} = &- \big(\mathbf{M}(\mathbf{x}) - \mathbf{M}(\mathbf{x}^*)\big)\mathbf{w}^* - \big(\mathbf{A}(\mathbf{x}) - \mathbf{A}(\mathbf{x}^*)\big)\mathbf{u}^* \\ &+ \big(\mathbf{g}(\mathbf{x}, \mathbf{u}) - \mathbf{g}(\mathbf{x}^*, \mathbf{u}^*)\big) - \mathbf{M}(\mathbf{x}^*)\mathbf{d}_{\mathbf{w}} \\ &+ \mathbf{M}(\mathbf{x}(0))\, \bar{\mathbf{e}}_{\mathbf{w}}(0),\end{aligned} \tag{4.1e}$$

where (4.1d)–(4.1e) are taken from [41, equation (5.16)] with an additional dependence of $\mathbf{f}^{\mathrm{W}}$ on velocity, and $\bar{\mathbf{e}}_{\mathbf{w}}(0) = \bar{\mathbf{w}}^*(0) - \bar{\mathbf{w}}(0)$. Note that $\bar{\mathbf{w}}^*$ denotes the vector which consists of the values of the exact solution $w = (V, z)^\top$ at the nodes, whereas $\mathbf{w}^*$ is constructed in [41] as a Ritz projection of w.

The following stability estimate for (4.1d)–(4.1e) was proved in [41, §5.4, Part (A.3)]. The additional dependence of $\mathbf{f}^{\mathrm{W}}$ on velocity brings no essential difference.

$$
\begin{aligned}
&\|\mathbf{e_u}(t)\|^2_{\mathbf{K}(\mathbf{x}^*(t))} + \|\mathbf{e_w}(t)\|^2_{\mathbf{K}(\mathbf{x}^*(t))} \\
&\leq C\int_0^t \Big(\|\mathbf{e_x}(s)\|^2_{\mathbf{K}(\mathbf{x}^*(s))} + \|\mathbf{e_v}(s)\|^2_{\mathbf{K}(\mathbf{x}^*(s))}\Big)\mathrm{d}s \\
&\quad + C\int_0^t \Big(\|\mathbf{e_u}(s)\|^2_{\mathbf{K}(\mathbf{x}^*(s))} + \|\mathbf{e_w}(s)\|^2_{\mathbf{K}(\mathbf{x}^*(s))}\Big)\mathrm{d}s \\
&\quad + C\int_0^t \Big(\|\mathbf{d_u}(s)\|^2_{\mathbf{M}(\mathbf{x}^*(s))} + \|\dot{\mathbf{d}}_\mathbf{u}(s)\|^2_{\star,\mathbf{x}^*(s)}\Big)\mathrm{d}s \\
&\quad + C\int_0^t \Big(\|\mathbf{d_w}(s)\|^2_{\mathbf{M}(\mathbf{x}^*(s))} + \|\dot{\mathbf{d}}_\mathbf{w}(s)\|^2_{\star,\mathbf{x}^*(s)}\Big)\mathrm{d}s \\
&\quad + C\|\mathbf{e_x}(t)\|^2_{\mathbf{K}(\mathbf{x}^*(t))} + C\|\mathbf{d_u}(t)\|^2_{\star,\mathbf{x}^*(t)} \\
&\quad + C\big(\|\mathbf{e_u}(0)\|^2_{\mathbf{K}(\mathbf{x}^0)} + \|\mathbf{e_w}(0)\|^2_{\mathbf{K}(\mathbf{x}^0)} + \|\bar{\mathbf{e}}_\mathbf{w}(0)\|^2_{\star,\mathbf{x}^0}\big).
\end{aligned}
\tag{4.2}
$$

The stability estimate for (4.1a) is the same as (3.52), i.e.,

$$
\|\mathbf{e_x}(t)\|^2_{\mathbf{K}(\mathbf{x}^*)} \leq C\int_0^t \|\mathbf{e_v}(s)\|^2_{\mathbf{K}(\mathbf{x}^*)}\,\mathrm{d}s + C\int_0^t \|\mathbf{e_x}(s)\|^2_{\mathbf{K}(\mathbf{x}^*)}\,\mathrm{d}s. \tag{4.3}
$$

The stability estimates for (4.1b)–(4.1c) are given by

$$
\begin{aligned}
\|\mathbf{e_v}\|_{\mathbf{K}(\mathbf{x}^*)} &\leq C(\|\mathbf{e_x}\|_{\mathbf{A}(\mathbf{x}^*)} + \|\mathbf{e_u}\|_{\mathbf{K}(\mathbf{x}^*)} + \|\mathbf{e_w}\|_{\mathbf{K}(\mathbf{x}^*)}) \\
&\quad + C(\|\mathbf{d_v}\|_{\mathbf{M}(\mathbf{x}^*)} + \|\widetilde{\mathbf{d}}_\mathbf{v}\|_{\star,\mathbf{x}^*} + \|\mathbf{d}_{\boldsymbol{\kappa}}\|_{\mathbf{M}(\mathbf{x}^*)}),
\end{aligned}
\tag{4.4}
$$

$$
\begin{aligned}
\|\mathbf{e}_{\boldsymbol{\kappa}}\|_{\mathbf{M}(\mathbf{x}^*)} &\leq C(\|\mathbf{e_u}\|_{\mathbf{M}(\mathbf{x}^*)} + \|\mathbf{e_w}\|_{\mathbf{K}(\mathbf{x}^*)} \\
&\quad + C(h^{-1}\|\mathbf{e_x}\|_{\mathbf{A}(\mathbf{x}^*)} + h^{-1}\|\mathbf{e_v}\|_{\mathbf{A}(\mathbf{x}^*)} + \|\mathbf{d}_{\boldsymbol{\kappa}}\|_{\mathbf{M}(\mathbf{x}^*)}),
\end{aligned}
\tag{4.5}
$$

which can be obtained through replacing $\|\mathbf{e_u}\|_{\mathbf{K}(\mathbf{x}^*)}$ by $\|\mathbf{e_u}\|_{\mathbf{K}(\mathbf{x}^*)} + \|\mathbf{e_w}\|_{\mathbf{K}(\mathbf{x}^*)}$ in the stability estimates proved in (3.54)–(3.55).

The stability estimate for the whole system in (4.1) can be obtained by substituting (4.4) into (4.3) + $\epsilon\times$(4.2), which yields

$$
\begin{aligned}
&\|\mathbf{e_x}(t)\|^2_{\mathbf{K}(\mathbf{x}^*(t))} + \epsilon\|\mathbf{e_u}(t)\|^2_{\mathbf{K}(\mathbf{x}^*(t))} + \epsilon\|\mathbf{e_w}(t)\|^2_{\mathbf{K}(\mathbf{x}^*(t))} \\
&\leq C\int_0^t \Big(\|\mathbf{e_x}(s)\|^2_{\mathbf{K}(\mathbf{x}^*(s))} + \|\mathbf{e_u}(s)\|^2_{\mathbf{K}(\mathbf{x}^*(s))} + \|\mathbf{e_w}(s)\|^2_{\mathbf{K}(\mathbf{x}^*(s))}\Big)\mathrm{d}s \\
&\quad + C\int_0^t \Big(\|\mathbf{d_u}(s)\|^2_{\mathbf{M}(\mathbf{x}^*(s))} + \|\dot{\mathbf{d}}_\mathbf{u}(s)\|^2_{\star,\mathbf{x}^*(s)}\Big)\mathrm{d}s \\
&\quad + C\int_0^t \Big(\|\mathbf{d_w}(s)\|^2_{\mathbf{M}(\mathbf{x}^*(s))} + \|\dot{\mathbf{d}}_\mathbf{w}(s)\|^2_{\star,\mathbf{x}^*(s)}\Big)\mathrm{d}s \\
&\quad + C\int_0^t \Big(\|\mathbf{d_v}(s)\|^2_{\mathbf{M}(\mathbf{x}^*(s))} + \|\widetilde{\mathbf{d}}_\mathbf{v}(s)\|^2_{\star,\mathbf{x}^*(s)} + \|\mathbf{d}_{\boldsymbol{\kappa}}(s)\|^2_{\mathbf{M}(\mathbf{x}^*(s))}\Big)\,\mathrm{d}s \\
&\quad + C\epsilon\|\mathbf{e_x}(t)\|^2_{\mathbf{K}(\mathbf{x}^*(t))} + C\|\mathbf{d_u}(t)\|^2_{\star,\mathbf{x}^*(t)} \\
&\quad + C\big(\|\mathbf{e_u}(0)\|^2_{\mathbf{K}(\mathbf{x}^0)} + \|\mathbf{e_w}(0)\|^2_{\mathbf{K}(\mathbf{x}^0)} + \|\bar{\mathbf{e}}_\mathbf{w}(0)\|^2_{\star,\mathbf{x}^0}\big).
\end{aligned}
\tag{4.6}
$$

By choosing a sufficiently small constant ϵ, the term $C\epsilon\,\|\mathbf{e_x}(t)\|^2_{\mathbf{K}(\mathbf{x}^*(t))}$ can be absorbed by the left-hand side. Then we can apply the Gronwall's inequality and use the consistency estimates, which can be established in the usual way, similarly as in [41]. This yields the following error bound:

$$\|\mathbf{e_x}(t)\|_{\mathbf{K}(\mathbf{x}^*(t))} + \|\mathbf{e_u}(t)\|_{\mathbf{K}(\mathbf{x}^*(t))} + \|\mathbf{e_w}(t)\|_{\mathbf{K}(\mathbf{x}^*(t))} \le Ch^k.$$

Substituting this result into (4.4), we also obtain

$$\|\mathbf{e_v}(t)\|_{\mathbf{K}(\mathbf{x}^*(t))} \le Ch^k.$$

This can be combined with the error estimates for the Ritz projection and the interpolation (see Theorem 3.1 and [23, Proposition 2.7]) to yield the desired results in Theorem 2.2. □

5 Numerical examples

In this section, we present numerical results to illustrate the convergence of the proposed method as proved in Theorems 2.1 and 2.2, as well as the performance of the proposed velocity for improving the mesh quality in simulation of several different curvature flows. All the numerical experiments are performed by using the open-source finite element software NGSolve; see [50].

5.1 Convergence tests of mean curvature flow

We consider the evolution of closed self-shrinkers under mean curvature flow (see [24]), with the following type of flow map:

$$X(p,t) = \sqrt{1-t}\,X(p,0) \quad \text{for } p \in \Gamma_0, \tag{5.1}$$

for which the exact solution of the velocity equations (1.9b)–(1.9c) can be written down explicitly. In fact, as a self-shrinker under mean curvature flow, the normal component of the shrinking velocity (which can be obtained by differentiating (5.1) in time)

$$v_s = -\frac{1}{2(1-t)}\mathrm{id} \quad \text{on} \quad \Gamma(t) \tag{5.2}$$

coincides with the velocity of the surface under mean curvature flow. Meanwhile, by applying the Laplace–Beltrami operator to the shrinking velocity above, we have

$$\Delta_{\Gamma(t)} v_s = \frac{1}{2(1-t)} Hn \quad \text{on} \quad \Gamma(t), \quad \text{with } \kappa = \frac{1}{2(1-t)} H \ \text{ in (1.9c)}.$$

As a result, the shrinking velocity v_s is exactly the proposed velocity determined by (1.9b)–(1.9c).

We consider two examples of such self-shrinkers with flow map as in (5.1), i.e., the self-shrinking sphere S^2 and self-shrinking Angenent's torus T^2; see [1]. Both surfaces can be parametrized by

$$F(s,\theta,t) = \sqrt{1-t}\,(\rho(s)\cos(\theta), \rho(s)\sin(\theta), z(s)). \tag{5.3}$$

The profile curve of the self-shrinking sphere S^2 is given by $\rho(s)^2 + z(s)^2 = 4$, where s is the arc-length parameter. The profile curve of the Angenent's torus T^2 can be solved from the following equations (by the shooting method):

$$\rho'(s) = \sin\alpha(s), \quad z'(s) = \cos\alpha(s), \tag{5.4a}$$

$$\alpha'(s) = \left(\frac{1}{\rho(s)} - \frac{\rho(s)}{2}\right)\cos\alpha(s) + \frac{z(s)}{2}\sin\alpha(s), \tag{5.4b}$$

$$\rho(0) = \rho_0, \quad z(0) = 0, \quad \alpha(0) = 0, \tag{5.4c}$$

where ρ_0 is a parameter to be determined to make the solution a closed curve, see [24, (5.2)]. Since T^2 is a rotational hypersurface, its mean curvature can be analytically expressed as

$$H \circ F(s,\theta,t) = -\frac{1}{2\sqrt{1-t}}(\rho(s)\cos\alpha(s) - z(s)\sin\alpha(s)) = \frac{1}{2(1-t)}F\cdot(n\circ F),$$

which implies that

$$H = \frac{1}{2(1-t)}\mathrm{id}\cdot n \quad \text{on } \Gamma(t). \tag{5.5}$$

Moreover,

$$n\circ F(s,\theta,t) = n\circ F(s,\theta,0). \tag{5.6}$$

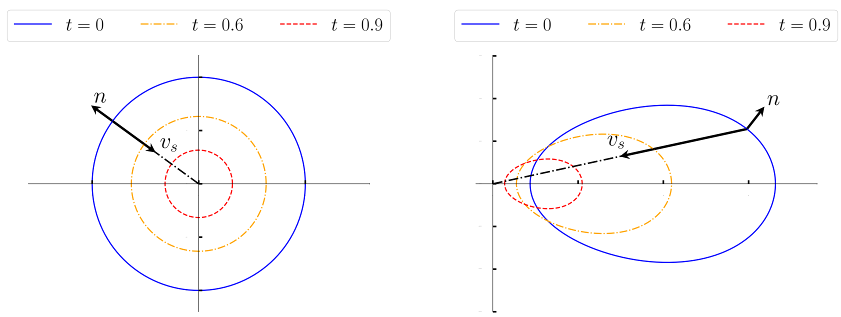

(A) Shrinking spheres (B) Shrinking Angenent's torus

Fig. 1: Exact profile curves of the self-shrinkers at $t = 0, 0.6$ and 0.9.

The profile curves of the sphere and the Angenent Torus are presented in Figure 1, which determine the surface through the parametrization in (5.3).

According to the exact position given in (5.1), the error of the numerically computed flow map $X_h(p,t)$ is given by (up to an interpolation error of the initial surface)

$$e_X(p,T) = X_h(p,T) - \sqrt{1-T}X_h(p,0), \quad p \in \Gamma_h^0.$$

From the formulae of the exact velocity (5.2), mean curvature (5.5) and normal vector field (5.6), it is easy to measure the errors of these geometrical quantities. The H^1-norm errors of the numerical solution and the convergence rates are presented in Figure 2 for finite elements of degree $k = 1, 2, 3$ at $T = 0.4$. The backward Euler method in (5.8) is used for temporal discretization, with a sufficiently small stepsize so that the errors from temporal discretization can be neglected in observing the convergence of spatial discretizations (when the mesh size h is refined). From Figure 2 we can see that the proposed method has kth-order convergence in the H^1 norm. The cases $k = 2, 3$ are proved in this article (similarly as [40,41]). The numerical results indicate that the result still holds in the case $k = 1$, though it has not been proved yet. Rigorous proof of the convergence of the method (as well as the methods in [40, 41]) in the case $k = 1$ is still challenging.

5.2 Convergence test of Willmore flow

We compute the convergence rate of the proposed method on Willmore flow by using a stationary solution: a sphere with radius $R = 2$, over the time interval $T = [0, 1]$. To compute the convergence rate, we generate a sequence of meshes with mesh sizes $h_0 \approx 0.4$ and $h_m \approx 2^{-1/2}h_{m-1}$. The backward Euler scheme is used for time discretization, and the corresponding time steps are chosen as $t_0 = 0.1$ and $t_m = 2^{-k/2}t_{m-1}$ for evolving surface FEM of degree k in space discretization.

The initial values for $H_h(\cdot, 0)$, $V_h(\cdot, 0)$, $n_h(\cdot, 0)$ and $z_h(\cdot, 0)$ in (2.5) are set by nodal interpolation of their exact expression in the case of a sphere. Then, $v_h(\cdot, 0)$ and $\kappa_h(\cdot, 0)$ are solved from (2.5b)-(2.5c) after initializing $V_h(\cdot, 0)$ and $n_h(\cdot, 0)$.

The H^1-norm errors between the numerical solution and the exact solution and their convergence rates are presented in Figure 3. When mesh size decreases, the convergence rates of H^1-norm errors match the theoretical order $\mathcal{O}(h^k)$ for $k = 2, 3$. For $k = 1$, the first order convergence rate of H^1-norm errors can also be obtained in numerical experiment.

5.3 Performance in improving the mesh quality (for mean curvature flow)

We compare the performance of the proposed method (2.2) with the BGN algorithm in [8] by considering the mean curvature flow of a two-dimensional

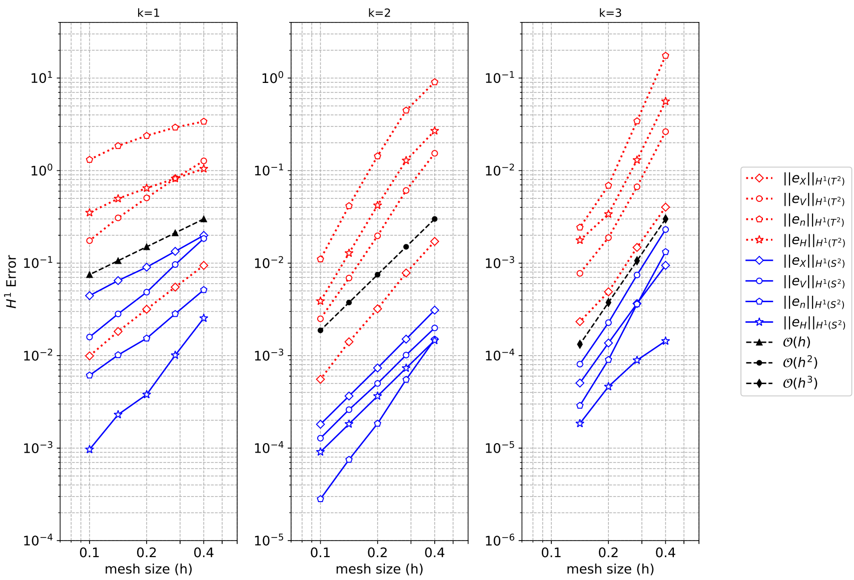

Fig. 2: The H^1 errors of geometrical quantities under the mean curvature flow for scheme (2.2) with $k = 1, 2, 3$ at $T = 0.4$.

surface with the following initial parameterization:

$$F(\theta, \varphi) := \begin{pmatrix} \cos\varphi \\ \left(0.6\cos^2\varphi + 0.4\right)\cos\theta\sin\varphi \\ \left(0.6\cos^2\varphi + 0.4\right)\sin\theta\sin\varphi \end{pmatrix}, \quad \theta \in [0, 2\pi), \quad \varphi \in [0, \pi], \quad (5.7)$$

which is a benchmark example proposed in [33]. It is known that the methods with tangential velocity to improve the mesh quality, including the BGN algorithm in [7–9] and the method with DeTurck's trick [33], can successfully approximate the mean curvature flow with the initial parametrization (5.7), which eventually evolves to a sphere. It is also known that the methods without tangential velocity often fail to approximate this problem well, i.e., the mesh becomes distorted and the nodes become clustered, which make the computation breakdown before the surface evolves to a sphere and necessitate a mesh redistribution method, see [25, Example 4.4].

We present the numerical simulation in Figure 5 by the proposed method in (2.2), or equivalently in (2.9), with a simple linearly implicit time-stepping

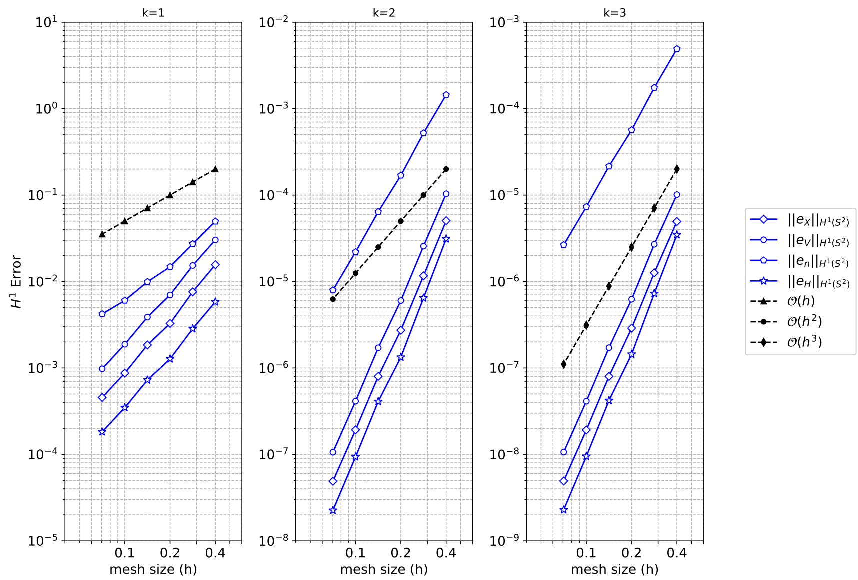

Fig. 3: The H^1 errors of geometrical quantities for a sphere S^2 with $R = 2$ under the Willmore flow for scheme (2.5) with $k = 1, 2, 3$ at $T = 1$.

method:

$$\frac{\mathbf{x}^{m+1} - \mathbf{x}^m}{\tau_m} = \mathbf{v}^{m+1}, \tag{5.8a}$$

$$\mathbf{B}(\mathbf{x}^m, \mathbf{n}^m)\mathbf{v}^{m+1} = -\mathbf{M}(\mathbf{x}^m)\mathbf{H}^{m+1}, \tag{5.8b}$$

$$\mathbf{B}(\mathbf{x}^m, \mathbf{n}^m)^\top \boldsymbol{\kappa}^{m+1} + \mathbf{A}^{[3]}(\mathbf{x}^m)\mathbf{v}^{m+1} = \mathbf{0}, \tag{5.8c}$$

$$\mathbf{M}^{[4]}(\mathbf{x}^m)\frac{\mathbf{u}^{m+1} - \mathbf{u}^m}{\tau_m} + \mathbf{A}^{[4]}(\mathbf{x}^m)\mathbf{u}^{m+1} = \mathbf{f}(\mathbf{x}^m, \mathbf{u}^m, \mathbf{v}^m), \tag{5.8d}$$

where the initial triangulation contains 2682 vertices and 5360 elements, and the time step size is chosen as $\tau = 0.05h^2$. Since the mean curvature and normal vector field are computed from the discretization (5.8d), the accumulated errors during evolution may make the numerical curvature and normal deviate from the geometrical quantities of the discrete surface. In another word, the fundamental relation (1.1) that links position, mean curvature and normal can be ruined. The incompatibility between the curvature and the position may finally prevent the surface from shrinking to a sphere. To overcome the drawback of the evolution equation during long time simulation, one solution is to start with a better discrete surface approximation with small mesh size so that the errors of the mean curvature, the normal and the position can be well controlled. Another numerical remedy is to reset the mean curvature and the normal according to the discrete position when the relative error between the numerical curvature and the geometrical one in L^2 norm reaches a threshold. In this experiment, once the relative error reaches 10%, we reset the data of H and n according to the position of the discrete mesh. For polyhedral surface, we reset the normal n_h^m at each vertex by the weighted normal introduced in [8] and the mean curvature by solving

$$\int_{\Gamma_h^m} H_h^m \chi_H = \int_{\Gamma_h^m} \nabla_{\Gamma_h^m} \cdot (n_h^m)\chi_H, \quad \forall \chi_H \in S_h[\mathbf{x}].$$

For high order discrete surface, we reset the normal and the mean curvature via an L^2 projection of the geometrical mean curvature and normal of the curved mesh. The re-initialization procedure only modifies the mean curvature and the normal and leaves the discrete position unchanged so that it has little influence in mesh quality. In this example, with a threshold of 10%, we need to perform re-initialization 5 times at $T = 0.086, 0.0904, 0.09086, 0.090975$ and 0.090988.

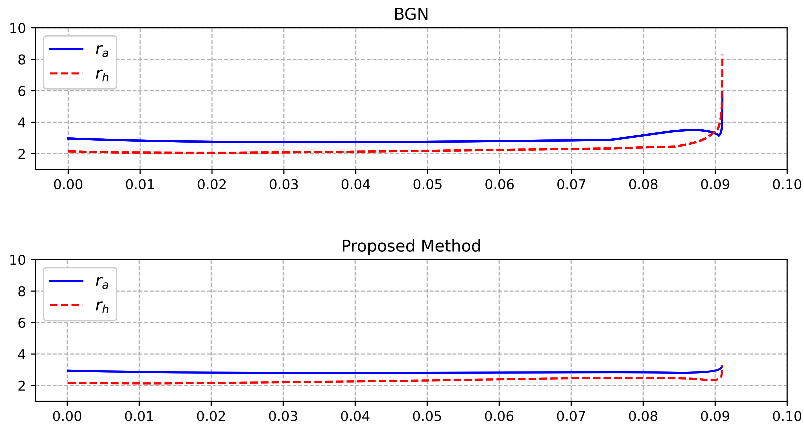

Fig. 4: Mesh quality of the evolution of a 2-dimensional dumbbell surface (5.7) under the mean curvature flow for the BGN method and (2.2). Re-initialization procedure with a threshold (10%) is performed when using (2.2).

For comparison, we also present the numerical results computed by the BGN algorithm in Figure 5. We see that the proposed method can successfully approximate the surface until it evolves to a sphere with similar mesh quality as the BGN algorithm. To measure mesh quality, we follow the treatment in [8, P. 4926] and use the indices r_a and r_h to denote the ratio of the maximal element area to the minimal area and the ratio of the maximal edge length to

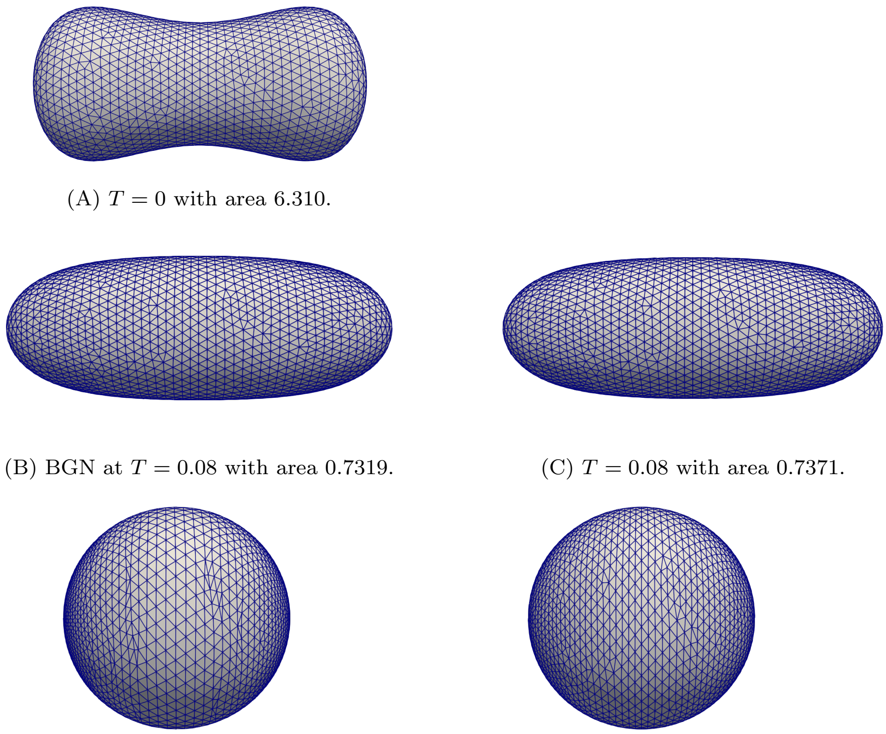

(A) $T = 0$ with area 6.310.

(B) BGN at $T = 0.08$ with area 0.7319.

(C) $T = 0.08$ with area 0.7371.

(D) BGN at $T = 0.0909924$ with area 1.413×10^{-5}.

(E) $T = 0.0909924$ with area 1.379×10^{-5}.

Fig. 5: Comparison of the proposed method (2.2) with the BGN method in [8] with initial parametrization (5.7). The images are rescaled. Re-initialization procedure with a threshold (10%) is performed when using (2.2).

the minimal one. The plot of mesh quality during evolution is demonstrated in Figure 4. It is clearly observed that the mesh quality is well preserved, even around the singularity.

5.4 Performance in improving the mesh quality (for surface diffusion of curve)

We consider the evolution of a "flower" shape curve under surface diffusion flow, with initial parametrization

$$\begin{aligned} x &= [1 + 0.65\sin(7\theta)]\cos\theta, \\ y &= [1 + 0.65\sin(7\theta)]\sin\theta, \quad \text{for } \theta \in [0, 2\pi], \end{aligned} \tag{5.9}$$

which is a benchmark problem considered in [5, 38]. The computation of this problem requires either mesh redistribution or certain tangential velocity to prevent the nodes from clustering.

We solve this problem by the proposed evolving surface FEM in (2.5) with $k = 2$ for the system of equations in (1.11) with $Q = 0$, which is a reformulation of surface diffusion flow; see [41]. The evolution equations (2.5e)-(2.5f) are fully discretized as follows:

$$
\begin{aligned}
&\int_{\Gamma_h^m} \frac{H_h^{m+1} - H_h^m}{\tau_m} \chi_H - \int_{\Gamma_h^m} \nabla_{\Gamma_h^m} V_h^{m+1} \cdot \nabla_{\Gamma_h^m} \chi_H \\
&\quad - \int_{\Gamma_h^m} (v_h^m \cdot \nabla_{\Gamma_h^m} H_h^{m+1} - |A_h^m|^2 V_h^{m+1}) \chi_H = 0, \\
&\int_{\Gamma_h^m} \frac{n_h^{m+1} - n_h^m}{\tau_m} \cdot \chi_n - \int_{\Gamma_h^m} \nabla_{\Gamma_h^m} z_h^{m+1} \cdot \nabla_{\Gamma_h^m} \chi_n \\
&\quad - \int_{\Gamma_h^m} (v_h^m \cdot \nabla_{\Gamma_h^m} n_h^{m+1} + (H_h^m A_h^m - (A_h^m)^2) z_h^{m+1}) \cdot \chi_n \\
&= 2 \int_{\Gamma_h^m} (A_h^m \nabla_{\Gamma_h^m} H_h^m) \cdot (\nabla_{\Gamma_h^m} \chi_n \, n_h^m) \\
&\quad + \int_{\Gamma_h^m} \left(|\nabla_{\Gamma_h^m} H_h^m|^2 n_h^m + (A_h^m)^2 \nabla_{\Gamma_h^m} H_h^m \right) \cdot \chi_n .
\end{aligned}
$$

In this case, both the mean curvature and the normal vector of the initial curve change rapidly at the concave corners, bringing great difficulty to accurately compute H_h and n_h via (2.5f)-(2.5g) for long time evolution. To resolve this problem, we generate a fine initial mesh with 5040 nodes. A small mesh size is crucial to obtaining accurate mean curvature and normal via the evolving equations so that no re-initialization procedure is needed during evolution. As for the initial data of H_h and n_h, we use an L^2 projection of the corresponding geometrical quantities of the discrete mesh by virtue of the curved element. Moreover, we use variable time step ($\tau = 10^{-3} T_i$ for $t \in [T_{i-1}, T_i]$ with $T_i = 10^i$ and $i = -12, \cdots, -4$) to resolve the rapid smoothing process of H and n. Afterwards, a uniform time step $\tau = 10^{-6}$ is used for $t \in [10^{-4}, 8 \times 10^{-3}]$.

The numerical simulation of the "flower" shape curve driven by surface diffusion is presented in Figure 6 at $T = 0, 10^{-5}, 10^{-4}, 10^{-3}$ with local magnification to show details of node distribution. The initial discrete curve has smaller mesh size around the concave corners. As shown in the subplots (F), (G), (H) in Figure 6, which are of the same scale, the nodes around the concave corner become almost equidistributed at $T = 10^{-3}$. For long time evolution, the evolving curves at $T = 0.003, 0.005, 0.006$ and 0.008 are presented in the third row of Figure 6 to show the final stationary shape, which is a circle. The mesh quality measured by the ratio of the longest edge length to the shortest one is presented in the last plot of Figure 6. It demonstrates that the proposed method can yield approximations with good mesh quality in this benchmark problem, which in the case of no tangential velocity, will lead to clustering of nodes and breakdown of computation.

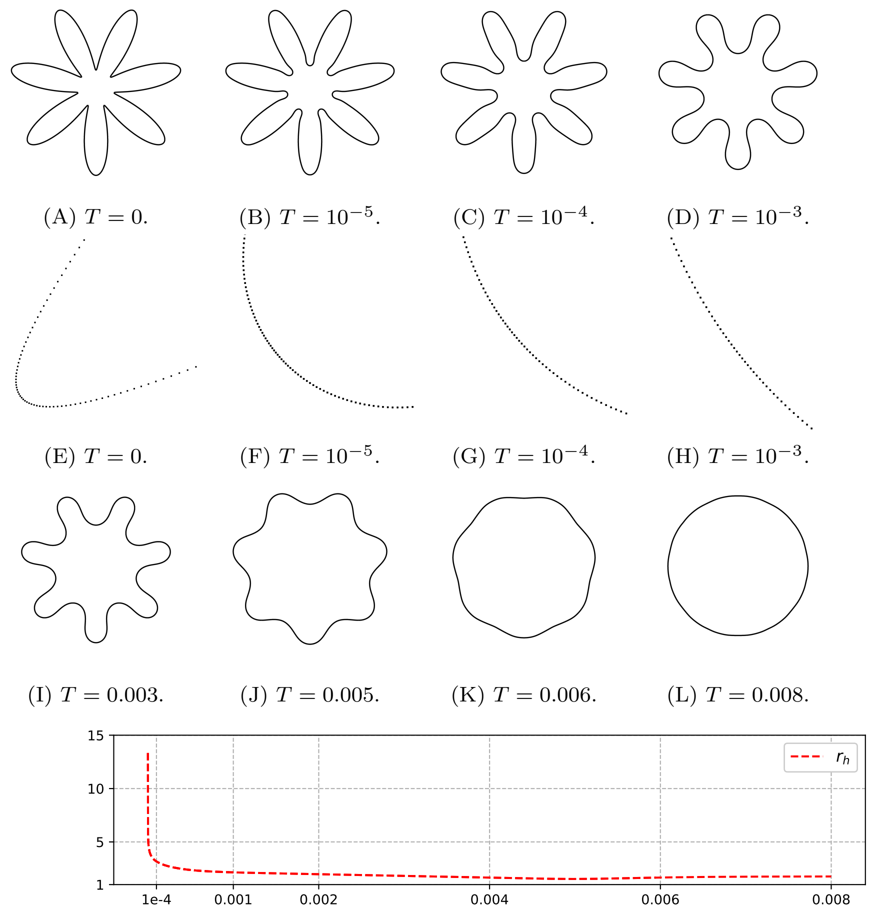

Fig. 6: Evolution of the "flower" shape curve driven by surface diffusion. In the first two rows, we present the evolving curves at $T = 0, 10^{-5}, 10^{-4}, 10^{-3}$, and locally magnify the node distribution around the corner at $\theta = 3\pi/14$ (see (5.9)). The last picture shows that the mesh quality r_h is well preserved during evolution.

5.5 Performance in improving the mesh quality (for Willmore flow of surface)

We consider the evolution of a "cell" shape surface under Willmore flow, see also [9, 41]. In this experiment, the initial hypersurface is parameterized by

$$F(\theta, \varphi) := \begin{pmatrix} 2\cos\varphi\cos\theta \\ 2\cos\varphi\sin\theta \\ (1 - 0.7(\cos^2\varphi - 1)^2)\sin\varphi \end{pmatrix}, \quad \theta \in [0, 2\pi), \quad \varphi \in \left[-\frac{\pi}{2}, \frac{\pi}{2}\right],$$

which is generated by rotating a profile curve in x-z plane around z-axis. In Figure 7(A), we present the initial profile curve and the rotational surface

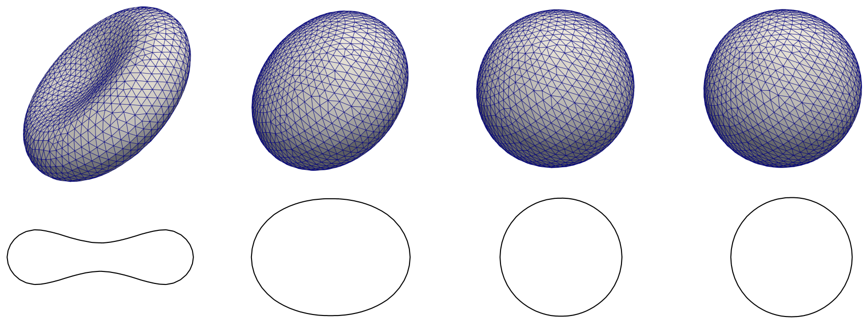

(A) $T = 0$. (B) $T = 0.3$. (C) $T = 1$. (D) $T = 1.5$.

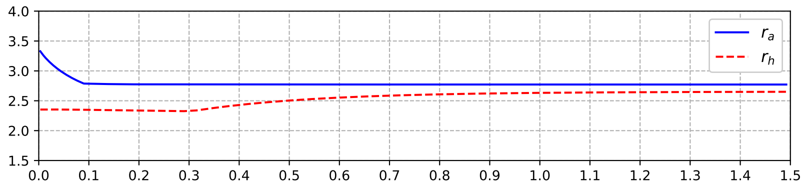

Fig. 7: Evolution of the "cell" shape surface driven by Willmore flow. We show the evolving surfaces and their profile curves in x-z plane at $T = 0,\ 0.3,\ 1,\ 1.5$. In the last plot, we present the mesh quality measured by r_a and r_h during evolution.

which has 3008 elements and 1506 vertices. In this experiment, we use the evolving surface FEM with $k = 2$ in space and a uniform time step $\tau = 10^{-3}$. The initial data of H_h, n_h, V_h and z_h are set by interpolating the analytic expressions according to the initial parameterization.

In Figure 7, we show four screenshots of the evolving surface and their profile curves at $T = 0, 0.3, 1, 1.5$. It is observed that at $T = 1$, the surface almost becomes a sphere and stays stationary afterwards. The last plot in Figure 7 demonstrates the preservation of mesh quality during evolution.

6 Conclusion

In this article, we have introduced an artificial tangential velocity, which is constructed by considering a limiting situation in the BGN method [7–9], into the KLL formulations of mean curvature flow and Willmore flow [40, 41]. We have proved optimal-order H^1-norm convergence of the proposed method with finite elements of degree $k \geqslant 2$ for both mean curvature flow and Willmore flow. The numerical tests show that the proposed evolving surface FEM with finite elements of degree $k \geqslant 1$ has kth-order convergence. The rigorous proof for the case $k = 1$ still remains open. The numerical simulations in this article show that the proposed method performs well and improves the mesh quality for some benchmark examples.

Acknowledgement

This work is supported in part by a grant from the Research Grants Council of the Hong Kong Special Administrative Region, China (GRF Project No. PolyU15300920), and an internal grant of The Hong Kong Polytechnic University (Project ID: P0034902, Work Programme: W15D).

Appendix: $\mathbf{L^2}$ projection of products of finite element functions

In this appendix, we prove the following results for any two finite element functions $w_1, w_2 \in S_h[\mathbf{x}^*]$.

Lemma A

$$\begin{aligned}&\|w_1 w_2 - P_{\Gamma_h[\mathbf{x}^*]}(w_1 w_2)\|_{L^2(\Gamma_h[\mathbf{x}^*])}\\ &\leq Ch^2 \|w_1\|_{H^1(\Gamma_h[\mathbf{x}^*])} \|w_2\|_{W^{1,\infty}(\Gamma_h[\mathbf{x}^*])},\end{aligned} \tag{A.1}$$

$$\begin{aligned}&\|\nabla_{\Gamma_h[\mathbf{x}^*]}(w_1 w_2 - P_{\Gamma_h[\mathbf{x}^*]}(w_1 w_2))\|_{L^2(\Gamma_h[\mathbf{x}^*])}\\ &\leq Ch \|w_1\|_{H^1(\Gamma_h[\mathbf{x}^*])} \|w_2\|_{W^{1,\infty}(\Gamma_h[\mathbf{x}^*])}.\end{aligned} \tag{A.2}$$

Inequalities (A.1)–(A.2) imply that the L^2 projection of a product $w_1 w_2$ (of finite element functions) approximates itself with some kind of superconvergence. These results are known for finite element functions on the Euclidean space, but need to be proved for surface finite elements. These estimates can also be extended to product of three functions by a similar proof, e.g.,

$$\begin{aligned}&\left\|\nabla_{\Gamma_h[\mathbf{x}^*]}\left(w_1 w_2 w_3 - P_{\Gamma_h[\mathbf{x}^*]}(w_1 w_2 w_3)\right)\right\|_{L^2(\Gamma_h[\mathbf{x}^*])}\\ &\leq Ch \|w_1\|_{H^1(\Gamma_h[\mathbf{x}^*])} \|w_2\|_{W^{1,\infty}(\Gamma_h[\mathbf{x}^*])} \|w_3\|_{W^{1,\infty}(\Gamma_h[\mathbf{x}^*])}.\end{aligned} \tag{A.3}$$

Remark A.1 From the following proof we see that the L^2 projection in (A.1)–(A.2) can be changed to interpolation, i.e.,

$$\begin{aligned}&\|w_1 w_2 - I_{\Gamma_h[\mathbf{x}^*]}(w_1 w_2)\|_{L^2(\Gamma_h[\mathbf{x}^*])}\\ &\leq Ch^2 \|w_1\|_{H^1(\Gamma_h[\mathbf{x}^*])} \|w_2\|_{W^{1,\infty}(\Gamma_h[\mathbf{x}^*])},\end{aligned} \tag{A.4}$$

$$\begin{aligned}&\|\nabla_{\Gamma_h[\mathbf{x}^*]}(w_1 w_2 - I_{\Gamma_h[\mathbf{x}^*]}(w_1 w_2))\|_{L^2(\Gamma_h[\mathbf{x}^*])}\\ &\leq Ch \|w_1\|_{H^1(\Gamma_h[\mathbf{x}^*])} \|w_2\|_{W^{1,\infty}(\Gamma_h[\mathbf{x}^*])}.\end{aligned} \tag{A.5}$$

□

Proof (Proof of Lemma A) We take the piecewise linear interpolated surface $\Gamma_h^1 = \Gamma_h^1[\mathbf{x}^*]$ as a bridge to transform the classical results on Euclidean space to the high-order piecewise polynomial surfaces $\Gamma_h^k = \Gamma_h[\mathbf{x}^*]$ of degree k. To this end, we recall the following construction of the piecewise polynomial surface Γ_h^k of degree k as well as the isoparametric finite element space on Γ_h^k; see [23].

As discussed in Section 2.4, we assume that h is sufficiently small so that there exists a lift mapping $a : \Gamma_h^1 \to \Gamma$ along the normal direction of Γ. Let

$S_h^k(\Gamma_h^1)$ be the finite element space of degree k on the piecewise linear surface Γ_h^1. Then Γ_h^k is defined as $a_k(\Gamma_h^1)$ where a_k is the finite element interpolation of a in $S_h^k(\Gamma_h^1)^3$. The push forward by a_k defines a lift from Γ_h^1 to Γ_h^k, denoted by a superscript ℓ_k. For any function φ on Γ_h^1 we can define its lift φ^{ℓ_k} as a function on Γ_h^k satisfying the relation $\varphi^{\ell_k} \circ a_k = \varphi$. The isoparametric finite element spaces on Γ_h^k is defined through the lift, i.e.,

$$S_h(\Gamma_h^k) = S_h(\Gamma_h^1)^{\ell_k} = \{v \in H^1(\Gamma_h^k) : v \circ a_k \in S_h^k(\Gamma_h^1)\}. \tag{A.6}$$

The following norm equivalence results induced by ℓ_k are shown in [23]: For $w \in W^{1,p}(\Gamma_h^k)$ and $1 \le p \le \infty$,

$$C_0^{-1}\|w\|_{L^p(\Gamma_h^k)} \le \|w \circ a_k\|_{L^p(\Gamma_h^1)} \le C_0\|w\|_{L^p(\Gamma_h^k)}, \tag{A.7}$$

$$C_1^{-1}\|\nabla_{\Gamma_h^k} w\|_{L^p(\Gamma_h^k)} \le \|\nabla_{\Gamma_h^1}(w \circ a_k)\|_{L^p(\Gamma_h^1)} \le C_1\|\nabla_{\Gamma_h^k} w\|_{L^p(\Gamma_h^k)}. \tag{A.8}$$

For a curved triangle $\tilde{T}$ of the piecewise polynomial surface Γ_h^k, we adopt the standard notation for the Sobolev space $W^{k,p}(\tilde{T})$ of functions possessing up to kth-order tangential derivatives in $L^p(\tilde{T})$, as defined in [31, Definition 2.11]. Let T be the corresponding flat triangle on Γ_h^1 such that $\tilde{T} = a_k(T)$. Then the following results hold (see [23, (2.20)]):

$$\|\nabla^j_{\Gamma_h^1}(w \circ a_k)\|_{L^p(T)} \le C_j \sum_{1\le m\le j} \|\nabla^m_{\Gamma_h^k} w\|_{L^p(\tilde{T})} \quad \text{for} \quad 1 \le j \le k. \tag{A.9}$$

The finite element interpolation $\tilde{I}_h^k : C(\Gamma_h^k) \to S_h(\Gamma_h^k)$ is defined as

$$\tilde{I}_h^k w = \big(I_h^k(w \circ a_k)\big)^{\ell_k},$$

where $I_h^k : C(\Gamma_h^1) \to S_h(\Gamma_h^1)$ is the piecewise polynomial interpolation of degree k on the piecewise flat triangular surface Γ_h^1 interpolating Γ. This implies that

$$w - \tilde{I}_h^k w = \big(w \circ a_k - I_h^k(w \circ a_k)\big)^{\ell_k}. \tag{A.10}$$

Therefore, for the L^2 projection $P_{\Gamma_h^k} : H^1(\Gamma_h^k) \to S_h(\Gamma_h^k)$, we obtain the following estimates for $w_1, w_2 \in S_h(\Gamma_h^k)$:

$$
\begin{aligned}
&\|w_1w_2 - P_{\Gamma_h^k}(w_1w_2)\|_{L^2(\Gamma_h^k)} \\
&\le \|w_1w_2 - \tilde{I}_h^k(w_1w_2)\|_{L^2(\Gamma_h^k)} \\
&\le C\|(w_1w_2) \circ a_k - I_h^k((w_1w_2) \circ a_k)\|_{L^2(\Gamma_h^1)} \\
&\le Ch^{k+1}|(w_1w_2) \circ a_k|_{H_h^{k+1}(\Gamma_h^1)} \\
&\le Ch^{k+1} \sum_{T\in\mathcal{T}_h} \sum_{i=0}^{k+1} \Big\|\nabla^i_{\Gamma_h^1}(w_1 \circ a_k)\Big\|_{L^2(T)} \Big\|\nabla^{k+1-i}_{\Gamma_h^1}(w_2 \circ a_k)\Big\|_{L^\infty(T)} && \text{(A.11)} \\
&\le Ch^{k+1} \sum_{T\in\mathcal{T}_h} \sum_{i=1}^{k} \Big\|\nabla^i_{\Gamma_h^1}(w_1 \circ a_k)\Big\|_{L^2(T)} \Big\|\nabla^{k+1-i}_{\Gamma_h^1}(w_2 \circ a_k)\Big\|_{L^\infty(T)} && \text{(A.12)} \\
&\le Ch^2\|w_1\|_{H^1(\Gamma_h^k)}\|w_2\|_{W^{1,\infty}(\Gamma_h^k)}, && \text{(A.13)}
\end{aligned}
$$

where (A.12) utilizes the property that $w_1 \circ a_k$ and $w_2 \circ a_k$ are polynomials of degree k, i.e.,

$$\nabla^{k+1}_{\Gamma_h^1}(w_1 \circ a_k) = \nabla^{k+1}_{\Gamma_h^1}(w_2 \circ a_k) = 0,$$

and (A.13) uses the inverse inequality and the norm equivalence relations in (A.8). The transformation from curved triangles to flat triangles in the above argument is essential.

The tangential gradient of the L^2 projection error can also be transformed to the piecewise flat surface Γ_h^1 as follows:

$$\begin{aligned}
&\|\nabla_{\Gamma_h^k}(w - P_{\Gamma_h^k} w)\|_{L^2(\Gamma_h^k)} \\
&\le \|\nabla_{\Gamma_h^k}(w - \tilde{I}_h^k w)\|_{L^2(\Gamma_h^k)} + \|\nabla_{\Gamma_h^k}(\tilde{I}_h^k w - P_{\Gamma_h^k} w)\|_{L^2(\Gamma_h^k)} \\
&\le \|\nabla_{\Gamma_h^k}(w - \tilde{I}_h^k w)\|_{L^2(\Gamma_h^k)} + Ch^{-1}\|\tilde{I}_h^k w - P_{\Gamma_h^k} w\|_{L^2(\Gamma_h^k)} \\
&\le \|\nabla_{\Gamma_h^k}(w - \tilde{I}_h^k w)\|_{L^2(\Gamma_h^k)} + Ch^{-1}\|\tilde{I}_h^k w - w\|_{L^2(\Gamma_h^k)} \\
&\le C\|\nabla_{\Gamma_h^1}(w \circ a_k - I_h^k(w \circ a_k))\|_{L^2(\Gamma_h^1)} + Ch^{-1}\|w \circ a_k - I_h^k(w \circ a_k)\|_{L^2(\Gamma_h^1)}.
\end{aligned}$$

Then, by repeating the arguments in the proof of (A.13), we obtain (A.2). □

References

1. S. Angenent. Shrinking doughnuts. Nonlinear diffusion equations and their equilibrium states, 3 (Gregynog, 1989), Progr. Nonlinear Differential Equations Appl., pages 21–38. Birkhäuser, 1992.
2. E. Bänsch, P. Morin, and R. Nochetto. Surface diffusion of graphs: variational formulation, error analysis, and simulation. *SIAM J. Numer. Anal.*, 42(2):773–799, 2004.
3. E. Bänsch, P. Morin, and R. Nochetto. A finite element method for surface diffusion: The parametric case. *J. Comput. Phys.*, 203(1):321–343, 2005.
4. W. Bao, W. Jiang, Y. Wang, and Q. Zhao. A parametric finite element method for solid-state dewetting problems with anisotropic surface energies. *J. Comput. Phys.*, 330:380–400, 2017.
5. W. Bao and Q. Zhao. A structure-preserving parametric finite element method for surface diffusion. *SIAM J. Numer. Anal.*, 59(5):2775–2799, 2021.
6. J. Barrett, K. Deckelnick, and R. Nürnberg. A finite element error analysis for axisymmetric mean curvature flow. *IMA J. Numer. Anal.*, 41(3):1641–1667, 2021.
7. J. Barrett, H. Garcke, and R. Nürnberg. A parametric finite element method for fourth order geometric evolution equations. *J. Comput. Phys.*, 222(1):441–467, 2007.
8. J. Barrett, H. Garcke, and R. Nürnberg. On the parametric finite element approximation of evolving hypersurfaces in $\mathbb{R}^3$. *J. Comput. Phys.*, 227(9):4281–4307, 2008.
9. J. Barrett, H. Garcke, and R. Nürnberg. Parametric approximation of Willmore flow and related geometric evolution equations. *SIAM J. Sci. Comput.*, 31(1):225–253, 2008.
10. J. Barrett, H. Garcke, and R. Nürnberg. Eliminating spurious velocities with a stable approximation of viscous incompressible two-phase Stokes flow. *Comput. Methods Appl. Mech. Engrg.*, 267:511–530, 2013.
11. J. Barrett, H. Garcke, and R. Nürnberg. A stable parametric finite element discretization of two-phase Navier–Stokes flow. *J. Sci. Comput.*, 63(1):78–117, 2015.
12. J. Barrett, H. Garcke, and R. Nürnberg. Parametric finite element approximations of curvature-driven interface evolutions. In *Handbook of Numerical Analysis*, volume 21, pages 275–423. Elsevier, 2020.
13. S. Bartels. A simple scheme for the approximation of the elastic flow of inextensible curves. *IMA J. Numer. Anal.*, 33(4):1115–1125, 2013.

14. A. Bonito, R. Nochetto, and M. Pauletti. Parametric FEM for geometric biomembranes. *J. Comput. Phys.*, 229(9):3171–3188, 2010.
15. K. Deckelnick. Error estimates for a semi-implicit fully discrete finite element scheme for the mean curvature flow of graphs. *Interfaces Free Bound.*, 2:341–359, 2000.
16. K. Deckelnick and G. Dziuk. Convergence of a finite element method for non-parametric mean curvature flow. *Numer. Math.*, 72(2):197–222, 1995.
17. K. Deckelnick and G. Dziuk. On the approximation of the curve shortening flow. In *Calculus of variations, applications and computations (Pont-à-Mousson, 1994)*, volume 326 of *Pitman Res. Notes Math. Ser.*, pages 100–108. Longman Sci. Tech., Harlow, 1995.
18. K. Deckelnick and G. Dziuk. Error analysis for the elastic flow of parametrized curves. *Math. Comput.*, 78(266):645–671, 2009.
19. K. Deckelnick, G. Dziuk, and C. Elliott. Error analysis of a semidiscrete numerical scheme for diffusion in axially symmetric surfaces. *SIAM J. Numer. Anal.*, 41(6):2161–2179, 2003.
20. K. Deckelnick, G. Dziuk, and C. M. Elliott. Fully discrete finite element approximation for anisotropic surface diffusion of graphs. *SIAM J. Numer. Anal.*, 43(3):1112–1138, 2005.
21. K. Deckelnick, J. Katz, and F. Schieweck. A C^1-finite element method for the Willmore flow of two-dimensional graphs. *Math. Comput.*, 84(296):2617–2643, 2015.
22. K. Deckelnick and R. Nürnberg. Error analysis for a finite difference scheme for axisymmetric mean curvature flow of genus-0 surfaces. *SIAM J. Numer. Anal.*, 59(5):2698–2721, 2021.
23. A. Demlow. Higher-order finite element methods and pointwise error estimates for elliptic problems on surfaces. *SIAM J. Numer. Anal.*, 47(2):805–827, 2009.
24. G. Drugan, H. Lee, and X. Nguyen. A survey of closed self-shrinkers with symmetry. *Results Math.*, 73(1):32, 2018.
25. B. Duan, B. Li, and Z. Zhang. High-order fully discrete energy diminishing evolving surface finite element methods for a class of geometric curvature flows. *Ann. Appl. Math.*, 37(4):405–436, 2021.
26. G. Dziuk. An algorithm for evolutionary surfaces. *Numer. Math.*, 58(1):603–611, 1990.
27. G. Dziuk. Convergence of a semi-discrete scheme for the curve shortening flow. *Math. Models Methods Appl. Sci.*, 4(4):589–606, 1994.
28. G. Dziuk. Computational parametric Willmore flow. *Numer. Math.*, 111(1):55–80, 2008.
29. G. Dziuk and K. Deckelnick. Error analysis of a finite element method for the Willmore flow of graphs. *Interfaces Free Bound.*, 8(1):21–46, 2006.
30. G. Dziuk and C. Elliott. Finite elements on evolving surfaces. *IMA J. Numer. Anal.*, 27(2):262–292, 2007.
31. G. Dziuk and C. Elliott. Finite element methods for surface PDEs. *Acta Numer.*, 22:289–396, 2013.
32. G. Dziuk, D. Kröner, and T. Müller. Scalar conservation laws on moving hypersurfaces. *Interfaces Free Bound.*, 15(2):203–236, 2013.
33. C. Elliott and H. Fritz. On approximations of the curve shortening flow and of the mean curvature flow based on the DeTurck trick. *IMA J. Numer. Anal.*, 37(2):543–603, 2017.
34. G. Fu. Arbitrary Lagrangian–Eulerian hybridizable discontinuous Galerkin methods for incompressible flow with moving boundaries and interfaces. *Comput. Methods Appl. Mech. Eng.*, 367:113158, 2020.
35. S. Ganesan, A. Hahn, K. Simon, and L. Tobiska. ALE-FEM for two-phase and free surface flows with surfactants. In *Transport Processes at Fluidic Interfaces*, Advances in Mathematical Fluid Mechanics, pages 5–31. Springer International Publishing, 2017.
36. E. Hebey. *Sobolev Spaces on Riemannian Manifolds*. Lecture Notes in Mathematics. Springer-Verlag, 1996.
37. G. Huisken. Flow by mean curvature of convex surfaces into spheres. *J. Differ. Geom.*, 20(1):237–266, 1984.
38. W. Jiang and B. Li. A perimeter-decreasing and area-conserving algorithm for surface diffusion flow of curves. *J. Comput. Phys.*, 443:110531, 2021.
39. B. Kovács. High-order evolving surface finite element method for parabolic problems on evolving surfaces. *IMA J. Numer. Anal.*, 38(1):430–459, 2018.
40. B. Kovács, B. Li, and C. Lubich. A convergent evolving finite element algorithm for mean curvature flow of closed surfaces. *Numer. Math.*, 143(4):797–853, 2019.

41. B. Kovács, B. Li, and C. Lubich. A convergent evolving finite element algorithm for Willmore flow of closed surfaces. *Numer. Math.*, (149):595–643, 2021.
42. B. Kovács, B. Li, C. Lubich, and C. Power Guerra. Convergence of finite elements on an evolving surface driven by diffusion on the surface. *Numer. Math.*, 137(3):643–689, 2017.
43. B. Li. Convergence of Dziuk's linearly implicit parametric finite element method for curve shortening flow. *SIAM J. Numer. Anal.*, 58(4):2315–2333, 2020.
44. B. Li. Convergence of Dziuk's semidiscrete finite element method for mean curvature flow of closed surfaces with high-order finite elements. *SIAM J. Numer. Anal.*, 59:1592–1617, 2021.
45. A. Mierswa. Error estimates for a finite difference approximation of mean curvature flow for surfaces of torus type, PhD Thesis, Otto-von-Guericke-Universität, Magdeburg, 2020.
46. P. Pozzi. Computational anisotropic Willmore flow. *Interfaces Free Bound.*, 17(2):189–232, 2015.
47. P. Pozzi and B. Stinner. Convergence of a scheme for elastic flow with tangential mesh movement. 2022.
48. R. Rusu. An algorithm for the elastic flow of surfaces. *Interfaces Free Bound.*, 7(3):229–239, 2005.
49. R. Rusu. Numerische analysis für den Krümmungsfluss und den Willmorefluss, PhD Thesis, University of Freiburg, Freiburg im Breisgau, 2006.
50. J. Schöberl. C++11 implementation of finite elements in NGSolve, 2014, ASC Report 30/2014, Institute for Analysis and Scientific Computing, Vienna University of Technology.
51. E. M. Stein. *Singular Integrals and Differentiability Properties of Functions*. Princeton mathematical series 30. Princeton University Press, 1970.
52. V. Thomee. *Galerkin Finite Element Methods for Parabolic Problems*. Number 25 in Springer Series in Computational Mathematics. Springer-Verlag, second edition, 2006.
53. C. Ye and J. Cui. Convergence of dziuk's fully discrete linearly implicit scheme for curve shortening flow. *SIAM J. Numer. Anal.*, 59(6):2823–2842, 2021.
54. Q. Zhao, W. Jiang, and W. Bao. A parametric finite element method for solid-state dewetting problems in three dimensions. *SIAM J. Sci. Comput.*, 42(1):B327–B352, 2020.